Cold, Dry, and Alone:

Quantifying Hibernation Traits in Dryland Bats of the Southwest

by

Hayden Hutcherson

A Thesis Presented in Partial Fulfillment
of the Requirements for the Degree
Master of Science

Approved October 2023 by the
Graduate Supervisory Committee:

Heather Bateman, Chair
Marianne Moore
Jesse Lewis

ARIZONA STATE UNIVERSITY

December 2023

ABSTRACT

As white-nose syndrome (WNS) spreads across North America, generating baseline data on bats hibernating outside of the affected area is critical. To illustrate, despite the imminent arrival of *Pseudogymnoascus destructans* (*Pd*) to Arizona (AZ), little is known about bat hibernation in the Southwest. With the current amount of information, if *Pd* spreads throughout the state, detection of cases would be limited, and severity of disease and magnitude of mortality impossible to accurately estimate. Thus, my study monitored hibernating bats in AZ to increase knowledge and investigate potential WNS impacts on these populations. Utilizing passive acoustic monitoring, internal cave surveys, environmental monitoring, and thermal imaging, my study quantified microclimate preferences, hibernation lengths, hibernation behaviors, population dynamics, and species compositions of bats hibernating in three north-central AZ caves. Hibernation lasted between 104 and 162 days, from late October through mid-March, during which time bats (primarily *Corynorhinus townsendii* and *Myotis* species) roosted at locations with an average of 4.7ºC (range = -0.2ºC – 12.1ºC), 59.6% relative humidity (range = 39.6% - 75.9%), and 0.4 kPa water vapor pressure deficit (range = 0.2 kPa – 0.8 kPa). A maximum of 40 individuals were observed in any hibernacula and clustering behavior occurred in only 4.1% of torpid bats. Bats selected cold and dry roost sites within caves. Results suggest *Pd* could proliferate on some bats hibernating in colder areas of AZ hibernacula, yet the range of observed roost humidities was lower than optimal for *Pd* growth. Hibernation length in north-central AZ is longer than predicted for *Myotis* species at similar latitudes and may be long enough to pose over-winter survival risks if WNS emerges in AZ populations. Yet, a natural tendency for mid-

winter activity, which I observed by multiple species, may allow for foraging opportunities and water replenishment, and therefore promote survival in bats utilizing these arid and cold habitats in winter. Additionally, the relatively solitary behaviors I observed, including virtually no clustering activity and a maximum of 40 bats per hibernacula, may keep rates of *Pd* transmission low in these Southwest bat populations.

DEDICATION

To Bryce and Shocklee- for making all the days "the good days"

ACKNOWLEDGMENTS

I sincerely thank my graduate committee for their invaluable expertise and guidance throughout this research endeavor. Dr. Marianne Moore, your mentorship, guidance, friendship, and unwavering commitment have been nothing short of exceptional. You worked hard to ensure that my graduate career progressed smoothly, and I admire and appreciate your dedication to our research. Dr. Jesse Lewis and Dr. Carol Chambers, thank you for your continuous feedback and guidance during my graduate career. Your wisdom and expertise have greatly contributed to my academic journey.

Angie McIntire, thank you for your expertise and mentorship in bat ecology. Your friendship and guidance have been invaluable. You have shown me the immense impact that a career in bat research can have. A big thank you to Harrison Tamayo, Heidi Kitchel, Jabe Kahawaii, and Bryce Bunn for being an excellent field crew, enduring cold camping trips and snowy hikes in the pursuit of bat research. Thank you to my adopted lab mates, Brett Montgomery, Maggie Huck, and Annika Enloe- your support and friendship have made this journey far better. And to my family, I want to express my heartfelt gratitude for your unwavering support, genuine interest, and constant encouragement throughout this journey.

I am grateful to the following agencies and individuals: The U.S. Fish and Wildlife Service and Arizona State University's Graduate and Professional Association for funding this research; the College of Integrative Sciences and Arts of Arizona State University for educational support; and the Hopi Tribe, Arizona State Trust, Tom Gilleland, and the Coconino National Forest for allowing access to our study sites.

TABLE OF CONTENTS

Page

LIST OF TABLES

LIST OF FIGURES

CHAPTER 1

GENERAL INTRODUCTION

Arid-adapted bats

Arid climates are characterized by extreme temperatures and dry conditions that often have predictable wet seasons with unpredictable precipitation (Whitford & Wade, 2002). Wildlife inhabiting dryland ecosystems contend with sparse resources, dramatic temperature extremes, and persistently dry surroundings (Prăvălie, 2016). Despite these challenges and difficulties, dryland ecosystems maintain high biodiversity (Maestre et al., 2012). Wildlife living in arid environments require evolutionary adjustments that enable their survival. Yet, these environments are understudied, and the extent of adaptations that facilitate survival of wildlife in dryland habitats remains largely unknown (Maestre et al., 2012).

Small mammals with high surface area to volume ratios may face increased evaporative water loss and challenges to maintain suitable body temperatures as compared with larger-bodied species (Altringham, 2011; Speakman & Thomas, 2003). Despite this, many small mammals have adapted to live in arid regions worldwide. Bats represent a group of small mammals with behavioral and physiological adaptations that are beneficial to living in drylands and their diversity in these ecosystems can be quite high (e.g., Strong, 2010).

Because bats are nocturnal, their activity is constrained to periods without direct solar radiation, reducing evaporative water loss (Carpenter, 1969; Herreid & Schmidt-Nielsen, 1966). Some arid-adapted bats can survive extended periods of time without free water (Geluso, 1978) by concentrating their urine (Carpenter, 1969). But experiments on

three desert-dwelling species of bats revealed that insectivorous bats cannot obtain water from their diets alone and must utilize additional water resources (Carpenter, 1969). The ability to fly to sources of free water is likely a contributing factor to the success of bats in arid regions (Carpenter, 1969). Globally, both higher aspect ratio and wing loading (i.e., more efficient, speedier flight) are prevalent in arid-adapted bats (Conenna et al., 2021), which may reduce energy expenditure while accessing scattered water resources.

When water or food resources are limited and ambient temperatures exceed or fall below thermoregulatory zones, bats either migrate to find more suitable conditions (Altringham, 2011) or enter torpor (Altringham, 2011; Speakman & Thomas, 2003). Torpor reduces total evaporative water loss (Ben-Hamo et al., 2013; Carpenter, 1969; Herreid & Schmidt-Nielsen, 1966) and bats may use short-term torpor during summer, known as aestivation, to reduce the effects of water loss in high heat (Geiser et al., 2019). Bats can also use prolonged deep torpor in winter (i.e., hibernate) when temperatures are low and food resources are limited (Altringham, 2011; Speakman & Thomas, 2003).

Hibernation presents bats with challenges related to water loss. Hibernation is composed of bouts of torpor, interrupted by arousals during which bats drink water (Perry, 2013; Thomas & Geiser, 1997; Whiting et al., 2021), feed (e.g., Hope & Jones, 2012; O'Farrell & Bradley, 1970), and mate, among other activities (see Boyles et al., 2006). Herreid and Schmidt-Nielsen (1966) estimated that *Eptesicus fuscus* loses 2% of its body mass in water each day of hibernation and should limit torpor bouts to one to two days maximum if adaptations that reduce evaporative water loss (EWL) do not exist. Yet, Brack Jr. and Twente (1985) and Twente et al. (1985) observed *E. fuscus* torpor bouts

lasting up to 72 days, although the majority lasted between seven and 25 days. This suggests that physiological adaptations to limit water loss during hibernation must exist.

EWL is the combination of cutaneous water loss (CWL) and water loss via external respiration. Of the species studied, CWL makes up a larger proportion of EWL in hibernating bats than expected when compared to CWL in similarly sized rodents (Herreid & Schmidt-Nielsen, 1966; Klüg-Baerwald & Brigham, 2017). Based on the same species, EWL is high in bats roosting in arid conditions, relative to bats in more humid environments (Klüg-Baerwald & Brigham, 2017). Yet, when measured under the same dry conditions, arid-adapted bats have reduced EWL compared to bats of the same species that are humid-adapted (Klüg-Baerwald & Brigham, 2017). To this end, a thicker stratum corneum may reduce CWL and allow bats in arid climates to escape high rates of CWL and EWL (Klüg-Baerwald & Brigham, 2017).

Bat Hibernation in Arizona

Arizona is part of the American southwest with 52 ecoregions identified across the 295,254 km^2 state, ranging from desert lowlands to subalpine habitats (Griffith et al. 2014). The aridity index (the ratio of precipitation to evapotranspiration) ranges from 0.05 to 0.3, classifying Arizona as hyper-arid to arid statewide across all ecoregions (Zomer et al., 2022). Arizona is topographically diverse, with elevations ranging from 21 to 3,851 meters above sea level. In the summer, temperatures can reach up to 50ºC at lower elevations. At higher elevations, average low temperatures in winter reach -10ºC. Daily temperature can fluctuate 50-60ºC, especially in winter when humidity is lower (University of Arizona, n.d.). The unique geography of Arizona encompasses over 2,400 documented caves (Arizona Cave Survey, 2017).

Across the state, there are 28 species of bats (A. McIntire, pers. comm.), and up to 24 species remain in Arizona year-round (Adams, 2003), although not all these bats hibernate. With harsh winters at higher elevations, a large diversity of hibernating species, and ample subterranean habitat, Arizona is a potential hotspot for bat hibernation. Yet, little research has been conducted to quantify bat hibernation behavior, ecology, and physiology in the state. Presented here are the results of a comprehensive literature review on bat hibernation in Arizona, including information regarding the ecological and physiological factors influencing bat overwintering strategies in an arid southwestern region. Understanding the distribution and specific habitat requirements of hibernating bats in Arizona is imperative for managing imperiled species and addressing threats posed by climate change, habitat alteration, and novel diseases. By synthesizing results from existing research, this review aims to highlight knowledge gaps and potential management and conservation challenges.

More than 50 years before I conducted this review, Hoffmeister (1970) reported the distribution of Arizona bats in summer and winter. Hoffmeister estimated that *Corynorhinus townsendii*, *Eptesicus fuscus*, *Parastrellus hesperus*, *Myotis californicus*, and *M. thysanodes* (among others) were found statewide in summer but only inhabited areas south of the Mogollon rim in winter. Cockrum et al. (1996) corroborated the presence of *M. thysanodes*, *M. californicus*, *P. hesperus*, *E. fuscus*, and *C. townsendii* south of the Mogollon Rim during winter (November-March) in Mohave County, Arizona, as well as *M. yumanensis*, *M. volans*, and *M. ciliolabrum*. Yet, Cockrum et al. (1996) predicted that *Antrozous pallidus*, among others, hibernated at higher elevations on the Colorado Plateau, where conditions may be more favorable for hibernation. If

correct, this would expand the known range of some bat species during winter. Hoffmeister (1970) acknowledged that "insufficient investigation" by many researchers in his collaborative study may have resulted in a lack of winter observations, and winter ranges may be more widespread than he reported.

In southern Arizona, Hayward (1961) observed *M. velifer* hibernating at high elevations, which was estimated to be the northern extent of their hibernating range. *M. velifer* was found roosting at cave temperatures between 3ºC and 11ºC. Roosting position was related to ambient temperature and bats shifted from fully exposed when cave temperatures were ~10ºC to inconspicuous and in rock crevices as temperatures dropped to 4-5ºC. These bats did not cluster, and at the time of publication, there were no reports of large clusters of bats during winter in any part of Arizona.

Cross (1965) expected *P. hesperus* to hibernate in southern Arizona based on low levels of activity during winter. On warmer winter days, Cross (1965) observed *P. hesperus* activity at dusk, indicating their presence in winter, but he recorded no direct observations of hibernating *P. hesperus* in this part of the state. Hayward (1961) also observed active *M. velifer* in winter and he predicted they were foraging.

In 2013 and 2014, 128 caves and mines across Arizona were surveyed for suitability as hibernacula and presence of torpid bats by the Arizona Game and Fish Department and Bat Conservation International (Corbett et al., 2017). Results revealed small groups of *C. townsendii*, *E. fuscus*, *M. californicus/ciliolabrum*, *M. thysanodes*, *M. velifer*, and *P. hesperus* hibernating across Arizona, roosting solitarily between 3ºC and 13ºC. These observations represent the earliest published observations of these species hibernating north of the Mogollon Rim. While it is plausible that this indicates a range

expansion over the past five decades since Hoffmeister (1970) published his range maps, it is more probable that increased research efforts simply revealed the presence of these species during winter in northern Arizona.

Pérez et al. (2020) closely studied several caves on the Colorado Plateau, north of the Mogollon rim, that were identified by Corbett et al. (2017) as hibernacula. This was the first published study to use repeated cave surveys to systematically survey and monitor hibernating bats for their behaviors and ecological requirements. Pérez et al. (2020) found small groups (n≤23) of *C. townsendii*, *E. fuscus*, *P. hesperus*, and *Myotis spp.* hibernating throughout winter, and most individuals roosted solitarily. Hibernating bats roosted in caves between 6.2ºC and 17.6ºC, however, the authors of this work readily acknowledge that more accurate measurements of roost temperatures and humidities were needed (M.S. Moore, pers. comm.).

Several cave and mine surveys completed by the Arizona Game and Fish Department revealed hibernating colonies of *C. townsendii* (range: 1-39 individuals) across sites in southeastern and southwestern Arizona (Schmidt, 1995; Tim K. Snow, 1996, 1998). Site elevations ranged from 1,370 m to nearly 2,200 m in elevation.

This review of bat hibernation in Arizona reveals several key findings. Groups of hibernating bats in this state are characterized by relatively small sizes (<40 individuals). Notably, there appears to be no considerable amount of clustering behavior expressed, which hints at a dispersed distribution across numerous roost sites in both the northern and southern regions of Arizona. Additionally, Arizona bats tend to hibernate at temperatures below 13ºC. But, despite prior research on hibernation, substantial gaps persist in our understanding of bat hibernation ecology, behavior, and physiology in

Arizona. Specifically, what is the geographical extent of hibernation in the state? How does hibernation differ on a latitudinal gradient and across different elevations of Arizona? Are there notable differences in hibernation ecology between species? Are these findings indicative of all hibernating bats in Arizona? And how does bat hibernation ecology in Arizona compare to what has been observed in adjacent states and other regions of North America?

Further investigations into population dynamics, geographical distribution, and roost preferences are crucial for guiding effective monitoring initiatives that target hibernating bat communities. Quantifying microclimate preferences and physiological responses during hibernation will enhance our understanding of the adaptive strategies employed by bats in arid environments. This knowledge is essential for assessing their vulnerability to threats like white-nose syndrome and the ecological consequences of climate and human-driven habitat changes.

White-nose Syndrome

White-nose syndrome (WNS) is a fungal epizootic that has caused significant impacts on the ecology and conservation of some cavernicolous bats (see Hoyt et al., 2021). WNS has resulted in >90% declines in populations in three affected species (*M. septentrionalis*, *M. lucifugus*, and *Perimyotis subflavus*; Cheng et al., 2021), over six million deaths (Coleman, 2015), and local extinctions (Frick et al., 2010, 2015, 2016; Langwig et al., 2012). WNS is caused by the fungus *Pseudogymnoascus destructans* (*Pd,* formerly *Geomyces destructans*; Gargas et al., 2009; Lorch et al., 2011; Minnis & Lindner, 2013) and is characterized by white, fuzzy fungal growth on the ears, muzzle, and wings of infected bats (Blehert et al., 2009). Based on phylogenetic analyses of *Pd*,

isolates, and experimental inoculations of naïve bats, WNS was most likely introduced into North America from Eurasia (Puechmaille et al., 2011; Warnecke et al., 2012). In contrast to North American bats, Eurasian bats colonized by *Pd* do not suffer similar rates of mortality (Wibbelt et al., 2013). Instead, possibly due to coevolution between host and pathogen, bats in Eurasia exhibit external characteristics of WNS with confirmed colonization of *Pd* but without the pathogenesis seen in North America (Bandouchova et al., 2018; Puechmaille et al., 2010).

Since its discovery in 2006 near Albany, New York (Blehert et al., 2009), WNS has spread in all directions and now occurs in 40 states and eight Canadian provinces. To date, there are no confirmed cases of WNS in Arizona, but the pathogen is presumed present in California and confirmed in New Mexico, where disease has been observed in some hibernating *M. velifer*. *Pd* was first detected in northwestern Arizona in 2019, but at levels too low to confirm and warrant placement on the official spread map (U.S. National Park Service, 2019). To date, no clinical manifestations of WNS have been observed in Arizona.

During an active WNS infection, *Pd* invades the skin of bats during hibernation and secretes destructin-1, a collagen-degrading enzyme (O'Donoghue et al., 2015). Fungal hyphae erode bat wing epithelia, fill hair follicles, and invade connective tissue, creating lesions on wings and other skin membranes (Meteyer et al., 2009). Lesions are associated with a suite of physiological issues for infected bats, including some systemic immune responses (Moore et al., 2011, 2013), local inflammatory response at the site of infection (Field et al., 2015), increased evaporative water loss (Cryan et al., 2013; McGuire et al., 2017; Willis et al., 2011) and increased metabolic rate (McGuire et al.,

2017; Verant et al., 2014). Higher rates of evaporative water loss and metabolic rate are correlated with increased frequency of arousals from torpor (Reeder et al., 2012; Warnecke et al., 2012), resulting in the premature depletion of fat reserves, which may be a primary cause of death from WNS (Blehert et al., 2009; Meteyer et al., 2009). Associated immune responses may not clear *Pd* infections and the energy required to mount an immune response may also deplete fat stores prematurely (Moore et al., 2013). WNS-associated mortality is highest during late hibernation and may begin roughly 85 days after exposure (Langwig et al., 2012; Lorch et al., 2011; Reeder et al., 2012). If WNS-infected bats survive hibernation they may exhibit an immune reconstitution inflammatory syndrome, which may compound wing damage developed during hibernation (Meteyer et al., 2012).

Genetic sequencing at eight loci supports a clonal expansion of *Pd* in North America (Rajkumar et al., 2011). Whole-genome sequencing of *Pd* shows that 100% of isolates from North America contained the MAT1-1 locus, completely lacking the MAT1-2 locus mating type necessary for a sexual phase to occur (Drees et al., 2017). While *Pd* appears to reproduce primarily by asexual conidia in North America, Palmer et al. (2014) discovered the heterothallic, sexual reproductive phase in Europe. Both mating types were isolated from soil in Europe (Palmer et al., 2014) providing evidence that a sexual stage is possible. Due to recombination during sexual phases, unique and more pathogenic strains could arise in North America, which could evade host defenses and lead to even greater impacts on hibernating bats (Minnis & Lindner, 2013). Yet, it is also possible that recombination could lead to less pathogenic strains of *Pd*, a trait that could increase in the *Pd* population through genetic drift if other linked traits are advantageous.

Pd is a cold-loving fungus that grows between 3ºC and 20ºC (Blehert et al., 2009). Optimal conditions for proliferation include temperatures between 12ºC and 16ºC (Verant et al., 2012) and high relative humidity (Marroquin et al., 2017). These conditions overlap with conditions selected by many species of bat during hibernation (Altringham, 2011; Haase et al., 2021). *Pd* is saprotrophic (Reynolds et al., 2015) and can persist in cave sediments without the presence of bat hosts (Hoyt et al., 2015; Lorch et al., 2013). Bats are the primary vector of *Pd* through bat-to-bat and bat-to-cave transfer (Lorch et al., 2011; Warnecke et al., 2012), and colony size and clustering behaviors are positively related to transmission rates (Langwig et al., 2012). Due to *Pd*'s persistence in hibernacula without bats (Hoyt et al., 2015; Lorch et al., 2013), bats may be reinfected upon entering hibernation through cave-to-bat transfer of spores. Campbell et al. (2020) discovered that conidia of *Pd* can survive for up to 180 days at elevated temperatures on bat fur, well above its optimal growth temperature. This has implications for long-term survival of *Pd* within hibernacula, between seasons, and especially across large geographic areas as bats disperse. Some bats may travel several hundred kilometers between hibernacula and summer roosts (e.g., Davis & Hitchcock, 1965), aiding spread of *Pd*. Some migratory bats have been confirmed with *Pd* present on their body surfaces (i.e., positive for exposure) without showing cutaneous invasion diagnostic of WNS (i.e., negative for infection; White-Nose Syndrome, n.d.). These species apparently serve as spreaders of *Pd* without being impacted themselves (Bernard et al., 2015). Additionally, it is likely that infected cave sediments are spread between caves by human recreational activities (e.g., cave sediments on shoes) and contribute to the spread of WNS (Reynolds et al., 2015).

WNS is confirmed in 12 species of bats, including *E. fuscus, M. velifer, M. leibii, M. thysanodes, M. grisescens, M. sodalis, M. lucifugus, M. volans, M. septentrionalis, M. evotis, P. subflavus,* and *M. yumanensis. Pd* has been detected on an additional eight species, without diagnostic symptoms of WNS. These species include *Lasiurus borealis*, *Tadarida brasiliensis, C. rafinesquii*, *Lasionycteris noctivagans*, *C. townsendii, C. townsendii virginianus*, *C. townsendii ingens, and M. ciliolabrum.* Based on research in eastern populations, some species of bats are more resistant to WNS than others either physiologically, behaviorally, or both (Frank et al., 2014; Moore et al., 2018). For example, under experimental conditions, *E. fuscus* increased torpor bout length in response to a WNS infection and showed a less pathogenic infection compared to *M. lucifugus*, in which hibernation behavior did not change (Moore et al., 2018). Despite similar rates of exposure, resistant bats may exhibit lower mortality (Cheng et al., 2021). Current information on hibernating bats in the Southwest is insufficient to determine which species will be exposed to *Pd* and which of those are likely to exhibit WNS symptoms and mortality (But see: Haase et al., 2021). Research on WNS has been an interdisciplinary effort (Bure & Moore, 2019), and collaboration between entities should continue in understudied parts of North America to address additional conservation concerns.

Additional Pressures

In addition to emerging infectious diseases, climate change may also pose a significant threat to bats, especially in arid environments. Current climate models for the southwestern United States predict these areas will become drier, with less precipitation, and exhibit warmer winters and more extreme weather events (Archer & Predick, 2008).

Festa et al. (2023) found that climate change may force species to adapt to new conditions, cause migrations to more suitable conditions elsewhere, or cause extreme contractions in species ranges. Examples of climate change induced range shifts have already been observed (e.g., Lundy et al., 2010). In bats, Ancillotto et al. (2016) observed a significant range expansion northward in just four decades for the *Pipistrellus kuhlii*. Modeling results indicated that the increase in winter temperatures, an effect of climate change, was the primary driver of range shifts (Ancillotto et al., 2016). If, as projected, winters in the southwestern United States become warmer and drier, hibernating bats may experience impacts as they seek climates more suitable for hibernation. However, warmer winters could also lead to increased insect activity and potentially benefit bats, although the effects of climate change on insects varies geographically and may have already caused significant declines in insect abundance in the Southwest (Harvey et al., 2023). Delineating the current geographic distributions of species and monitoring of bats across all seasons should be prioritized to predict and assess the effects of climate change on bats in arid climates in the coming decades.

Additionally, it is possible that climate change will directly affect the climate and ecology of subterranean habitats of which many cavernicolous bats depend (Vaccarelli et al., 2023). This may lead to changes in temperature and humidity within these sites, changing the availability of habitat for both native and invasive organisms (Vaccarelli et al., 2023). Yet, there is little data quantifying changes in subterranean features and organisms and additional monitoring of underground habitats should be prioritized.

Bats also face many pressures related to human expansion. Worldwide, bats face the substantial challenge of habitat modification, by logging, agricultural expansion, and

urban development (Frick et al., 2020). Additionally, there is the possibility of reverse zoonotic transmission of infections from humans to bats, as exemplified by Sars-CoV-2 (Olival et al., 2020). Human recreational or purposefully destructive activity within caves during sensitive times of year for bats (i.e., hibernation, maternity roosting) is also recognized as a significant threat to bats (Mickleburgh et al., 2002).

Effective management of Arizona's bats becomes a formidable challenge when there is a lack of comprehensive knowledge on these species. If managers aim to protect roosting habitats using measures like seasonal or total cave/mine closures, it is imperative to identify and understand which sites are critical for hibernating bats and which sites are not utilized. This requires robust scientific research and monitoring programs to determine the ecological requirements of each species. Prioritizing monitoring efforts and conducting research to assess species abundance and distribution is essential to ensure that management efforts are effectively targeted towards colonies and species most in need. Our current understanding of Arizona bat distributions during winter is inadequate for detecting potential range shifts of hibernating bat species within the state. Additionally, there is presently no established baseline for the hibernation physiology, ecology, and behavior of Arizona bats under natural conditions, against which changes in hibernating colonies can be discerned and management plans be scientifically designed and implemented.

CHAPTER 2

BAT HIBERNATION BEHAVIOR, ECOLOGY, AND PHYSIOLOGY IN ARIZONA

Introduction

Bats expend considerable amounts of energy to survive overwintering in habitats with low ambient temperatures (Altringham, 2011; Speakman & Thomas, 2003). Body heat is easily lost to the environment by small mammals, such as many North American insectivorous bats, that have high surface area to volume ratios (Altringham, 2011; Speakman & Thomas, 2003). During winter, energy demands of maintaining a constant body temperature above ambient temperature exceeds energy intake, due to the lack of available food and low ambient temperatures in temperate regions during winter (Stawski et al., 2014). Survival is achieved by migrating to warmer climates (Altringham, 2011), entering torpor (Altringham, 2011; Speakman & Thomas, 2003), or utilizing a mixture of these strategies (Auteri, 2022).

Hibernation is defined by long bouts of torpor with periodic arousals (Geiser and Ruf, 1995). It is an adaptive strategy when ambient temperatures are low and food resources are limited (Geiser, 2013). In temperate regions, bats generally enter hibernation in late October and emerge in April (e.g., Johnson et al., 2017; Lesiński, 1986) although hibernation varies widely on a latitudinal gradient (Perry, 2013) and can last as long as eight months in some northern populations (e.g., Norquay & Willis, 2014). Survival through winter depends primarily on the amount of energy stored before winter, how much energy is consumed throughout winter (particularly during arousals), and the duration of time along which ambient temperatures are low (Humphries et al., 2002).

During hibernation, bat metabolism is reduced to 1-5% of basal metabolic rate (Geiser, 2013), allowing body temperatures to fall within 1-2ºC of ambient temperatures (Altringham, 2011; Webb et al., 1996). Low metabolic rates reduce total water loss and promote energy conservation (Ben-Hamo et al., 2013). Despite it being adaptive to keep arousals throughout the winter to a minimum, healthy bats arouse every 10-20 days (Geiser & Ruf, 1995; Thomas et al., 1990) to drink water (Perry, 2013; Thomas & Geiser, 1997; Whiting et al., 2021) and perform other tasks (see Boyles et al., 2006), though there is considerable species-specific variation in torpor bout length (e.g., Jackson et al., 2022).

North American hibernating bats face environmental challenges during winter and are now faced with a novel infectious disease, white-nose syndrome (WNS). WNS, a fungal epizootic, poses additional survival risks for many species of cavernicolous, hibernating bats across the continent and has already caused more than six million deaths (Coleman, 2015). 90% population declines have occurred in three hibernating bat species (*M. septentrionalis*, *M. lucifugus*, and *Perimyotis subflavus*; Cheng et al., 2021) leading to local extinctions in some species (Frick et al., 2010, 2015, 2016; Langwig et al., 2012).

Pseudogymnoascus destructans (*Pd,* formerly *Geomyces destructans*; Gargas et al., 2009; Lorch et al., 2011; Minnis & Lindner, 2013) the causal agent of WNS, is a cold-loving fungus that grows between 3ºC and 20ºC (Blehert et al., 2009), optimally between 12 and 16ºC (Verant et al., 2012) and at high relative humidities (Marroquin et al., 2017). *Pd* invades the skin of bats during hibernation, creating lesions on wings and other skin membranes (Meteyer et al., 2009). It increases the frequency of arousals in hibernating bats leading to premature depletion of energy stores (Reeder et al., 2012;

Warnecke et al., 2012). WNS-associated mortality is highest during late hibernation and may begin roughly 85 days after exposure in some species (Langwig et al., 2012; Lorch et al., 2011; Reeder et al., 2012). Bats are the primary vectors of WNS through bat-to-bat and bat-to-cave transfer (Lorch et al., 2011; Warnecke et al., 2012), and larger colonies and clustering behaviors are positively related to transmission rates (Langwig et al., 2012). Since the discovery of WNS near Albany, NY in 2006, WNS has spread in all directions and now occurs in 40 states and eight Canadian provinces.

Knowledge on bat hibernation ecology and physiology in North America is based mostly on Eastern and Northern hibernating populations, and there is a noticeable knowledge gap on bat hibernation traits in the Southwest (Weller et al., 2018). My study was conducted in Arizona (AZ) which is considered hyper-arid to arid statewide (Zomer et al., 2022). Arizona is topographically diverse, and conditions at lower elevations and latitudes in AZ can exceed 50ºC in summer while higher latitudes can remain below 0ºC during winter months (Hammer, 2006). Twenty-eight species of bats are present in Arizona (A. McIntire, pers. comm.), with up to 24 species as year-round residents (Adams, 2003). Colonies of hibernating *C. townsendii*, *Myotis spp*., *Parastrellus hesperus*, and *E. fuscus* have been documented in the northern and southern reaches of the state (Corbett et al., 2017; Hayward, 1961; Pérez et al., 2020), although bat behavior and physiology during hibernation in AZ is still largely unknown. To date, there are no confirmed cases of WNS in AZ, but the pathogen's presence and some mortality is confirmed in several surrounding states (White-Nose Syndrome, 2023). The U.S. Fish and Wildlife Service recognizes and funds priority research as part of the National Response to WNS. Currently, the priority list includes "research to produce critical

knowledge relevant to management decisions and actions for hibernating bats" (White-nose Syndrome Research for Conservation Grants, 2021). Because WNS is spreading across North America, Weller et al. (2018) described the need for characterizing bat hibernacula in the West as urgent.

Like bat hibernation ecology, the majority of information about WNS and its effects on bats is based on limited species primarily studied in a laboratory setting or in eastern North America. It remains unclear how bats hibernating in arid environments will respond to *Pd* and WNS. Thus, my study addresses knowledge gaps and generates a baseline dataset of bat hibernation traits in AZ to understand the natural behavior, ecology, and physiology of bats in AZ, explore adaptations that bats in AZ may express to hibernate successfully in arid environments, and assess what risk WNS may pose to dryland hibernating bats. Specifically, I set out to 1) quantify the relative abundance of bats in hibernacula, the diversity of species observed, and document hibernating bat behavior (i.e., clustering activity, roosting behavior) across hibernacula, 2) estimate torpid body temperatures and the tendency for hibernating bats to arouse upon non-tactile disturbance, 3) analyze microclimate selection tendencies, 4) estimate total hibernation length and winter activity for bats in north-central AZ, and 5) explore these observed hibernation traits in the context of WNS to identify risk factors for bats hibernating in AZ. This dataset provides a baseline that can be used to help detect changes in abundance of bats hibernating in AZ. My findings increase our understanding of bat hibernation in arid environments and contribute to broader conservation efforts, with potential implications related to hibernating bats in other dryland ecosystems.

Methods

Study Area

This study was conducted in north-central Arizona (AZ), north of the Mogollon Rim (Figure 1). I repeatedly surveyed three main hibernation sites (hibernacula) within 85 km of Flagstaff, AZ and separated by an average of 94 km. All sites are considered arid by Zomer et al. (2022). Sites were selected from a Bat Conservation International report indicating presence of bats in winter (Corbett et al., 2017) and accessibility, using off-road vehicles, for most of the hibernation period. Research was conducted over five years between 2018 and 2023. Initial protocols were generated in 2018-2019 (Year 1) and 2019-2020 (Year 2) when each site was monitored between August and April and colony size, species composition, and roosting behaviors were documented (Pérez et al., 2020). Due to a moratorium on bat research during the outbreak of Sars-CoV-2 and a gap in funding, no data were collected during the 2020-2021 field season (Year 3). Research resumed in Year 4 (2021-2022) and a final year of data collection took place in Year 5 (2022-2023). Cave names are omitted to protect sensitive hibernating bat colonies.

Cave 1 is 1626 meters above sea level (asl) and in the Conifer Woodlands and Savannas ecoregion (Griffith et al., 2014), dominated by pinyon (*Pinus spp.*) and juniper (*Juniperus spp.*). Typical annual precipitation is between 500-635 mm. It is a single-opening, limestone cave consisting of several large rooms and tall ceilings reaching a maximum height of 3.8 m. The cave is used by javelina, pack rats, rattlesnakes, and large carnivores. Cave 1 is located on gated private land, so it receives little human disturbance.

Cave 2 is in the Coconino National Forest at 2264 meters asl. It is in a transition zone between Montane Coniferous Forest and Montane and Subalpine Grasslands (Griffith et al., 2014) dominated by ponderosa pine (*Pinus ponderosa*) and mixed grass species with typical annual precipitation between 500-635 mm. This site is a basalt lava tube with three single-entrance passages, the longest one being 274 meters in length (Corbett et al., 2017). Ceiling heights range from 0.5 meters to 4 meters. This is a publicly accessible site used by recreationists primarily in summer. The forest road leading to this cave is usually closed in winter and appears to receive very little use during that time.

Cave 3 is partially on Hopi Tribal land and partially on Arizona State Trust land at 1733 meters asl. Located in the Northeast Arizona Shrub-Grassland ecoregion (Griffith et al., 2014), this site is dominated by several grass species, is mostly devoid of trees, and is grazed by livestock. Typical annual precipitation is between 130-250 mm. Cave 3 is a fissure running 313 m long and up to 9 m deep (Corbett et al., 2017). Some sections of the cave are fully exposed (i.e., no ceiling). Cave 3 connects to a nearby cave through a small opening that was not surveyed. This is an easily accessible site without off-road vehicles and may receive some human disturbance, especially for rockhounding. This site is also used by nesting ravens and mountain lions (M.S. Moore, pers. comm.).

Caves 4-12 were additional caves that I surveyed one to three times to assess the presence of bats during hibernation across a larger geographic area within AZ. I surveyed caves 4-6 in February 2022. Caves 4-6 are in the Coconino National Forest and in the Montane Coniferous Forest (Griffith et al., 2014) above 2100 meters asl. Cave 4 is a relatively shallow basalt lava cave with a single large opening and daylight throughout

the entire cave. Cave 5 is a small, single opening cave, with a two-meter vertical scramble, into a single room with a max height of ~3 meters. Cave 6 is a shallow, single-opening lava cave with a max height of ~1.5 meters. Caves 4-6 are challenging to access in the winter and most likely receive little human disturbance year-round.

I added Caves 7-12 to our surveys in Year 5. Cave 7 is in the Prescott National Forest at 1922 meters asl in the Mogollon Transition Conifer Forests ecoregion (Griffith et al., 2014). This single-entrance site is easily accessible from paved roads and receives heavy human visitation. Cave 7 heights range from 1 meter to ~7 meters. Caves 8-10 are in the Coconino National Forest at 2100 meters asl. They are all within 4.8 km of Cave 2, are single-opening basalt lava tubes, and are in the Montane Coniferous Forest ecoregion (Griffith et al., 2014). During the winter, Caves 8-10 are only accessible via backcountry skis and receive little to no human disturbance during these months. Cave 11 is in the Coronado National Forest at 1555 meters asl in the Lower Madrean Woodlands ecoregion (Griffith et al., 2014). Cave 12 is in the Miller Peak Wilderness Area at 2045 meters asl in a Madrean Pine-Oak and Mixed Conifer Forest (Griffith et al., 2014).

Data Collection

Internal Cave Surveys. To quantify hibernating colony size, species composition, and hibernation behavior in three focal caves, I conducted monthly internal cave surveys at Caves 1-3 between October 2021 and March 2022, except in December 2021. In Year 5, I surveyed these sites in November 2022, January 2023, and February 2023 (Supplementary Material Appendix A; Table A1). Because of time constraints from backcountry skiing and snowshoeing to Cave 2 as well as weather concerns in January 2023, there was only time to do maintenance checks on equipment and a full survey was

not completed. I conducted additional reconnaissance internal surveys at Caves 4-6 once during hibernation in Year 4, at Caves 7-10 once during hibernation in Year 5, and at Caves 11 and 12 once during late hibernation/early emergence in Year 5. Because Caves 11-12 were surveyed after our defined hibernation period, data from these two sites are not included. Teams consisted of two to six people who were trained in data collection techniques to limit disturbance to roosting bats (Supplementary material Appendix C, Figure C1). We used a double-observer technique to ensure at least two people would examine all accessible sections of each cave (Supplementary material Appendix C, Figure C2). During surveys, two observers would begin the survey on opposite cave walls, looking for bats with a headlamp and handheld light from ground level to the ceiling, behind and within cave features. At the end of each room, the two observers would switch walls and make a return trip using the same approach, always looking for bats in the same manner on the opposite wall from the other observer. This technique was repeated in every room, and all accessible surfaces of caves were surveyed by at least two people. We counted the number of individual roosting bats and used photography to record and confirm species identifications. To avoid altering the behaviors of roosting bats, we did not handle bats and did not collect morphometric measurements. For this reason, some bats, especially *Myotis*, were only identified to the genus level.

I recorded locations of each roosting bat on cave maps. I measured cluster size at each roosting individual by quantifying the number of bats that were in direct contact with the focal individual. I quantified the roost height from the floor directly below each roost location using a laser distance tool (GLM165-40; ±0.16 cm; Robert Bosch Tool Corporation; Farmington Hills, MI). Roost position was recorded on a binned scale from

1-4. Position 1 was used for a fully exposed bat. Position 2 corresponded to a bat partially concealed in a cave feature (i.e., crack, cup, etc.) with >50% of the bat exposed. In position 3, <50% of the bat was exposed and position 4 was used when less than 10% of the bat was exposed (i.e., only an ear was visible; Figure 2).

My team followed all WNS decontamination protocols set forth by the United States Fish and Wildlife Service to prevent the potential spread of *Pd* between caves (White-Nose Syndrome Disease Management Working Group, 2020). Additionally, following recommendations set forth by the Arizona Game and Fish Department to reduce the risk of transmitting SAR-CoV-2 to bats, each crew member was vaccinated against SARS-CoV-2, PCR tests through Arizona State University were used one to two days prior to each survey, and we used rapid antigen tests prior to entering each site. Crew members that tested positive for SARS-CoV-2 did not attend field trips. All crew members wore N95 masks while in caves.

Thermal Imaging. The temperature of the ventral surface of a bat is highly correlated with internal bat body temperature (Audet & Fenton, 1988), so thermal imaging of bat body surfaces was collected to estimate torpid bat body temperature (T_{sk}; Supplementary material Appendix C, Figure C8-9). Thermal images were captured for each roosting bat using a FLIR T540 thermal camera (Teledyne; Wilsonville, OR, ±2°C) beginning in November 2021. For the first several surveys, still images were taken of each roosting bat. Beginning in January 2022, I used a video setting to record each bat in thermal mode and visual mode for at least 30 seconds to ensure the highest quality image for extracting temperature data. Images and videos were collected as quickly as possible

after locating each bat (typically within the first minute) to record roosting T_{sk} prior to disturbance that may have occurred due to our presence.

To estimate the tendency of bats hibernating in AZ to arouse upon non-tactile disturbance, repeated images of each bat were collected opportunistically (i.e., not along a specific time course) several times throughout each survey in Year 4. Typically, I reimaged each bat within one hour of the preceding image to assess changes in T_{sk} in response to our presence. Subsequent images collected at individual bats spanned up to 360 minutes following the first image. In Year 5, I did not estimate the tendency for bats to arouse upon non-tactile disturbance, so a single thermal video of each roosting bat was collected to increase survey efficiency and reduce time spent in hibernacula.

Microclimate Conditions. To explore microclimate preferences, I measured environmental conditions at bat roost sites and throughout each cave system. At each roosting bat, I measured the temperature of the cave wall within 10 cm of each bat using a Fluke thermometer (62 Max Mini Infrared Thermometer, ±1.0°C, Everett, WA) and recorded the relative humidity as close to each roosting bat as possible. In Year 4 (2021-2022), humidity was recorded using a Kestrel 3000 (±1.0% relative humidity; ±0.4°C; ±1.04-1.66% wind speed, Boothwyn, PA) which was hung from cave features and left undisturbed near the roosting bats (0.1 meters-4 meters) for 1-10 minutes while the relative humidity measurement stabilized. Due to low airflow and extremely cold temperatures in caves, it is possible the Kestrel 3000 did not stabilize during the recorded time but recorded skewed relative humidity in Year 4. Upon discovering the skewed data, a validation study was launched. Two Kestrel 3000s, one Kestrel 5200 Professional (±2.0% relative humidity; ±0.5°C; ±3% wind speed, Boothwyn, PA), and one HOBO

data logger (model U23-001A; ±0.2°C; ±2.5% from 10% to 90% RH, Onset Computer Corporation, Bourne, MA) were attached to a single telescoping pole (Supplementary material Appendix C, Figure C3). This apparatus measured relative humidity adjacent to roosting bats for five minutes. The HOBO logger recorded every five seconds during this time, and relative humidity from the three Kestrels was recorded manually at the end of the five-minute period. Statistical analyses revealed significantly different relative humidities between the Kestrels and the HOBO data logger in most cases (Kruskal-Wallis Cave 1: $H=0.31$, $df=4$, $p<0.01$; Cave 3: $H=0.43$, $df=4$, $p<0.01$), further supporting the assumption that relative humidity data recorded using the Kestrel 3000 in Year 4 was skewed to report significantly lower humidity readings. To increase accuracy and consistency in our humidity measurements, I only used a HOBO data logger in Year 5 (2022-2023). The HOBO logger was positioned horizontally and attached to the end of a telescoping pole, then held within 0.5 m of each roosting bat for five consecutive minutes all the while recording relative humidity every 10 seconds. The final relative humidity recording of the five-minute period was used for analysis.

I deployed nine battery-powered HOBO data loggers (HOBO model U23-001A; ±0.2°C; ±2.5% from 10% to 90% RH; Onset Computer Corporation, MA) in Caves 1-3 in December 2021. Loggers were set to record temperature and relative humidity every 15 minutes. One logger was placed outside of each cave in the shade near acoustic monitors to collect external conditions. Five additional loggers were deployed in Cave 2 in January 2023 to increase coverage of cave conditions. Data was downloaded in June 2022 and November 2022, and loggers were immediately redeployed. I collected internal loggers from each site in February 2023 and external loggers in May 2023. Loggers were

randomly dispersed through each cave system to cover the range of available cave conditions. They were placed horizontally in cave features, obscured by rocks, and camouflaged using dark foam that did not cover the sensor (Supplementary material Appendix C, Figure C4). Placements ranged from 0.35 m to 6.29 m from the floor. I positioned loggers in areas where roosting bats had been observed and additional locations that were within reach. The external logger at Cave 2 went missing and was never recovered, so external condition data from the 2021-2022 winter was not collected; however, it was replaced in June 2022, and I successfully recorded external conditions during Year 5.

In Year 5, I deployed HOBO loggers in six additional caves to gather conditions of other caves that may be used as hibernacula (Figure 1). Loggers in Caves 7, 8, 9, and 10 were deployed in January 2023 and collected in May 2023. Loggers in Caves 11 and 12 were deployed in March 2023. These loggers were also placed horizontally, camouflaged using dark foam that did not cover the sensor, but were set to record temperature and relative humidity every two hours.

Additional climatic variables (precipitation, barometric pressure, etc.) were downloaded from the National Oceanic Atmospheric Association weather station closest to each site (https://www.ncei.noaa.gov/cdo-web/). Daily moon phase data was accessed from The Astronomical Applications Department of the U.S. Naval Observatory (https://aa.usno.navy.mil/data/MoonFraction).

Acoustic Monitoring. Passive acoustic monitoring was conducted at each site using Wildlife Acoustics SM4FS automated recording units (ARU) and an omni-directional SMM-U2 microphone (Maynard, MA). Calls were recorded in full spectrum.

One detector was placed outside each of Caves 1-3 within 20 m of cave entrances, as in Bernard & McCracken (2017). I attached microphones to telescoping poles, which were secured to trees or stabilized with rebar (Supplementary material Appendix C, Figure C5-7). Microphones were at least two meters above ground level in low clutter areas. ARUs used 128 GB SD cards (SanDisk Ultra Plus, 130 MB/s, Milpitas, CA) and were powered using rechargeable D-batteries (Powerex Rechargeable D NiMH Batteries, 1.2V, 10,000 mAh) until solar panels (Faunatech 20-watt solar panel connected to 12V 7 Ah SLA battery) were deployed in December 2021. Solar panels were south facing, mounted to trees at Caves 1 and 2 and on the ground at Cave 3, and secured with steel cables and padlocks. Cave 3 had solar panel malfunctions in May 2022 and November 2023, so instead I used rechargeable D-batteries at this site, which were replaced every two weeks. ARUs recorded calls nightly from September 2021 through May 2022 and from September 2022 through May 2023, starting 30 minutes before sunset and ending 30 minutes after sunrise. ARUs were launched with the following settings: Gain: 12dB, 16K; High Filter: OFF; Sample Rate: 256kHz; Min Duration: 1.5ms; Max Duration: None; Min Trigger Freq: 7kHz; Trigger Level: 12dB; Trigger Window: 2; Seconds Max Length: 15; Seconds Compression: None.

Analysis

I performed all data analysis using R version 4.2.1 (R Core Team, 2022) and R Studio (RStudio Team, 2020). All data were non-normally distributed, determined using a Shapiro-Wilk test for normality ($p<0.05$) and transformations did not improve normality, so I proceeded with non-parametric tests.

Hibernating Bat Group Size, Species Composition, and Behavior. Chi-squared tests compared species composition and colony sizes using data from Years 1-5 (2018-2023). I analyzed roost characteristics (roost height from floor, cluster size, and roost position) and tested for differences between species and caves using the Kruskal-Wallis H-test, followed by Dunn's Multiple Comparison *post hoc* test to check for specific pair-wise differences. These analyses only included data from Years 4 and 5 since survey personnel were consistent across both years and my protocol was solidified and refined by this time.

Torpid Body Temperature and Tendency to Arouse. Thermal image processing was completed in FLIR Thermal Studio (version 1.9.66). I estimated T_{sk} from each video using the scale bar provided in the video, and determined if the roosting bat's T_{sk} was above ambient by more than ~1ºC or normothermic (~35ºC). For bats imaged repeatedly in Year 4, T_{sk} was estimated from each video and compared to subsequent videos collected over the course of the survey. For each repeatedly imaged bat, I determined if T_{sk} increased by more than 1ºC over the course of the survey, and if it did, I examined the data further to determine if the bat reached normothermic body temperatures and/or returned to temperatures representative of torpor. Species-specific tendencies were not evaluated because image quality differed between *C. townsendii*, roosting exposed, and *Myotis* spp., which often roosted in obscured positions.

Microclimate Selection. To assess microclimate selection, I used data from January and February of Year 5 only (2023), which included data from two internal surveys at each of Caves 1 and 3, one internal survey in February 2023 at Cave 2, and continuous cave condition data at each site. Year 4 data was not used due to Kestrel 3000

malfunctions. Based on our acoustic monitoring efforts that estimated hibernation length using bat nightly activity at each site, I assumed data collected in January and February were accurate representations of bat hibernation microclimate selections at these sites.

Relative humidity can be misleading regarding evaporative water loss from hibernating bats (Kurta, 2014), so I converted relative humidity to absolute humidity and water vapor pressure deficit. Water vapor pressure deficit was determined by taking the difference between the measured saturated vapor pressure (calculated based on relative humidity) and the measured actual vapor pressure (calculated using the recorded temperature). For comparisons between bat roost condition and available cave conditions from 24 hours prior to a survey, hourly recordings per logger were used since daily variance per logger was wide in some cases. In other analyses (i.e., comparisons between caves and years), daily average recordings were used. Days where loggers were placed or retrieved were excluded from analysis.

Data from each month was analyzed separately because conditions varied significantly between months (Kruskal-Wallis $df=1$, $p<0.01$), and this allowed us to avoid problems related to pseudo-replication of bat observations. Sites were combined for analysis to assess bat selection of conditions on the larger geographic scale and were analyzed separately to assess site-specific patterns. For each month, only a subset of the HOBO data was used. Bats arouse periodically and may relocate within hibernacula every one to 25 days (e.g., Brack Jr. and Twente 1985), though arousal patterns have not been described for these specific groups of hibernating bats. Thus, hourly recordings per logger spanning a 24-hour period from one day, five days, 10 days, 20 days, and 25 days preceding each survey date were each tested against bat roost conditions to account for

the conditions that existed when bats may have selected a particular roost location and entered torpor. Cave conditions varied significantly across all data collected one, five, 10, 15, 20, and 25 days prior to each survey (Kruskal-Wallis df=1, $p<0.01$). However, available cave condition and bat roost condition distributions were significantly different regardless of which 24-hour period was used (Kolmogrov Smirnov df=1, $p<0.05$). Presumably, bat roost conditions vary over time similarly to cave condition variation over time, so I present differences using cave conditions from the 24-hour period preceding each bat survey, which were most reflective of conditions at the time I observed bats.

Nonparametric tests were used for all analyses because most data were non-normally distributed (Shapiro-Wilks $p<0.05$) and transformations did not improve distributions. A two-sample Kolmogorov-Smirnov test was used to directly compare the distribution of measured bat roost conditions, including temperature, relative humidity, absolute humidity, and water vapor pressure deficit, to available cave conditions within each cave. I analyzed all species together and separately tested for species-specific preferences. Significantly different distributions ($p<0.05$) indicated a non-random distribution of bats across available conditions. A nonsignificant result indicated bats were randomly dispersed across the available cave conditions, with no evidence of selecting for specific temperature and humidities.

Interspecific roost differences within caves, intraspecific roost differences between caves, and differences in cave conditions between sites, months, and 24-hour HOBO sampling periods were tested using the Kruskal-Wallis H-test, followed by Dunn's Multiple Comparison *post hoc* test. Comparisons of species preferences between sites were performed with *C. townsendii* and *Myotis spp.*, which had sufficient sample

sizes to make meaningful comparisons. A significance of less than p=0.05 indicated significantly different conditions between groups.

Acoustic Analysis and Hibernation Length. All bat acoustic calls were processed using SonoBat (version 4.4.5; Szewczak 2017). Files containing characteristic bat pulses were automatically determined as bat-call files by Sonobat software. Several species of bats in Arizona echolocate at frequencies ~8 kHz, so I evaluated all calls 5 kHz and above. I used the Northern-Arizona auto-classifier with an acceptable call quality threshold of 0.50 and a decision threshold of 0.90 within each call sequence. All calls characterized as bat calls by Sonobat were then manually vetted by evaluating each call's sonogram against reference files for Arizona species. I confirmed that all included calls met characteristic bat call criteria (i.e., no birds, insects, etc.). Species presence per recording night at each site was determined to evaluate species-specific differences in hibernation length and winter activity.

Due to ambiguity in *Myotis spp.* acoustic signatures, I grouped calls from this genus into the "50 kHz *Myotis*" group (characteristic frequency above 48 kHz) and the "40 kHz *Myotis*" group (characteristic frequency between 38 kHz and 48 kHz; Table 1). All other species were manually vetted to the species level when possible. When vetting to the species level was not possible, calls were grouped into high frequency bats (characteristic frequency above ~35 kHz) and low frequency bats (characteristic frequency below ~35 kHz; Table 1).

Calls were used as an index of relative activity and were not used to estimate total abundance since single bats may be detected multiple times in one night (Bernard & McCracken, 2017). Acoustic-nights were defined as the number of nights that acoustic

recorders were operating at each site. I designated nights of bat activity when at least one file containing characteristic bat calls was recorded. I summed the number of files with bat activity each night at each site to evaluate relative nightly activity. I adapted methods to determine hibernation length from Meyer et al. (2016) and Blejwas et al. (2021). To capture a conservative estimate of hibernation I selected the hibernation start date (entrance) as the first of three consecutive nights that nightly bat passes fell below 1% of the total bat passes for fall. I defined "fall" as all dates within the eight weeks prior to the autumnal equinox. For the hibernation end date (emergence), I selected the first of three consecutive nights that nightly bat passes exceeded 1% of total bat passes for the spring season, which I defined as all dates eight weeks prior to the spring equinox. Humphries et al. (2002) expected hibernation length to equal the number of days in a year where the mean nightly temperature < 0ºC, so I additionally estimated hibernation length at each of my sites using weather station temperature data.

I used multivariate modeling in program R (version 4.2.1; R Core Team, 2022) to determine which environmental variables were the most predictive of winter bat activity. Like Bernard & McCracken (2017) and Mallinger et al. (2023), my dependent variable was nightly bat activity defined as the total number of files with characteristic bat calls per night at each site. Every acoustic-night during the defined hibernation period from Years 4 and 5 at each site was used as the sample unit (n=1148 nights). As compared with Bernard & McCracken (2017), my study included a similar number of sample sites (i.e., hibernacula; n=3), multiple years of data collection, the same methods of estimating bat activity, and overlapping environmental predictor variables. My nightly bat activity data was non-normally distributed (Shapiro-Wilks $W=0.29$, $p<0.001$) and transformations

did not improve normality of data distributions, so I used nonparametric methods. I used base R to scale all predictor variables and standardize values (range=-3 - 3).

I used Spearman correlations from package Hmisc (2022) to test for significant pairwise correlations between each measured environmental variable and nightly bat activity. I selected environmental variables that correlated with bat activity with $\rho \geq |0.3|$ (Bolker et al., 2009; Supplementary Material Appendix B; Table B1). To reduce model complexity, I used only the most highly correlated measurement of each variable category. Using the temperature category as an example, daily average temperature, daily minimum temperature, and daily maximum temperature were all highly correlated with nightly bat activity ($\rho \geq |0.3|$), but daily average temperature was most highly correlated with bat activity ($\rho=0.56$), so daily average temperature was the temperature measurement I used in modeling (Supplementary Material Appendix B; Table B2). For other variable categories with average, maximum, and minimum measurements, the most highly correlated measurement of each category was selected.

Next, I used Spearman correlations to test for relationships between the selected environmental predictor variables (Supplementary Material Appendix B; Figure B1). I identified model sets of uncorrelated predictor variables ($\rho < 0.6$; Supplementary Material Appendix B; Table B2) and generated six *a priori* global models (Supplementary Material Appendix B; Table B3). For each *a priori* model set, I tested generalized linear models (GLM) and generalized linear mixed models (GLMM; package lme4; Bates et al., 2015), first with Poisson distribution, then with negative binomial distribution (penalized quasilikelihood estimation) to account for the overdispersion in my count data

(Supplementary Material Appendix B; Table B4). Within each *a priori* model set, every possible predictor variable combination was tested using additive effects.

Initially, I modeled each site separately using data from Years 4 and 5 combined. I followed this with models combining data from all sites and years, which produced similar results. I proceeded with analyzing data from all caves, and tested cave as a fixed effect (Supplementary Material Appendix B; Table B5). However, I was more interested in uncovering environmental factors driving bat activity with implications across a broader geographic scale over site specific differences, so I used cave as a random intercept effect. A lack of any overlap in atmospheric pressures between Cave 2 and the other two caves (Kruskal-Wallis $H=0.76$, $df=2$, $p<0.001$) also supported using cave as a random effect.

Due to the ratio of samples (n=1148) to parameters (n=4), I used Akaike Information Criterion (AIC) to rank and identify top performing models. To assess goodness of fit of top models, I examined quantile-quantile (q-q) plots, residual versus predicted plots, and nonparametric dispersion histograms using the R package DHARMa (Hartig, 2022). Finally, I evaluated the importance of including cave as a random intercept by calculating standard deviations of the random effect in each top model (Mallinger et al., 2023).

Results

Hibernating Bat Group Size, Species Composition, and Behavior

Between April 2018 and February 2023, we completed 63 internal cave surveys and recorded 727 observations of torpid bats. Bat abundance was greatest at Cave 1 in March 2019 with 85 roosting individuals observed. Cave 1 is a known maternity colony

for *C. townsendii* (M. Moore, pers. comm.). Relatively high bat abundance in March at Cave 1 may be influenced by the maternity colony and were not representative of the relative abundance I observed during hibernation, so hibernation analyses included only November through February at each site. Observed hibernating colony sizes ranged from five to 40 individuals. Hibernating groups were observed beginning in October, and they gradually increased each survey until counts of hibernating bats peaked in January and February, during all years (Figure 3). Maximum observed hibernating group size was 40 individuals in Cave 1 in February 2022. Controlling for survey effort by averaging across all surveys per year, observed hibernating colony sizes were 18.6, 16.3, 25.6 and 26.1 individuals, in Years 1-5 respectively. In Years 1, 2, and 5, hibernating colony sizes varied significantly among caves (Year 1: X^2=66.39, df=2, p<0.001;Year 2: X^2=6.0308, df=2, p=0.049;Year 4: X^2=5.9826, df=2, p=0.05; Year 5: X^2=7.01, df=2, p=0.03). Across all sites, observed hibernating colony sizes varied among years (X^2=61.20, df=3, p<0.001); however, colony size did not change significantly between years at Cave 3 (X^2=0.69, df=3, p=0.87; Figure 3).

The following results present data from Years 4 and 5 only, when survey personnel and internal cave survey protocols remained constant. Between November and February, I collected data from *C. townsendii* (n=153 observations), *E. fuscus* (n=27 observations), *P. hesperus* (n=6 observations), and *Myotis* spp. (n=217 observations), and one observation of a pair of *A. pallidus* roosting together (n=2 observations). Because of similarities in morphology and cryptic roosting locations, some bats could not be distinguished between *P. hesperus* and *Myotis* spp. (*P. hesperus*/*Myotis* spp.) or could not be identified at all (NA). Species compositions differed significantly between Years 4

and 5 at Cave 1 (X^2=46.67, df=5, p<0.001) but did not differ significantly between Years 4 and 5 at Caves 2 or 3 (Cave 2: X^2=3.50, df=4, p=0.48; Cave 3: X^2=3.97, df=4, p=0.41). Species compositions also varied among sites in each year (Year 4: X^2=59.554, df=8, p<0.001; Year 5: X^2=30.95, df=10, p<0.001; Figure 4). See Table 2 for species counts and relative abundance per year across Caves 1-3.

In Years 4 and 5, bats roosted at an average of 2.9 meters above ground, ranging from 0.5 meters to 11.3 meters (Table 3). Average roost height was significantly higher in Cave 3 compared to Caves 1 and 2 (Kruskal-Wallis H=0.062, df=2, $p_{1:3}$= 0.003, $p_{2:3}$<0.001). *C. townsendii* roosted at an average height of 3.16 meters above ground (range 0.53 m-6.60 m), significantly higher than *Myotis* spp. (Kruskal-Wallis H=0.067, df=4, p< 0.001), which roosted at an average of 2.67 meters above ground (range 0.52 m-11.32 m).

Roost positions did not vary significantly between caves (Kruskal-Wallis df=2, p=0.28; Table 3). *C. townsendii* roost position was significantly different from *Myotis* spp.*, E. fuscus,* and *P. hesperus/Myotis* spp. (Kruskal-Wallis H=0.65, df=5, p<0.001). *C. townsendii* roosted fully exposed in 98.7% of observations during hibernation, whereas *Myotis* spp. roosted fully exposed in only 7.3% of observations. Instead, the vast majority (93%) of *Myotis* spp. roosted inside of a cave feature (e.g., crack, cup, etc.) with only part of the body exposed. *P. hesperus* and *E. fuscus* were never observed roosting fully exposed and were always observed partially obscured within cave features. Clustering was observed in only 4.1% of total bat observations, and the largest cluster size was two bats. There were significantly more clusters of bats in Cave 1 than in Caves 2 and 3 (Kruskal-Wallis H=0.039, df=4, $p_{1:2}$<0.001, $p_{1:3}$=0.008), where eight occurrences of two-

bat clusters were observed. Cluster size was not significantly different between species (p=0.43).

Reconnaissance surveys of additional hibernacula revealed small colonies, ranging from zero to 22 individuals between November and February (Figure 5). At Caves 8 and 10, colonies up to 22 were observed in November, but repeated surveys in January revealed zero bats utilizing either cave as hibernacula. Despite all November observations being within the defined hibernation period, it is possible these observations may not be indicative of the hibernating colony at those sites as all bats were gone in January. Species found in Caves 8 and 10 included *C. townsendii* (n=5)*, E. fuscus* (n=1), and *Myotis* spp. (n=39), with no clustering activity observed.

Torpid Body Temperature and Tendency to Arouse

In Years 4 and 5, I thermally imaged bats on 426 occasions between November and February. Across all occasions, 0.9% of bats imaged in Year 4 and 1% of bats imaged in Year 5 showed surface body temperatures (T_{sk}) >2ºC above ambient at the time of initial observation. Across both years, T_{sk} ranged from 1ºC to 22ºC in Cave 1, -2.5ºC to 29.9ºC in Cave 2, and 0ºC to 12ºC in Cave 3 (Table 4).

On 173 occasions, I collected repeated thermal images of roosting bats. Repeated thermal imaging spanned up to 360 minutes after the time of the initial image, with an average maximum range between first and last images of 209.9 minutes. During 11% of repeated imaging occasions, bats raised their body temperatures 1-2ºC between the first image and the last image, but only one bat increased its T_{sk} to normothermic temperatures over the course of a survey. Of note, at Cave 2 in November 2022, one *C. townsendii*, for which I collected repeated images, unfurled its ears, then refurled them, all while

maintaining T_{sk} ~9ºC. Additionally, across both years and all sites, above-ground bat activity never increased significantly the night following an internal survey, according to my acoustic data.

Microclimate Selection

In Years 4 and 5, temperature, relative humidity, absolute humidity, and water vapor pressure deficit (WVPD) varied significantly among caves (Kruskal-Wallis: temperature: H=0.73, df=2, p<0.001; relative humidity: H=0.23, df=2; absolute humidity: H=0.44, df=2, p<0.001; WVPD: H=0.60, df=2, p<0.001; Table 5). Cave 1 was the warmest, most humid site, and exhibited the highest WVPD. Cave 2 was the coldest, driest site, and had the lowest WVPD. Cave 3 was intermediate in temperature, humidity, and WVPD. Although there were significant differences across sites, there was some overlap in cave conditions between sites. Overall, caves provided a buffer from external condition extremes and variability (Figure 6), but internal cave conditions did vary significantly throughout the winter (Kruskal-Wallis p<0.01; Supplementary Material Appendix A; Figure A1) and between years (Kruskal-Wallis: temperature: H=0.022, df=2, p<0.001; relative humidity: H=0.15, df=2, p<0.001; absolute humidity: H=0.032, df=2, p<0.001; WVPD: H=0.14, df=2, p<0.001). Specifically, compared to Year 4, caves in Year 5 were colder (Year 4 average temperature=5.56ºC; Year 5 average temperature=4.35ºC) and more humid (Year 4 average absolute humidity=3.79 g/ml; Year 5 average absolute humidity=4.27 g/ml).

Across all three caves in Year 5, bats generally roosted in cold and dry locations during hibernation (Table 5). Bats roosted between -0.2ºC and 12.1ºC, 39.6% and 75.9% relative humidity, 2.68 g/ml and 5.59 g/ml absolute humidity, and 0.16 kPa and 0.78 kPa

WVPD. I performed microclimate analysis only on Year 5 data and found that bat roost condition distributions for all measured variables were significantly different from the distributions of conditions available within caves when all sites were considered together (Fligner-Killeen df=1, $p<0.05$). In other words, bats roosted within a relatively narrow subset of available conditions, avoiding the highest and lowest temperatures and humidities (Figure 7). At each cave, when comparing bat roost conditions to cave conditions from 24 hours prior to each survey, distributions were significantly different for all measured variables, for every survey (Kolmogorov-Smirnov df=1, $p<0.05$), except for WVPD at Cave 1 in January (Kolmogorov-Smirnov D=0.19, df=1, p=0.29) and temperature at Cave 3 in January (Kolmogorov-Smirnov D=0.16, df=1, p=0.40).

In Year 5, there were no interspecific differences in roost temperature (Kruskal-Wallis df=4, p=0.23), relative humidity (Kruskal-Wallis df=4, p=0.96), absolute humidity (Kruskal-Wallis df=4, p=0.27), or WVPD (Kruskal-Wallis df=4, p=0.59). Although roost conditions did not differ significantly between *C. townsendii* and *Myotis* spp. (*C. townsendii* n=42 observations; *Myotis* spp. n=93 obs.) at any individual site, there were intraspecific differences in roost conditions between sites. Roost temperatures were significantly different between sites for *C. townsendii* and *Myotis* spp. (*C. townsendii*: Kruskal-Wallis H=0.70, df=2, $p_{1:2}<0.001$, $p_{1:3}=0.008$, $p_{2:3}<0.001$; *Myotis spp.*: Kruskal-Wallis H=0.69, df=2, $p_{1:2}<0.001$, $p_{1:3}<0.001$, $p_{2:3}<0.001$) where they utilized a narrower range of temperatures between -0.5ºC and 4.4ºC in Cave 2 and were more dispersed across temperatures between 2.1ºC and 12.1ºC in Caves 1 and 3. *Myotis* spp. roosted in significantly higher absolute humidity in Cave 1 than in Caves 2 and 3 (Kruskal-Wallis H=0.27, df=2, $p_{1:2}<0.01$, $p_{1:3}<0.01$, $p_{2:3}=0.394$); however, *C. townsendii* roost absolute

humidity did not vary significantly between caves (Kruskal-Wallis H=0.096, df=2, $p_{1:2}$=0.0924, $p_{1:3}$=0.0924, $p_{2:3}$=0.888). Both *C. townsendii* and *Myotis* spp. roosted at low WVPDs in Cave 2 (0.20 kPa – 0.28 kPa) compared to Caves 1 and 3, where they roosted between 0.22 kPa and 0.78 kPa (*C. townsendii*: Kruskal-Wallis H=0.64, df=2, $p_{1:2}$<0.01, $p_{1:3}$=0.179, $p_{2:3}$<0.01; *Myotis spp.*: Kruskal-Wallis H=0.54, df=2, $p_{1:2}$<0.01, $p_{1:3}$=0.028, $p_{2:3}$<0.01; Figure 8).

C. townsendii and *Myotis* spp. roost temperatures also differed intraspecifically between Years 4 and 5 (Kruskal-Wallis *C. townsendii*: H=0.097, df=1, p<0.001; *Myotis* spp.: H=0.027, df=1, p=0.02). *C. townsendii* roost sites were 1.76ºC colder in Year 5 compared to Year 4, roosting at an average of 4.05ºC, and *Myotis spp.* roost sites were 0.96ºC warmer in Year 5 compared to Year 4, roosting at an average of 4.91ºC. All other species' roost conditions did not vary between years (Kruskal-Wallis df=1, p>0.05).

Hibernation Length and Winter Activity

In Years 4 and 5 across all three sites, I collected a total of 583 recorder-nights of acoustic data and 565 recorder-nights of acoustic data, respectively. I detected thirteen species and species groups (i.e., 40 kHz *Myotis*) across sites in both years (Supplementary Material Appendix A; Table A2). Acoustic monitoring revealed significant seasonality in species detections (Supplementary Material Appendix A; Figure A2). The most active species group across all sites was 40 kHz *Myotis*, followed by 50 kHz *Myotis*, *C. townsendii*, *E. fuscus*, and *P. hesperus*.

Hibernation length was consistent across years (Table 6). Hibernation generally began in early November, and lasted through early March to early April, although this varied between sites (Figure 9). Hibernation was estimated to last between 117 and 152

days in Year 4, and between 104 and 166 days in Year 5. Hibernation lasted longer than predicted by temperature data, following methods from Humphries et al. (2002), at Caves 1 and 3 but lasted about as long as predicted at Cave 2 (Table 6). At Caves 2 and 3, species-specific hibernation lengths could be estimated. The 40 kHz *Myotis* group had the shortest overall hibernation period (Cave 2: 132 days (Year 4), 164 days (Year 5); Cave 3: 79 days (Year 4), 116 days (Year 5)). *C. townsendii* had the longest hibernation periods (Cave 2: 171 days (Year 4), 172 days (Year 5); Cave 3: 106 days (Year 4), 123 days (Year 5)) followed by the 50 kHz *Myotis* group (Cave 2: 157 days (Year 4), 168 days (Year 5); Cave 3: 115 days (Year 4), 125 days (Year 5)).

Winter bat activity varied significantly across sites (Kruskal-Wallis H=0.42, df=2, $p<0.01$) in both Years 4 and 5. Winter activity was greatest at Cave 1 [Percent of hibernation nights with activity (Year 4: 91%; Year 5: 95%)], lowest at Cave 2 (Year 4: 50%; Year 5: 33%), and relatively moderate at Cave 3 (Year 4: 80%; Year 5: 83%). Across all three caves in both Years 4 and 5, the 40 kHz *Myotis* group was the most active during hibernation with an average of 76 active nights (range 48-113) in Year 4 and 72 active nights (range 34-100) in Year 5 across all caves. In one instance, 40 kHz *Myotis* activity was recorded at temperatures as low as -12.3ºC, an almost identical observation as that of Bernard and McCracken (2017). *C. townsendii* was active on 37 nights, on average, during hibernation in both years (Year 4 range: 2-70; Year 5 range: 5-64). The 50 kHz *Myotis* group showed an average of 25 and 35 active nights (Year 4 range: 1-39; Year 5 range: 2-61) respectively and *E. fuscus* showed an average of 21 and 23 active nights (Year 4 range: 17-26; Year 5 range: 7-46) respectively. *P. hesperus* was

active only on 13 and 9 active nights, on average, in Years 4 and 5, respectively (Year 4 range: 0-39; Year 5 range: 0-26).

A priori model testing followed by model selection using AIC indicated that models including daily average external temperature, daily average pressure, daily maximum wind speed, and daily minimum cave internal temperature performed best (Table 7). These four predictor variables were included in top models across all modeling efforts (Supplementary Material Appendix B; Table B6-8). A negative binomial distribution had a better fit to my data compared with the Poisson distribution (Supplementary Material Appendix B; Figure B2-9). Cave as a random intercept had no significant impact on models (standard deviation<0.001), so I ultimately selected the generalized linear model (GLM) with a negative binomial distribution as the best fitting model.

Like Bernard and McCracken (2017), ambient temperature showed a strong, positive relationship with winter bat activity (Estimate ± SE: 1.02± 0.08; Figure 10; Table 8). Atmospheric pressure also showed a strong positive relationship with winter bat activity (Estimate ± SE: 1.10 ± 0.09; Figure 10; Table 8). Maximum daily wind speed correlated negatively with winter bat activity (-0.32 ± 0.07; Figure 10, Table 8). Minimum internal temperature was included in the top model; however, it did not show a significant relationship with winter activity (-0.07 ± 0.09; Figure 10, Table 8).

Discussion

Mine is the first study to routinely monitor and study groups of hibernating bats in north-central Arizona. I have generated a baseline dataset on the ecology, physiology, and behavior of bats hibernating in a geographic region that has received very limited

attention, as compared with other areas (e.g., eastern United States) where hibernating bats are more easily observable. My findings shed light on arid-adapted bat hibernation ecology, behavior, and physiology, and on the potential of white-nose syndrome (WNS) to develop in Arizona bats.

Bat Hibernation in Arizona

Hibernation in north-central AZ is characterized by small colonies of less than 40 individuals that peak in abundance in either January or February. Bats are dispersed throughout each cave system with very little to no clustering activity apparent. This contrasts populations in other parts of North America and in other parts of the Southwest (i.e., New Mexico) where several hundred individuals may cluster together (e.g., Jagnow, 1998). My findings reinforce information showing that bat hibernation ecology varies on the continental-scale (e.g., Hranac et al., 2021) and illuminates differences across a relatively small geographic area, the Southwest.

Corbett et al. (2017) found a similar lack of clustering activity and small colonies in their extensive cave survey project throughout Arizona. All but one of the sites with bats present (n=16) that Corbett et al. (2017) surveyed between January and February exhibited temperatures that overlapped with temperatures observed in hibernacula used in this study. For this reason, similarities in temperature between my study sites and hibernacula found throughout the state are evident. Additionally, small colonies of *C. townsendii* have been observed at similar elevations in the most southern part of Arizona. These hibernacula offer similar ambient temperatures to my study sites (Schmidt, 1995; Tim K. Snow, 1996, 1998). Based on the similarity between the limited number of other investigations and mine, these results may be indicative of bat hibernation throughout

Arizona. But because there are over 2,400 documented caves in Arizona (Arizona Cave Survey, 2017), it is possible these results do not encompass the behaviors of all bats overwintering in Arizona. For example, the hibernacula I monitored were never utilized by *M. velifer*, and had very few observations of *P. hesperus*, *E. fuscus*, and *A. pallidus*. All of these species are known to occur in Arizona throughout winter (Corbett et al., 2017; Hayward, 1961; Pérez et al., 2020), yet very little information regarding their hibernation ecology in Arizona exists, and these results may not capture hibernation tendencies of these species state-wide. I urge managers and researchers to collect more data of these kinds at additional sites throughout the state.

The low tendency of Arizona bats to arouse following disturbance was surprising. After four years of repeated surveys, hibernating colonies in each cave increased in relative abundance, though these increases may be attributed to methodological improvements rather than actual changes in abundance. Using passive acoustic monitoring, I found no significant increase in bat activity on nights following any internal survey. Generally, bat body temperatures increase during interbout arousals from near ambient to normothermic temperatures (~35ºC; but see Bachorec et al., 2021). Repeated thermal imaging of hibernating bats revealed only one bat (0.5% of Year 4 bat observations) that returned to normothermic body temperatures during internal surveys, which lasted up to seven hours with crews of up to six people. This supports the hypothesis that bats hibernating in Arizona have a low tendency to arouse upon non-tactile disturbance. Considering the single *C. townsendii* that unfurled and refurled its ears while maintaining low T_{sk}, the use of "cold arousals" following disturbance should be considered as a strategy employed by bats overwintering in Arizona (Bachorec et al.,

2021). A historical pattern of minimal human disturbance in some Arizona caves and common natural disturbances, such as nesting ravens and javelina activity within hibernacula (Twente, 1955a), may have driven the evolution of hibernation behaviors that consume minimal energy and suffice to cope with limited life-threatening disruptions. Additionally, because bats in Arizona hibernate in caves with low humidity (see "Microclimate Selection" section), reducing water loss may have been a primary driver in bat hibernation behavior in Arizona, and bats may exhibit a lower tendency to disturb to maintain a low arousal frequency. Boyles (2017) suggests that understanding site-specific disturbance regimes of bats will help managers understand the costs and benefits of research on hibernating bat populations. Here, I show that managers may enter Arizona hibernacula without detriment to hibernating colonies if non-tactile and efficient methods are used, although this should be evaluated on a site-specific basis.

Microclimate Selection

My results provide evidence that bats hibernating in Arizona select cold and dry roost sites, even when other conditions are available within the same cave. I observed bats roosting in caves that did not reach 100% relative humidity, though higher humidity sites were available, and bats utilized relatively dry roost sites within hibernacula. I did not observe any hibernating bats in Caves 8-10 which had suitable temperatures (<9.9ºC) and up to 100% relative humidity. But within 10 km of these sites, a significantly less humid cave (Cave 2), supported a stable hibernating bat colony. The selection of Cave 2 by hibernating bats, which is within a feasible travel distance for bats from Caves 8-10 suggests a preference for this location over the more humid sites. Other factors, such as

snowpack preventing winter aboveground activities, increased airflow within caves, among other possibilities, should also be considered as drivers of site selection.

Within caves, bats selected relatively dry roost locations and all bats roosted below 75.9% relative humidity. These roost sites are significantly drier than some roost sites in northeastern North America (e.g., Kurta & Smith, 2014), but have similar conditions to sites in Montana, Nevada, Colorado, Oregon, Utah, and Oklahoma (Haase et al., 2021). Under experimental conditions, arid-adapted bats show lower amounts of EWL than their humid-adapted counterparts when both are exposed to dry conditions (Klüg-Baerwald & Brigham, 2017). So, Arizona bats may express traits that allow them to roost in dry locations without suffering from detrimental EWL throughout hibernation. Additionally, in one species of bat, clustering with conspecifics reduced EWL by 30% (Boratyński et al., 2015), yet none of the bats I observed utilized this strategy. Thus, the selection of dry roost sites and lack of clustering behavior by bats hibernating in Arizona may indicate evolved tolerance to low humidities and ability to select sites based on factors other than high humidities.

When considered in relation to roost temperatures, the potential for evaporative water loss was relatively low in the three hibernacula, despite low humidities. For example, Cave 2 showed low absolute humidities, but roost sites exhibited low potential for EWL due to the cold temperatures resulting in low WVPD. At Caves 1 and 3, the more humid and warmer roost sites showed higher WVPD than at Cave 2, potentially driving more EWL at these sites. Thus, it may be a combination of roost humidity and temperature that acts as a driving force for roost site selection.

I observed bats exhibiting a preference for cold roost sites, while actively avoiding exposure to the most extreme cold temperatures. Bats roosted at temperatures between -0.2ºC and 12.1ºC, which are equivalent to roost temperatures observed in Colorado, Nevada, Oregon, Utah, Idaho, British Columbia, and Montana (e.g., Haase et al., 2021; Hayes et al., 2011; Gillies et al., 2014; Nagorsen et al., 1993), indicating similarities in roost selection by bats in Arizona and bats that hibernate at higher latitudes.

Optimal hibernation theory suggests that bats will choose to roost as close to the minimum available temperature (T_{min}) as possible to maximally reduce energy expenditure throughout hibernation (Boyles et al., 2020). But this constraint to roost near T_{min} varies based on how much energy is available, either stored as fat or available throughout winter (i.e., insects; Boyles et al., 2020). At Cave 2, the coldest site in my study both internally and externally, bats roosted at the lowest recorded roost temperatures. These bats may be so constrained by a harsh winter (extended periods of low temperatures), lack of available food, or duration of winter (see "Hibernation Length and Winter Activity" below) that they adaptively select the coldest possible roost locations. Bats as Caves 1 and 3 roosted at warmer temperatures and appeared to stray further from T_{min}, while still avoiding the warmest temperatures. Less extreme conditions, shorter duration of winter and potentially more available food (see "Hibernation Length and Winter Activity" below) at Caves 1 and 3 may allow more flexibility in roost temperature selection.

I observed a lack of interspecific variation in microclimate preferences between the two main species groups, *C. townsendii* and *Myotis* spp. These results may indicate

similar adaptations to arid hibernacula with suitably cold temperatures among species. I also observed intraspecific differences in roost selection between sites, which indicates that there is flexibility in hibernation strategies within species groups (e.g., Auteri, 2022; Klüg-Baerwald & Brigham, 2017). It is possible that a narrow range of condition utilization by roosting bats could be a function of small colonies, which couldn't physically be dispersed across a wider range of available cave conditions, biasing selection tendencies. Yet, because patterns persisted across caves, I suspect that the utilization of observed conditions may instead indicate microclimate selection tendencies. Exploring and quantifying the specific adaptations that enable Arizona bats to thrive in dry hibernacula could reveal underlying mechanisms with relevance to climate change and pathogen invasion through the skin.

Hibernation Length and Winter Activity

According to my estimates, hibernation lasted between 104 and 162 days across the three north-central Arizona hibernacula and varied along an elevational gradient. Variation across sites illuminated the different energetic costs of hibernation for bats within a relatively small geographic area that has diverse topography. Compared to modeling efforts (Hranac et al., 2021) and common methods to estimate hibernation length from climatic data (e.g., Humphries et al., 2002), hibernation in north-central Arizona is longer than expected at similar latitudes (e.g., Brack Jr. & Twente, 1985, Hayman et al., 2017). Hibernation lasted as long as in some areas of Nevada, Colorado, and Utah (Haase et al., 2021), and this likely places a considerable energetic strain on hibernating bats in Arizona.

I observed high levels of winter activity, specifically at the two lower elevation caves. Activity outside of hibernacula can be common in winter (e.g., Boyles et al., 2006; Bradley & O'Farrell, 1969; O'Farrell & Bradley, 1970). The use of deep torpor in combination with high levels of winter activity indicates that north-central Arizona bats may be considered winter "resistors" versus true hibernators (Auteri, 2022), but not at all sites (i.e., elevations) included in this study. Even in small geographic areas, researchers and managers should consider that significant differences in hibernation traits may exist on an elevational gradient. Modeling efforts revealed increased winter activity associated with warmer internal and external temperatures, low wind speeds, and higher pressures. In Nevada, O'Farrell and Bradley (1970) directly observed an increase in bat activity at warmer winter temperatures and during lower wind speeds. Similar to findings in Meyer et al. (2016) and Bernard and McCracken (2017), bat activity in my study was more strongly correlated with external temperatures than internal cave temperatures, potentially because air flow throughout cave systems can change based on external conditions, though with smaller magnitudes of change, and alert bats through atmospheric stimuli (Boratyński et al., 2015).

Some studies show that bats may feed during winter on warmer nights (Bernard et al., 2021; Hope & Jones, 2012; O'Farrell & Bradley, 1970; Speakman & Thomas 2003) and this may replenish fat stores (Boyles et al., 2020). In this study, bat activity increased above the threshold average temperature of 0ºC. High levels of winter activity at the two lower elevation sites (Caves 1 and 3) could indicate a foraging potential if insects were available (Bernard et al., 2021) which could allow bats at these lower-elevation sites to intermittently gain energy and withstand energetic constraints that hibernation presents.

In contrast, lower temperatures at Cave 2 may limit insect activity throughout winter. Without the ability to replenish fat stores, bats in Cave 2 may face the greatest hibernation-induced energetic strains across the three sites. Bats at Cave 2 showed the narrowest range of roost temperatures and roosted very close to the minimum temperature (T_{min}), which should reduce energy expenditures (Boyles et al., 2020). This pattern may be adaptive at Cave 2 since external temperatures may be too low to allow foraging opportunities needed to replenished fat. Because there may be an opportunity to feed and replenish fat stores, bats at Caves 1 and 3 may have more flexibility in their roost temperature selection, allowing them to stray further from T_{min} than bats at Cave 2, a pattern we observed at these two sites. Research to measure winter insect availability in the Southwest (Bernard et al., 2021) and winter feeding-specific activities is needed to understand the role insect availability plays on winter activity and other hibernation traits, such as roost temperature selections (Klüg-Baerwald et al., 2022).

Winter activity may be the result of bats arousing and relocating between hibernacula, which has been observed in some species of hibernating bats (e.g., Twente, 1955b). This pattern has been noted specifically in *C. townsendii* (e.g., Genter, 1986). Because colony sizes varied between each survey, it is likely that bats move within and possibly between hibernacula during winter, and this may account for some of the observed above-ground activity in winter.

Due to the aridity of my study area, evaporative water loss may also be a driving force for winter activity. Bats have higher total evaporative water loss (EWL) in drier conditions (Ben-Hamo et al., 2013), so it is adaptive for bats to roost in areas with low water vapor pressure deficit to reduce water loss and arousal frequency. At Cave 2 bats

selected roost sites with lower WVPD and the very low levels of winter activity at this site may be attributed to low rates of EWL and fewer arousals to replenish body water. In contrast, WVPD was higher at roosts in Caves 1 and 3, which increased the potential for EWL from the bats utilizing these locations. Higher levels of activity at Caves 1 and 3 may be attributed to roost sites with higher WVPD, higher rates of EWL, and necessarily more frequent arousals from torpor to drink water (Ben-Hamo et al., 2013; Klüg-Baerwald et al., 2022).

Across all sites, I observed interspecific differences in winter activity levels. It is possible that I captured fewer *C. townsendii* calls than *Myotis* spp. calls due increased attenuation of *C. townsendii* calls (Fenton, 1982), but the proximity of ARUs to cave entrances should have increased my ability to capture most calls. Therefore, I assume that the observed activity levels are indicative of actual relative activity levels. I found significantly more activity in *Myotis* spp. than in the larger-bodied species. Higher surface area to volume ratios seen in smaller-bodied bats leads to higher rates of EWL as compared with larger-bodied species (Conenna et al., 2021). *Myotis* spp. may be more vulnerable to evaporative water loss, forcing them to be more active throughout winter compared to the larger *C. townsendii* and *E. fuscus* to replenish more pronounced losses of body-water. This result indicates that interspecific differences exist in the use of "hibernation" versus "resisting" (Auterri, 2022) potentially due to differing physiologies between species. These findings emphasize the importance of variations in winter activity patterns among bat species, especially across elevational gradients even in small geographic areas.

Arizona Bat Risk to WNS

I observed virtually no clustering behavior across all caves, years, and species. Colonies were small with a maximum observed hibernating colony of 40 individuals. Because clustering activity and colony sizes are correlated with the transmission of *Pd* (Langwig et al., 2012), hibernating bats in Arizona may experience relatively low risk of exposure if *Pd* more substantially enters the state.

Caves 1, 2, and 3 exhibited temperatures that support growth of *Pd* (Blehert et al., 2009; Verant et al., 2012). However, these sites were drier than optimal for *Pd* growth (Marroquin et al., 2017), which could limit fungal mycelial growth. I observed bats tolerating a wide range of conditions but avoiding the coldest and warmest areas within each site. Bats roosted within the range of temperatures where *Pd* growth is possible (3ºC-20ºC; Blehert et al., 2009), but nearly all bats roosted below the *optimal* growth range (12ºC-16ºC; Verant et al., 2012). Bats roosted in relatively dry areas compared to the range of available humidities. Roost humidities observed in my study would not support optimal *Pd* mycelial growth according to Marroquin et al. (2017), which may lessen the spread of *Pd* throughout hibernacula, slow invasion of *Pd* into host tissues, and increase survival in hibernating bats exposed to the fungus (Haase et al., 2021).

Across the three study sites, hibernation lasted as long as in some areas of Nevada, Colorado, and Utah (Haase et al., 2021), which should be considered when discussing the risk WNS may pose to Arizona bats. Based on experiments on *Myotis lucifugus*, death from WNS can occur starting 85 days after exposure to *Pd* (Warnecke et al., 2012). If Arizona bats are exposed to *Pd* upon entering hibernacula, there may exist

an elevated risk of death from WNS as hibernation lasted between 104 and 162 days across all three sites during my study period.

Active WNS infections are correlated with higher arousal frequency and higher EWL (Reeder et al., 2012; Warnecke et al., 2012). If affected by WNS, bats hibernating in Arizona may have differing risks towards more frequent arousals and rates of EWL depending on the elevation at which they overwinter. If bats roosting at lower elevation sites are already adapted to arouse frequently to forage or replenish water, they may not be affected by even more frequent arousals caused by a WNS infection if bats are indeed foraging while active in winter (see "Hibernation Length and Winter Activity" section). But bats roosting at the higher elevations may be so energetically constrained, increased arousals caused by *Pd* may pose a significant risk of fat depletion and an increased risk of death from WNS. Additionally, as bats lose fat reserves, they trend toward utilizing colder microclimates, in general (Boyles et al., 2007). Bats at Cave 2, which may already be roosting at their energetic minimum, would have little ability to choose colder temperatures for energy savings upon infection by *Pd*. In contrast, bats at Caves 1 and 3 are not roosting at T_{min} or the highest humidities so they may be able to adjust roost locations and select colder and more humid sites, expend less energy, and potentially survive longer compared with bats at Cave 2. Thus, it is important to consider that different risks may be presented in a relatively small geographic area where there are considerable changes in elevation.

This study reveals that bats hibernating in Arizona have a low tendency to arouse upon non-tactile disturbance. Therefore, it may be possible for additional research aimed at addressing the risk of WNS to AZ bats to occur without negative effects on these

hibernating colonies. Yet, I caution that the tendency for bats to arouse should be monitored and studies should adapt accordingly.

Bats hibernating in Arizona exhibit a suite of traits suggesting a mix of protective factors that may lessen spread of *Pd* and severity of WNS combined with risk factors that may increase WNS impacts in these populations. Specifically, the selection of roost sites within possible *Pd* growth temperatures may provide adequate conditions for *Pd* proliferation. Long hibernation lengths may pose significant risks of death from WNS if bats are infected upon entering hibernation. Yet, small colonies, a lack of clustering activity, selection of dry roost sites, and a natural tendency for winter activity to either feed, drink, or relocate, may indicate Arizona bats are at low risk of being impacted by WNS. All factors considered, bats hibernating in AZ may have some behavioral and ecological advantages compared to other populations of bats that have been highly affected by WNS.

WNS is a complex disease, and these variables and others might have different effects on the virulence of *Pd* in Arizona compared to other regions of North America that are highly affected by WNS. Predicting the impacts of WNS lacks a straightforward and definitive approach, and inherent uncertainty exists about how WNS will play out in Arizona. Specifically, the species included in my study are different than the species most thoroughly studied in the context of WNS, for example, and most experimental studies are based on *M. lucifugus*. Not all species respond to WNS in the same way (Cheng et al., 2021; Frank et al., 2014; Moore et al., 2018), so results from other species and *M. lucifugus* experimental studies may not be applicable to the species hibernating in Arizona. Additionally, there are large knowledge gaps surrounding the physiology of bats

hibernating in Arizona, like how much fat bats in Arizona put on in the fall, if bats are foraging during winter, or the natural arousal frequency of individuals during hibernation. These knowledge gaps, among others, make it difficult to accurately predict the outcome for bats hibernating in Arizona if *Pd* becomes more prevalent in the state. My baseline dataset of colony sizes, species composition, and behavior throughout winter can be used as a point of comparison for managers in the future to understand if bats hibernating in Arizona are being impacted by WNS. Continual monitoring and research on Arizona bat populations should be prioritized to determine how my findings generalize to the broader geographic scale and to detect and respond to potential changes in abundance and/or behaviors.

Management Implications

I found bats roosting in caves with temperatures between -9.5ºC and 14.0ºC with an average of 4.3ºC. Relative humidities ranged from 22.4% and 90.8%, with an average of 63.3%. These observed values can guide managers when they are seeking out additional bat hibernacula in the state. Because cave conditions are relatively stable (Tuttle & Stevenson, 1978), managers could visit additional sites in October to November, before bats are in deep torpor, to assess the quality of hibernacula, reducing disturbance to hibernating colonies. When potentially suitable sites are found, they could be resurveyed between November and February, when I found bats hibernating in all sites. Managers should conduct internal surveys before the end of February if estimating hibernating colony sizes and behaviors are the goal, since emergence can begin in March. I found bats roosting in a range of positions, from fully exposed to almost completely obscured within cave features (e.g., only the tip of an ear exposed). Bats roosted between

0.5 meters and 11.3 meters from the cave floor, and in preliminary years, bats were observed nearly lying on the floor while in torpor (M.S. Moore, pers. comm.). I encourage anyone conducting internal surveys in Arizona to survey areas of caves where they would not normally expect to find roosting bats (i.e., in small cave features, near the ground, behind boulders).

If bats are exposed to *Pd* upon entering Arizona hibernacula, managers should monitor bats toward the end of January for signs and symptoms of WNS, as that would be ~85 days after exposure (Langwig et al., 2012; Lorch et al., 2011; Reeder et al., 2012). This would also be the appropriate time to swab bats and cave features for presence of *Pd*. To swab bats for *Pd* during winter or as bats begin to emerge from hibernation, managers should target their netting efforts to nights when average temperatures are above 0ºC in mid- to late March, above the threshold temperature at which I observed higher levels of bat activity. Here, I generated a foundational dataset that includes colony sizes and activity levels during winter. Managers can employ this dataset as a reference point to measure alterations in colony sizes or behaviors, providing a method to evaluate the impact or presence of WNS and other stressors.

Additional Research

The power of my study comes from systematic, repeated surveys at cave sites to characterize hibernation traits within and between years. My results are potentially indicative of behaviors and traits in other groups of hibernating bats statewide, but one limitation of this study is the relatively few caves sampled given the total number across the state. Additional research that focuses on systematically monitoring additional sites across AZ will provide further evidence to support my findings or illuminate behavioral

and ecological differences across a larger geographic area. Additionally, expanding this research to include more sites on a wider elevational gradient could provide further insight on the role of elevation in both hibernation length and winter activity.

My study also did not directly measure the physiology of bats hibernating in AZ. Additional research to quantify total evaporative water loss, torpor bout lengths, and energy consumption during hibernation may provide insights into the microclimate selection and winter activity levels that I observed. This research would bolster the general understanding of bat hibernation ecology in arid environments, and could provide a deeper understanding of the risk WNS, climate change, and habitat loss may pose to bats hibernating in AZ.

Additional research using radio-tracked individual bats before, during, and after hibernation should also be considered. This may help researchers identify additional hibernacula across the 2,400 documented caves in the state (Arizona Cave Survey, 2017), and could provide insights into individual movements between and within hibernacula during hibernation. This would further our understating of what factors may be influencing high levels of winter bat activity across the state.

Conclusion

This study presents a first dataset of hibernation traits for bats overwintering in Arizona, shedding light on the physiological adaptations and behaviors utilized by arid-adapted bats during winter. Based on the low disturbance rates I observed in hibernating bats and the use of passive methods (i.e., no direct handling) the results of my study accurately reflect the natural behaviors of Arizona bats during hibernation. Additionally, given that this study spanned multiple years, I was able to document the behavior,

ecology, and physiology of bats over time, encompassing years with varying levels of winter severity. Even with large variations in winter conditions, my results are consistent across years, providing further evidence that the data I collected was representative of the natural behavior of Arizona bats during winter. My study provides a baseline that wildlife managers and researchers can use as a reference point if WNS enters these systems or other stressors, like climate change and habitat modification, affect bat population stability in Arizona.

TABLES

Table 1. Groups of possible north-central Arizona bat species used for acoustic analyses. 50 kHz Myotis and 40 kHz Myotis groups were always grouped due to similarities in calls. All other species were identified to the species level when possible or grouped into high-frequency or low-frequency when necessary.

Acoustic Group	kHz Range	Species	Always grouped or attempted to ID to species
50 kHz *Myotis*	>~48kHz	*Myotis yumanensis* *Myotis californicus*	Always grouped
40 kHz *Myotis*	~40-48 kHz	*Myotis volans* *Myotis ciliolabrum* *Myotis velifer* *Myotis occultus/lucifugus* *Myotis auriculus*	Always grouped
High-frequency	>~40	*Parastrellus hesperus* *Lasiurus blossevillii*	Attempted to ID to species
Low-frequency	<~40	*Myotis evotis* *Lasiurus xanthinus* *Eptesicus fuscus* *Antrozous pallidus* *Lasionycteris noctivagans* *Corynorhinus townsendii* *Myotis thysanodes* *Tadarida Brasiliensis* *Lasiurus cinereus* *Nyctinimops macrotus* *Idionycteris phyllotis* *Eumops perotis* *Euderma maculatum*	Attempted to ID to species

Table 2. Total bat observations and percent composition across Caves 1-3, by species and year for internal cave surveys conducted between November and February in 2018-2023. **n**=the number of bats observed during hibernation per year, **percent**=the percent each species made up total observations per year, **yearly total**=total number of bat observations during hibernation per year. Species codes are as follows: ANPA=*Antrozous pallidus*; COTO=*Corynorhinus townsendii*; EPFU=*Eptesicus fuscus*; MY=*Myotis* spp.; PAHE=*P. hesperus*; PAHE/MY=undistinguished between *Parastrellus hesperus* and *Myotis* spp.; NA=unidentified.

	ANPA		COTO		EPFU		MY		PAHE		PAHE/MY		NA		Yearly Total
Year	n	Percent	n	Percent	n	Percent	n	Percent	n	Percent	n	Percent	n	Percent	n
2018-19	-	-	27	29.0%	4	4.3%	47	50.5%	7	7.5%	-	-	8	8.6%	93
2019-20	-	-	83	42.6%	3	1.5%	12	6.2%	6	3.1%	75	38.5%	16	8.2%	195
2021-22	-	-	94	40.9%	7	3.0%	105	45.7%	5	2.2%	18	7.8%	1	0.4%	230
2022-23	2	1.0%	59	28.2%	20	9.6%	112	53.6%	1	0.5%	11	5.3%	4	1.9%	209

Table 3. Roost height from floor, roost position, and cluster size measured at hibernating bat roost sites between November and February in Years 4 and 5. Variables are grouped by species or by cave. **n**=number of observed bats. Roost height from floor is measured in meters. Roost position was measured on a binned scale from 1-4: 1=fully exposed bat; 2=bat partially concealed in a cave feature (i.e., crack, cup, etc.) with >50% of the bat exposed; 3=bat was exposed <50%; 4=less than 10% of the bat was exposed (i.e., only an ear was visible). Cluster size was defined as the number of bats directly touching each other. Species codes are as follows: COTO=*Corynorhinus townsendii*; EPFU=*Eptesicus fuscus*; MY=*Myotis* spp.; PAHE/MY=undistinguished between *Parastrellus hesperus* and *Myotis* spp.; PAHE=*P. hesperus*.

Variable	Group	n	Mean	SD	Median	Min	Max	Range	SE
Roost Height (m)									
	COTO	152	3.09	1.18	3.02	0.53	6.6	6.06	0.1
	EPFU	27	2.8	1.13	2.61	1.17	6.15	4.98	0.22
	MY	216	2.63	1.3	2.55	0.52	11.32	10.8	0.09
	PAHE/MY	27	3.32	1.41	3.19	0.89	6.1	5.21	0.27
	PAHE	6	2.42	0.6	2.32	1.7	3.43	1.73	0.24
Roost Position									
	COTO	153	1.02	0.18	1	1	3	2	0.01
	EPFU	27	2.63	0.79	3	1	4	3	0.15
	MY	217	2.8	0.85	3	1	4	3	0.06
	PAHE/MY	27	3.37	0.79	4	2	4	2	0.15
	PAHE	6	2.67	0.52	3	2	3	1	0.21
Cluster Size									
	COTO	153	1.05	0.22	1	1	2	1	0.02
	EPFU	27	1.07	0.27	1	1	2	1	0.05
	MY	217	1.02	0.15	1	1	2	1	0.01
	PAHE/MY	27	1.04	0.19	1	1	2	1	0.04
	PAHE	6	1	0	1	1	1	0	0
Roost Height (m)									
	Cave 1	154	2.55	0.92	2.76	0.53	4.45	3.91	0.07
	Cave 2	146	2.47	0.67	2.55	0.52	3.95	3.43	0.06
	Cave 3	137	3.57	1.72	3.35	0.63	11.32	10.69	0.15
Roost Position									
	Cave 1	154	2.17	1.11	2	1	4	3	0.09
	Cave 2	146	2.24	1.13	2	1	4	3	0.09
	Cave 3	137	2.26	1.12	2	1	4	3	0.1
Cluster Size									
	Cave 1	154	1.1	0.31	1	1	2	1	0.02
	Cave 2	146	1	0	1	1	1	0	0
	Cave 3	137	1.01	0.12	1	1	2	1	0.01

Table 4. Minimum, maximum, and average bat body surface temperature per survey at each cave in Years 4 (2021-2022) and 5 (2022-2023). Species-specific differences were not evaluated.

			Bat Body Temperature		
Year	Cave	Month	Min	Max	Average
2021-22					
	Cave 1	November	9	18.4	11.8
		January	2.5	12.5	7.6
		February	2.5	12.5	5.6
	Cave 2	November	3.5	29.9	5.7
		January	0.5	3.8	1.8
		February	-2.5	3.5	-0.06
	Cave 3	November	8.2	11.2	9.9
		January	2.5	8.3	4
		February	0	10	2.8
2022-23					
	Cave 1	November	9	22	12.3
		January	1	10.5	4.6
		February	1.5	11	5.5
	Cave 2	November	0	9	3.8
		February	-2	2.5	-0.66
	Cave 3	November	4	12	7.12
		January	0	5.5	2.2
		February	1.5	11.5	4.5

Table 5. Temperature, relative humidity, absolute humidity, and water vapor pressure deficit measured by HOBO loggers at roosting bats within caves or by internal and external stationary HOBO loggers externally in January and February of Year 5.

		Temp (ºC)					Relative Humidity (%)					Absolute Humidity (g/m3)					Water Vapor Pressure Deficit (kPa)				
Group	n	Mean	Median	Min	Max	SD	Mean	Median	Min	Max	SD	Mean	Median	Min	Max	SD	Mean	Median	Min	Max	SD
Bat Roost (all species combined)		4.7	4.9	-0.2	12.1	2.8	59.6	60.0	39.6	75.9	8.8	4.0	4.1	2.6	6.3	0.8	0.4	0.4	0.2	0.8	0.1
Corynorhinus townsendii	42	4.1	4.4	-0.1	9.9	2.5	59.2	63.1	42.6	75.9	9.3	3.8	3.7	2.7	5.1	0.6	0.3	0.3	0.2	0.7	0.1
Myotis spp.	93	4.9	5.3	-0.2	12.1	3.1	58.9	59.6	39.6	74.0	8.9	4.0	4.0	2.6	6.3	0.8	0.4	0.4	0.2	0.8	0.1
Eptesicus fuscus	10	6.0	5.9	4.5	10.0	1.7	59.2	59.4	47.4	65.2	5.1	4.3	4.3	3.2	5.6	0.6	0.4	0.4	0.3	0.5	0.1
Parastrellus hesperus	1	4.3	4.3	4.3	4.3	NA	63.2	63.2	63.2	63.2	NA	4.1	4.1	4.1	4.1	NA	0.3	0.3	0.3	0.3	NA
P. hesperus/Myotis spp.	10	5.2	5.4	2.5	6.8	1.5	57.8	58.9	45.3	73.3	9.9	4.0	4.3	2.8	5.2	0.9	0.4	0.4	0.2	0.5	0.1
Internal Conditions (all caves combined)		4.3	3.8	-9.5	14.0	4.7	62.3	62.2	22.4	90.8	12.3	4.2	3.9	1.2	10.4	1.7	0.3	0.3	0.1	0.9	0.2
Cave 1		9.8	10.1	3.4	14.0	2.7	62.7	62.2	33.9	90.8	12.0	6.0	5.6	2.4	10.4	1.8	0.5	0.4	0.1	0.9	0.2
Cave 2		0.1	0.4	-9.5	9.3	2.6	68.1	68.7	27.9	91.7	10.3	3.4	3.4	1.2	5.9	0.9	0.2	0.2	0.1	0.8	0.1
Cave 3		3.6	3.9	-4.1	9.8	2.0	54.2	54.3	22.4	84.9	10.2	3.4	3.4	1.4	6.3	0.9	0.4	0.4	0.1	0.8	0.1
External Conditions (all caves combined)		1.1	0.6	-19.0	23.4	5.6	58.1	58.8	5.3	100.0	24.2	2.9	2.8	0.8	8.8	1.1	0.3	0.2	0.0	2.7	0.3
Cave 1		2.3	1.0	-11.1	23.4	6.8	56.9	55.6	5.3	100.0	27.4	3.0	2.8	0.9	8.8	1.2	0.4	0.3	0.0	2.7	0.5
Cave 2		-2.4	-2.5	-19.0	19.6	6.4	63.8	65.7	10.2	99.0	21.8	2.6	2.5	0.8	5.3	0.9	0.2	0.2	0.0	2.0	0.3
Cave 3		1.5	1.2	-7.0	13.4	3.6	56.7	57.9	11.8	100.0	21.2	3.0	2.9	0.8	6.7	1.1	0.3	0.3	0.0	1.4	0.2

Table 6. Estimated hibernation start and end dates, length of hibernation in days, and estimated hibernation length in days using temperature data only (Humphries et al. 2002) for Years 4 and 5.

Cave	Estimated Hibernation Start Date	Estimated Hibernation End Date	Hibernation Length	Estimated Hibernation Length from Climate Data
Cave 1	11/1/21	3/1/22	120	67
	11/9/22	3/10/23	121	86
Cave 2	10/23/21	3/24/22	152	152
	10/22/22	4/6/23	166	154
Cave 3	11/17/21	3/14/22	117	89
	11/20/22	3/4/23	104	101

Table 7. Akaike Information Criterion (AIC) values for a series of Generalized Linear Models (GLMs) with the response variable "total nightly bat activity" in relation to seven environmental variables (ET=daily average external temperature, IT=daily minimum internal temperature, W=daily maximum wind speed, P=daily average atmospheric pressure, IVPD=daily average internal water vapor pressure deficit (VPD), EVPD=daily average external VPD, and IRH=daily minimum internal relative humidity). K is the number of parameters. AIC is the AIC for each model, *Δ*AIC is the difference between the AIC of the best fitting model and the AIC of that model, AICWt is the weight of each model, Cum.Wt is the cumulative weight of models combined, and LL is the log-likelihood. Coefficients are listed for each variable that was included in each model in Table 8.

	K	AIC	Delta_AIC	AICWt	Cum.Wt	LL
ET + P + W + IT	6	2973.7	0	1	1	-1480.8
ET + P + IT	5	2988.9	15.23	0	1	-1489.5
ET + W + IVPD	5	3047.7	74.06	0	1	-1518.9
ET + W + IT + IVPD	6	3049.4	75.75	0	1	-1518.7
ET + W + IT + IRH	6	3053.6	79.9	0	1	-1520.8
ET + W + IRH	5	3068.6	94.91	0	1	-1529.3
EVPD + P + IT	5	3073.2	99.56	0	1	-1531.6
EVPD + P + W + IT	6	3074.0	100.33	0	1	-1531.0
ET + W + IT	5	3082.8	109.14	0	1	-1536.4
EVPD + W + IT + IRH	6	3179.7	206.06	0	1	-1583.9
EVPD + W + IT + IVPD	6	3182.8	209.08	0	1	-1585.4
EVPD + W + IT	5	3192.9	219.2	0	1	-1591.4
ET + IT + IVPD	5	3215.6	241.92	0	1	-1602.8
ET + IVPD	4	3215.7	242.05	0	1	-1603.9
EVPD + W + IVPD	5	3222.3	248.64	0	1	-1606.2
ET + IT + IRH	5	3232.1	258.39	0	1	-1611.0
ET + IRH	4	3237.2	263.53	0	1	-1614.6
EVPD + W + IRH	5	3249.7	275.98	0	1	-1619.8
ET + IT	4	3273.0	299.34	0	1	-1632.5
EVPD + IT + IVPD	5	3325.4	351.73	0	1	-1657.7
EVPD + IT + IRH	5	3327.1	353.46	0	1	-1658.6
EVPD + IT	4	3345.9	372.17	0	1	-1668.9
EVPD + IVPD	4	3349.8	376.07	0	1	-1670.9
EVPD + IRH	4	3379.1	405.41	0	1	-1685.5
ET + P + W	5	3380.4	406.71	0	1	-1685.2
ET + P	4	3393.3	419.6	0	1	-1692.6
EVPD + P	4	3486.7	513	0	1	-1739.3
EVPD + P + W	5	3488.7	514.99	0	1	-1739.3
P + IT	4	3505.8	532.15	0	1	-1748.9
P + W + IT	5	3505.9	532.22	0	1	-1748.0
ET + W	4	3514.8	541.1	0	1	-1753.4
W + IT + IRH	5	3555.6	581.91	0	1	-1772.8
W + IT + IVPD	5	3565.7	592.01	0	1	-1777.8
W + IT	4	3601.9	628.24	0	1	-1797.0
W + IVPD	4	3632.5	658.83	0	1	-1812.3
EVPD + W	4	3678.1	704.43	0	1	-1835.1
W + IRH	4	3688.9	715.19	0	1	-1840.4
ET	3	3704.0	730.28	0	1	-1849.0
IT + IRH	4	3713.3	739.57	0	1	-1852.6
IT + IVPD	4	3713.7	740.06	0	1	-1852.9
IT	3	3761.6	787.94	0	1	-1877.8
IVPD	3	3763.5	789.85	0	1	-1878.8
EVPD	3	3817.4	843.72	0	1	-1905.7
IRH	3	3823.7	849.97	0	1	-1908.8
P	3	4645.1	1671.39	0	1	-2319.5
P + W	4	4646.9	1673.24	0	1	-2319.5
W	3	4921.4	1947.72	0	1	-2457.7
Intercept	2	5076.1	2102.39	0	1	-2536.0

Table 8. Beta estimates for predictor variables included in the top generalized linear model with a negative binomial distribution (Table 7).

	β Estimate	Std. Error	z value	p-value
(Intercept)	1.52	0.08	20.19	<0.001
Daily Average External Temperature	1.02	0.08	12.85	<0.001
Daily Average Pressure	1.10	0.09	11.86	<0.001
Daily Maximum Wind Speed	-0.32	0.07	-4.65	<0.001
Daily Minimum Internal Cave Temperature	0.07	0.09	0.76	0.45

FIGURES

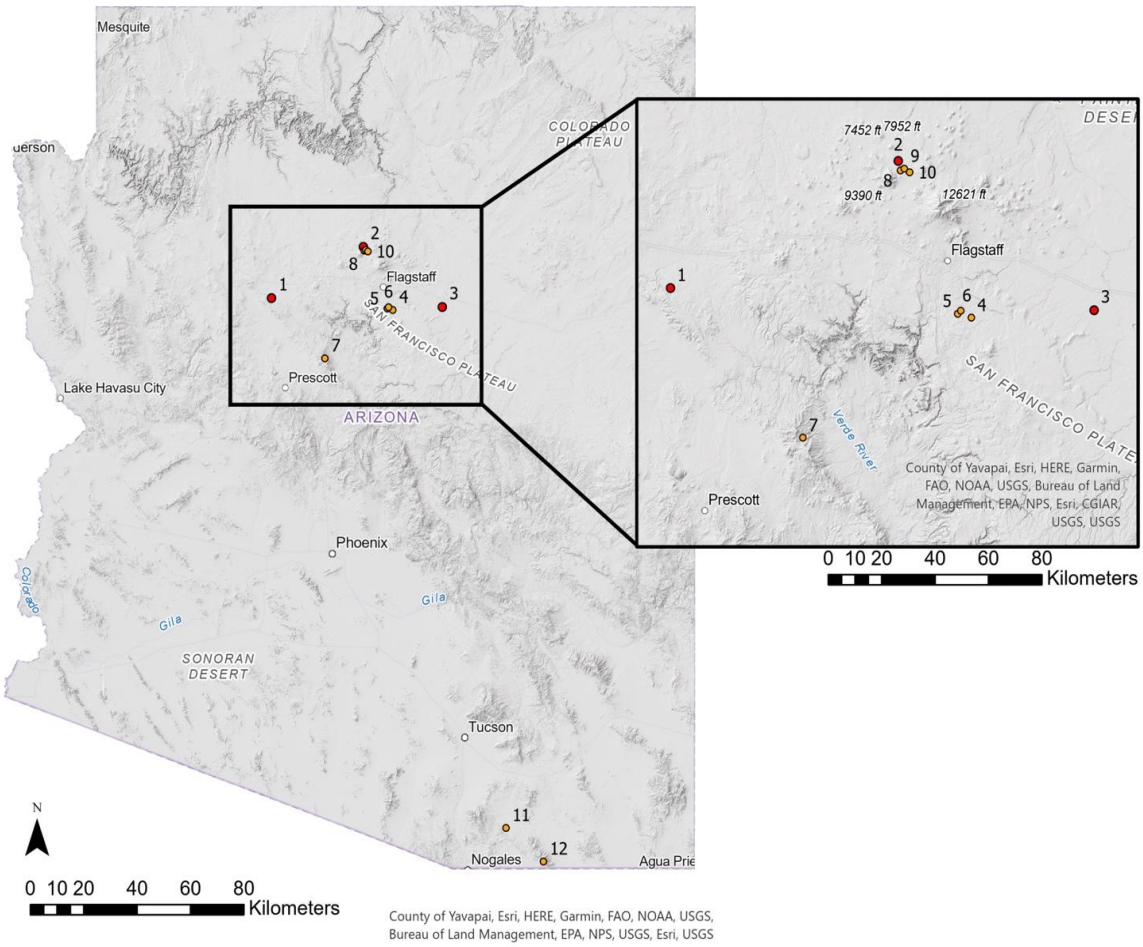

Figure 1. Locations of study sites across the state of Arizona. Red markers indicate primary study caves (Caves 1-3). Orange markers indicate caves where opportunistic surveys were conducted in Years 4 and 5 (Caves 4-12).

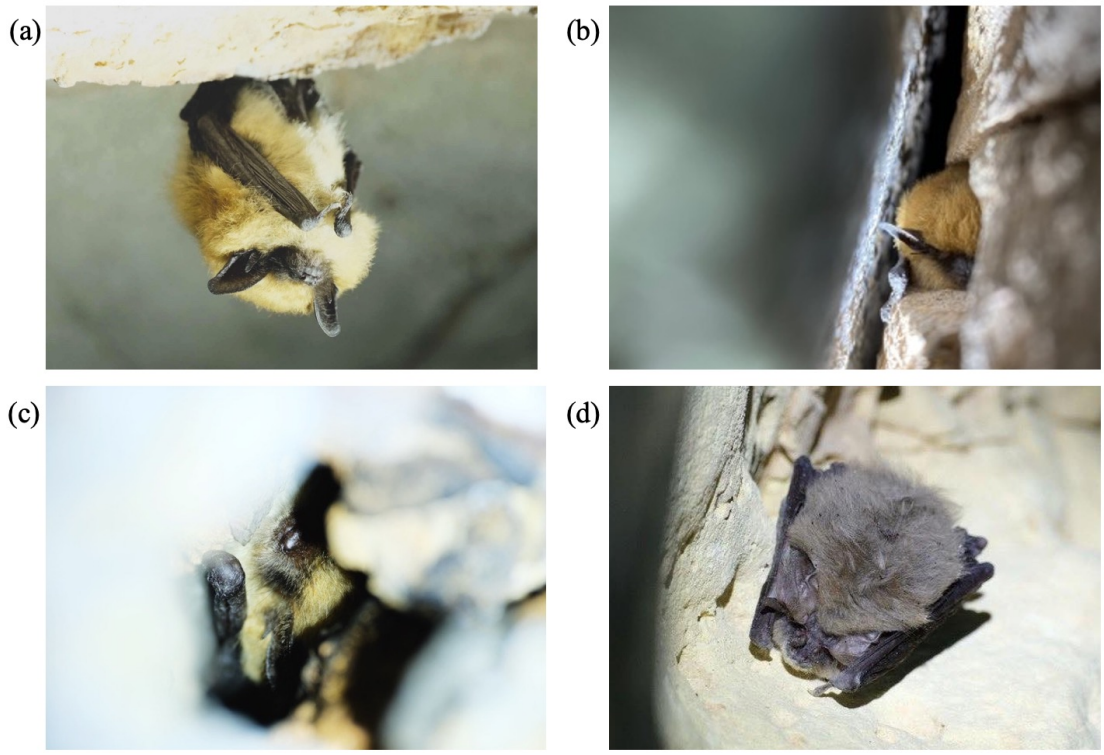

Figure 2. Different species of bats observed during hibernation in north-central Arizona. (a) Uncommon observation of a roosting *Myotis* spp. in a fully exposed position (Position 1). Note the pointed tragus, which was used for discrimination between *Myotis* spp. and *P. hesperus* (which has a blunt tragus). (b) A *Myotis* spp. roosting in a partially concealed position (Position 3) in Cave 5 during hibernation. (c) A *Myotis* spp. roosting in an inconspicuous position (Position 4) in Cave 2 during hibernation. (d) A *C. townsendii* roosting in a fully exposed position in Cave 3 during hibernation. Note the curled ears which are indicative of this species while it roosts.

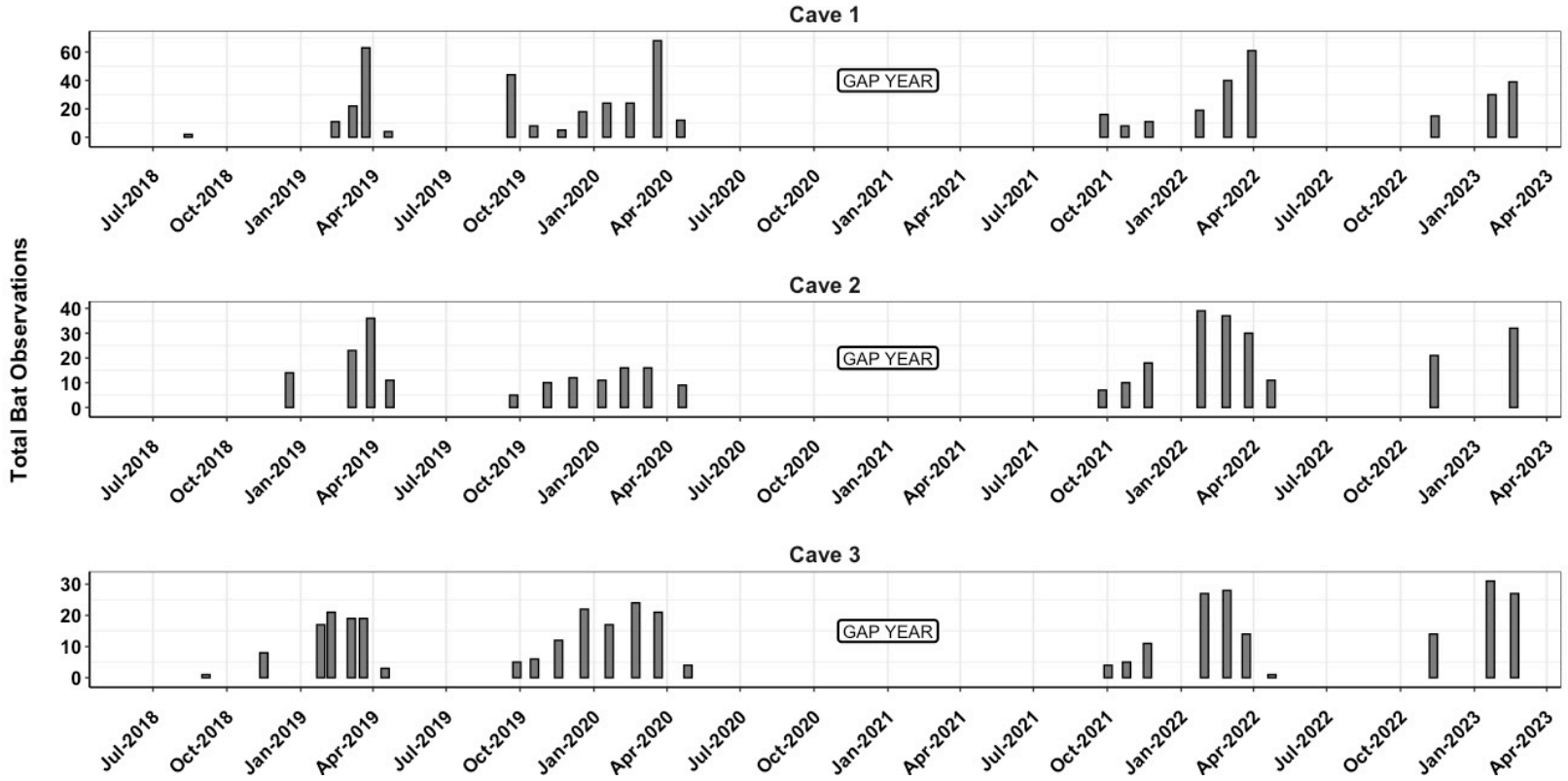

Figure 3. Total observations of hibernating bats across all surveys between 2018 and 2023 at each site. Blank spaces are months when internal surveys did not take place. Note different scales on Y axes.

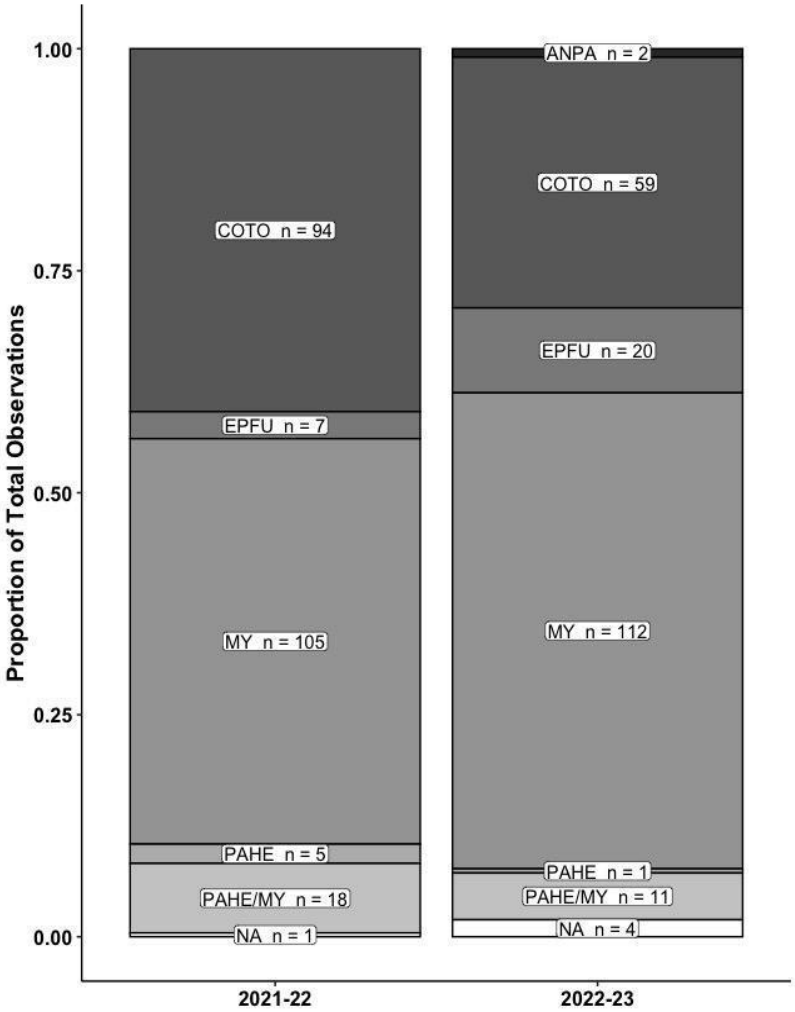

Figure 4. Species composition across all sites between November and February in 2021-2023. Numbers next to species ID represent the total count of observations for that species per year. Bars represent the proportion each species made up within a hibernation season. Species codes are as follows: MY=*Myotis spp.*; COTO= *Corynorhinus townsendii*; EPFU=*Eptesicus fuscus*; PAHE/MY=undistinguished between *Parastrellus hesperus* and *Myotis spp.*; PAHE=*P. hesperus*; ANPA=*Antrozous pallidus*; NA=unidentified.

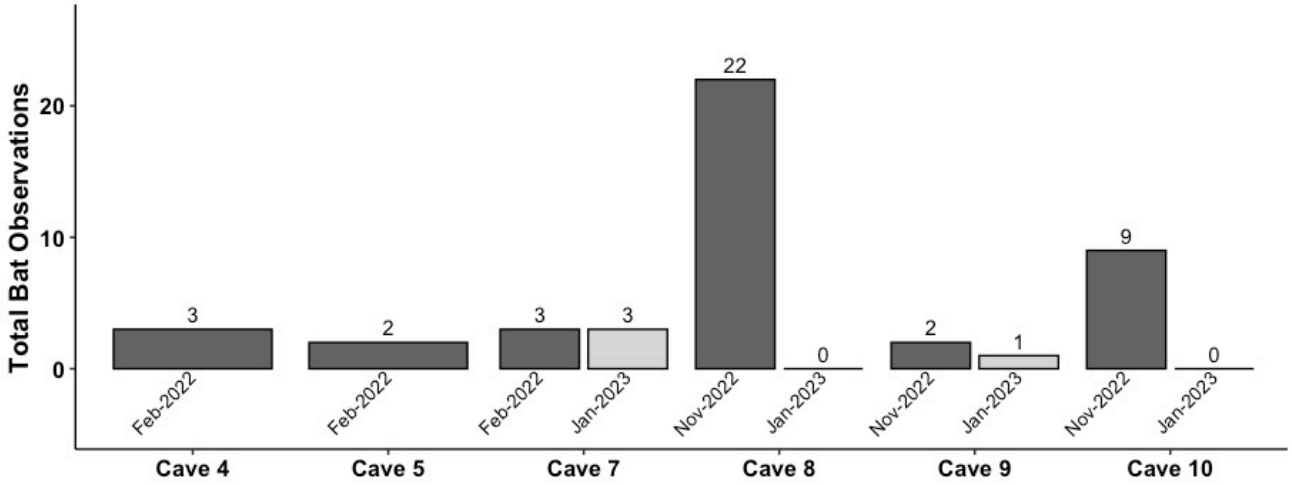

Figure 5. Counts of hibernating bats at Caves 4-10 in 2022-2023. Different colors represent different visits at the same site. Numbers above bars represent the total bat observations per visit.

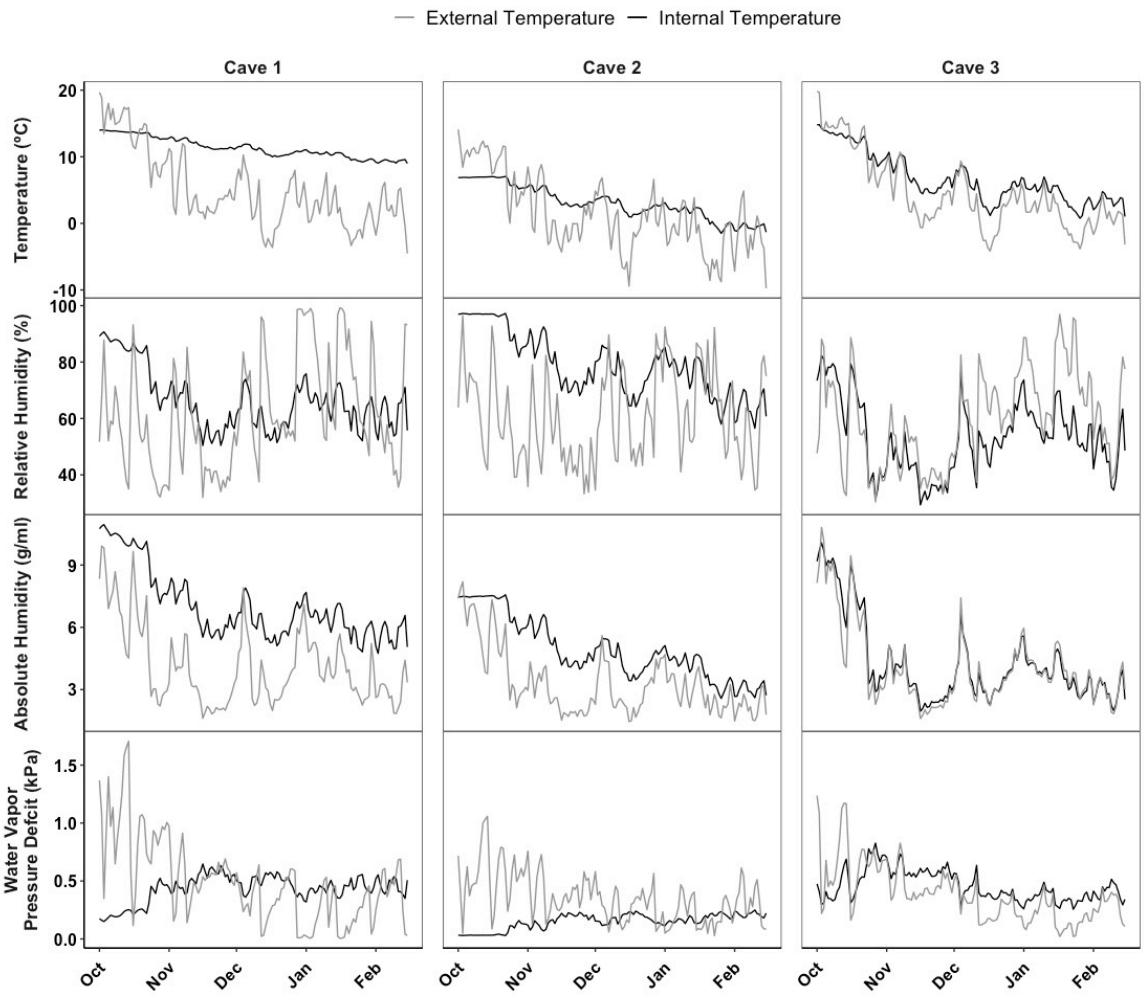

Figure 6. Internal (dark gray) versus external (light gray) cave conditions at each site between October 2022 and mid-February 2023. Data is averaged across all internal loggers per day at each site. External conditions are averaged across each day at each site.

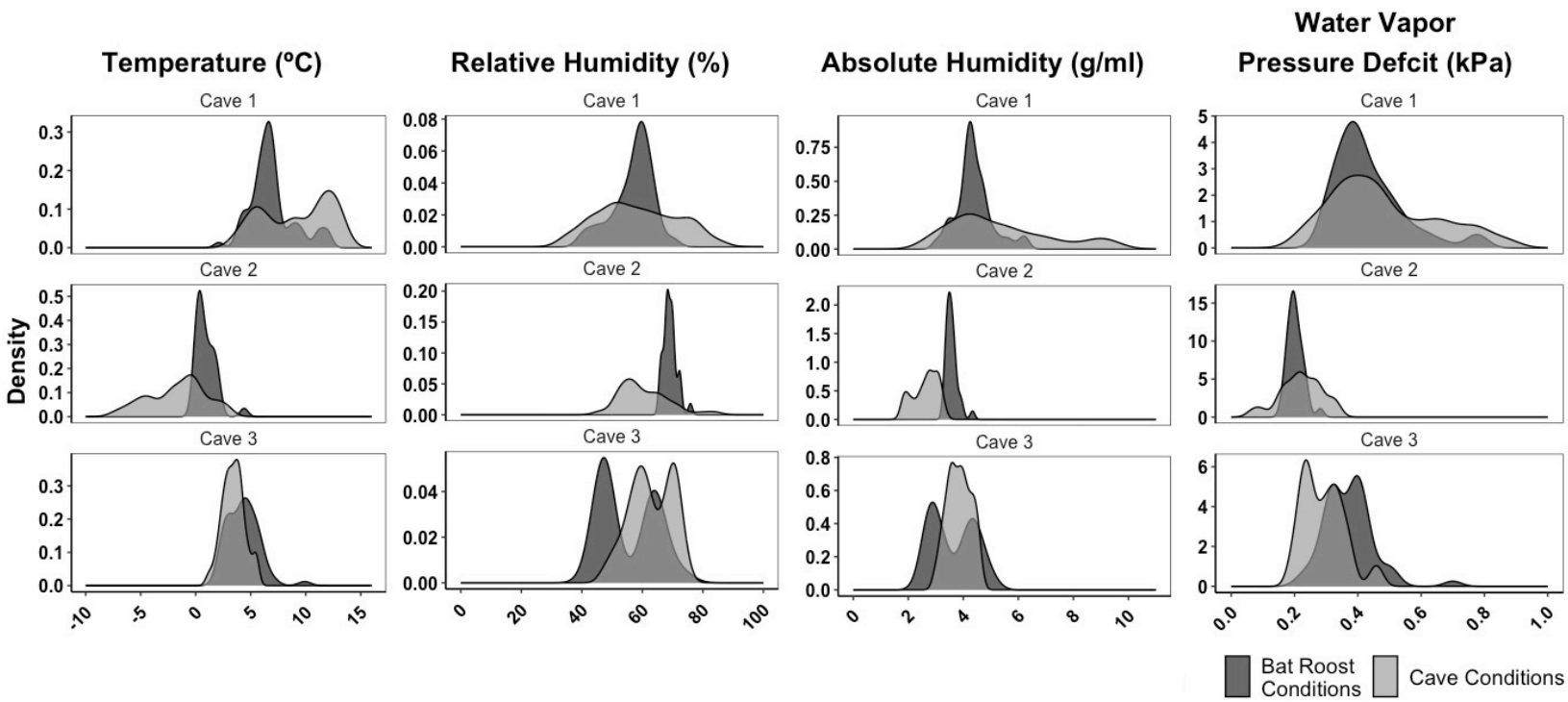

Figure 7. Distributions of cave conditions available to roosting bats from 24 hours prior to survey (light gray) compared to the distributions of bat roost conditions measured during the survey (dark gray) across all three sites during hibernation (January and February) of Year 5 (2023).

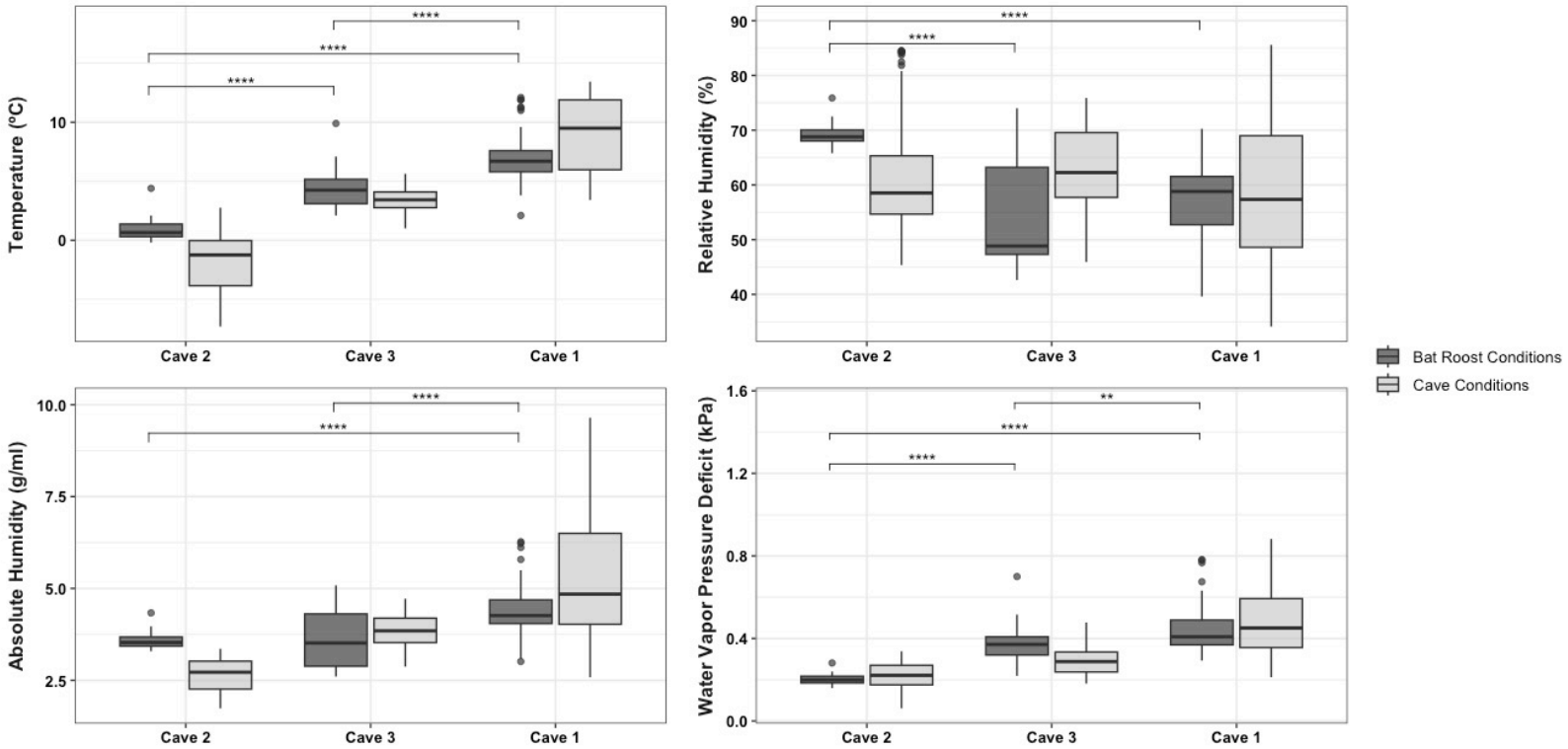

Figure 8. Comparison of bat roost conditions (*C. townsendii* and *Myotis* spp. only and combined as "Bat Roost Conditions") to available cave conditions (collected from the 24-hours prior to each survey) by cave in January and February of 2023. Note the order of caves on X-axis. Significantly different conditions at bat roost sites between each cave ($p<0.05$) are denoted with asterisks [Kruskal-Wallis (Bat roost: temperature: $H=0.71$, $df=2$, $p<0.001$; relative humidity: $H=0.48$, $df=2$, $p<0.001$; absolute humidity: $H=0.25$, $df=2$, $p<0.001$; WVPD: $H=0.58$, $df=2$, $p<0.001$); (Cave conditions: temperature: $H=0.83$, $df=2$, $p<0.001$; relative humidity: $H=0.0.34$, $df=2$, $p<0.001$; absolute humidity: $H=0.60$, $df=2$, $p<0.001$; WVPD: $H=0.53$, $df=2$, $p<0.001$)] .

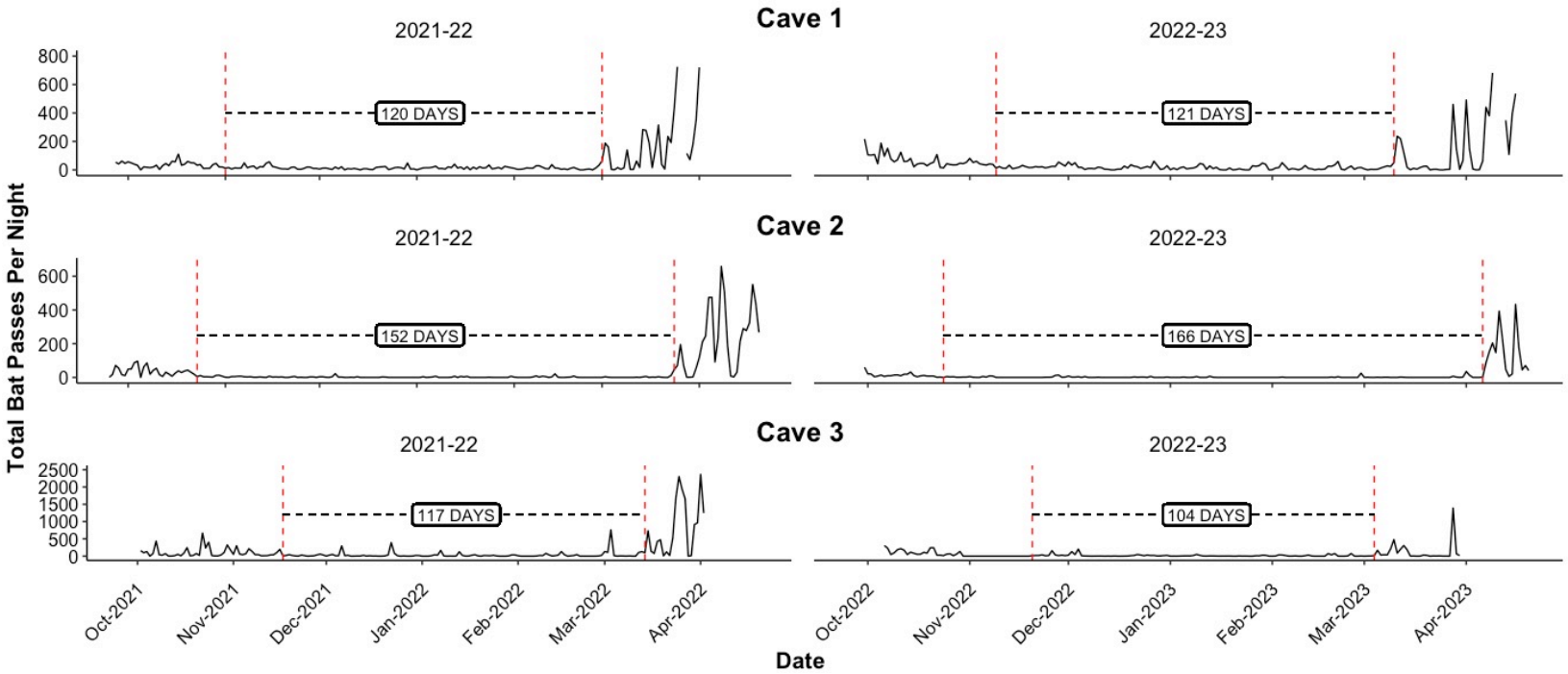

Figure 9. Panel of all acoustic calls (solid black line) over time with estimated hibernation start and end dates indicated with red dashed lines. Dates on the X-axis are consistent across all plots. Note different scales on the y-axis. Year 4 for all sites is indicated on the left column and Year 5 for all sites is on the right column.

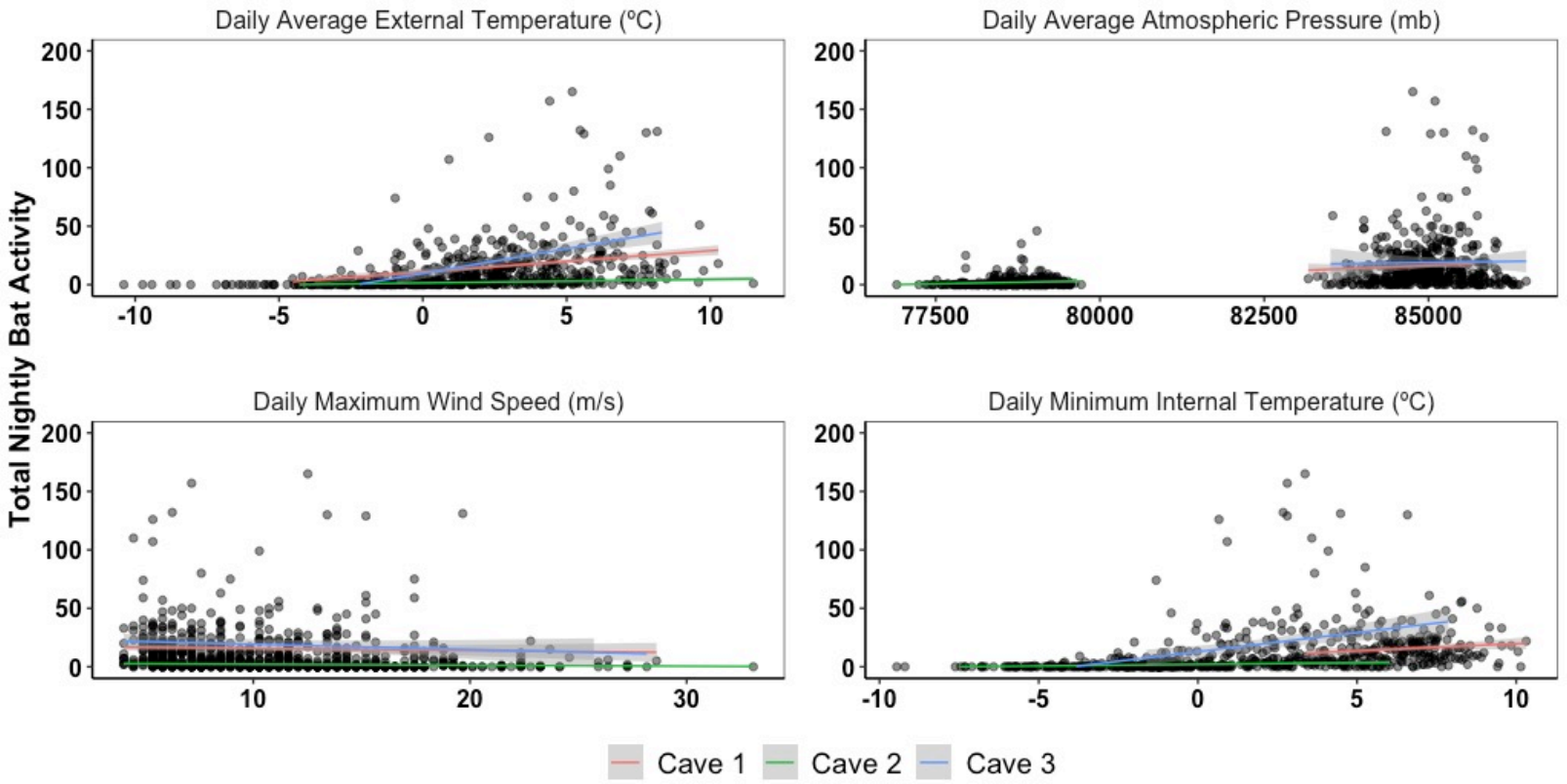

Figure 10. Nightly bat acoustic activity on the y-axis plotted against four environmental variables related to winter bat activity. Dots represent the total number of bat call files per night during the defined hibernation period at each site of Years 4 and 5. Each panel is a different variable, and all caves are considered together. Lines indicate the generalized linear model best-fit line by cave, and the gray shading around each line represents the 95% confidence interval. Correlation coefficients can be found in Supplementary Material Appendix B, Figure B1. Note different scales across plots.

REFERENCES

Adams, R. A. (2003). *Bats of the rocky mountain West: Natural history, ecology, and conservation*. University Press of Colorado.

Altringham, J. (2011). *Bats: From evolution to conservation* (2nd ed.). Oxford University Press.

Ancillotto, L., Santini, L., Ranc, N., Maiorano, L., & Russo, D. (2016). Extraordinary range expansion in a common bat: The potential roles of climate change and urbanisation. *The Science of Nature*, *103*(3), 15. https://doi.org/10.1007/s00114-016-1334-7

Archer, S. R., & Predick, K. I. (2008). Climate change and ecosystems of the southwestern United States. *Rangelands*, *30*(3), 23–28. https://doi.org/10.2111/1551-501X(2008)30[23:CCAEOT]2.0.CO;2

Arizona Cave Survey. (2017). *Arizona cave survey- documenting the caves of Arizona*. Arizona Cave Survey. http://arizonacaves.org/index.htm

Audet, D., & Fenton, M. B. (1988). Heterothermy and the use of torpor by the bat *Eptesicus fuscus* (Chiroptera: Vespertilionidae): A field study. *Physiological Zoology*, *61*(3), 197–204.

Auteri, G. G. (2022). A conceptual framework to integrate cold-survival strategies: Torpor, resistance and seasonal migration. *Biology Letters*, *18*(5), 20220050. https://doi.org/10.1098/rsbl.2022.0050

Bachorec, E., Bartonička, T., Heger, T., Pikula, J., & Zukal, J. (2021). Cold arousal—A mechanism used by hibernating bats to reduce the energetic costs of disturbance. *Journal of Thermal Biology*, *101*, 103107. https://doi.org/10.1016/j.jtherbio.2021.103107

Bandouchova, H., Bartonička, T., Berkova, H., Brichta, J., Kokurewicz, T., Kovacova, V., Linhart, P., Piacek, V., Pikula, J., Zahradníková, A., & Zukal, J. (2018). Alterations in the health of hibernating bats under pathogen pressure. *Scientific Reports*, *8*(1), Article 1. https://doi.org/10.1038/s41598-018-24461-5

Bates, D., Mächler, M., Bolker, B., & Walker, S. (2015). Fitting Linear Mixed-Effects Models Using lme4. Journal of Statistical Software, 67(1), 1–48. https://doi.org/10.18637/jss.v067.i01

Ben-Hamo, M., Muñoz-Garcia, A., Williams, J. B., Korine, C., & Pinshow, B. (2013). Waking to drink: Rates of evaporative water loss determine arousal frequency in hibernating bats. *Journal of Experimental Biology*, *216*(4), 573–577. https://doi.org/10.1242/jeb.078790

Bernard, R. F., Foster, J. T., Willcox, E. V., Parise, K. L., & McCracken, G. F. (2015). Molecular Detection of the Causative Agent of White-nose Syndrome on Rafinesque's Big-eared Bats (*Corynorhinus rafinesquii*) and Two Species of Migratory Bats in the Southeastern USA. *Journal of Wildlife Diseases*, *51*(2), 519–522. https://doi.org/10.7589/2014-08-202

Bernard, R. F., & McCracken, G. F. (2017). Winter behavior of bats and the progression of white-nose syndrome in the southeastern United States. *Ecology and Evolution*, *7*(5), 1487–1496. https://doi.org/10.1002/ece3.2772

Bernard, R. F., Willcox, E. V., Jackson, R. T., Brown, V. A., & McCracken, G. F. (2021). Feasting, not fasting: Winter diets of cave hibernating bats in the United States. *Frontiers in Zoology*, *18*(1), 48. https://doi.org/10.1186/s12983-021-00434-9

Blehert, D. S., Hicks, A. C., Behr, M., Meteyer, C. U., Berlowski-Zier, B. M., Buckles, E. L., Coleman, J. T. H., Darling, S. R., Gargas, A., Niver, R., Okoniewski, J. C., Rudd, R. J., & Stone, W. B. (2009). Bat white-nose syndrome: An emerging fungal pathogen? *Science*, *323*(5911), 227–227.

Blejwas, K. M., Pendleton, G. W., Kohan, M. L., & Beard, L. O. (2021). The Milieu Souterrain Superficiel as hibernation habitat for bats: Implications for white-nose syndrome. *Journal of Mammalogy*, *102*(4), 1110–1127. https://doi.org/10.1093/jmammal/gyab050

Bolker, B. M., Brooks, M. E., Clark, C. J., Geange, S. W., Poulsen, J. R., Stevens, M. H. H., & White, J.-S. S. (2009). Generalized linear mixed models: A practical guide for ecology and evolution. Trends in Ecology & Evolution, 24(3), 127–135. https://doi.org/10.1016/j.tree.2008.10.008

Boratyński, J. S., Willis, C. K. R., Jefimow, M., & Wojciechowski, M. S. (2015). Huddling reduces evaporative water loss in torpid Natterer's bats, *Myotis nattereri*. *Comparative Biochemistry and Physiology Part A: Molecular & Integrative Physiology*, *179*, 125–132. https://doi.org/10.1016/j.cbpa.2014.09.035

Boyles, J. G., Dunbar, M. B., & Whitaker Jr, J. O. (2006). Activity following arousal in winter in North American vespertilionid bats. *Mammal Review*, *36*(4), 267–280. https://doi.org/10.1111/j.1365-2907.2006.00095.x

Boyles, J. G., Johnson, J. S., Blomberg, A., & Lilley, T. M. (2020). Optimal hibernation theory. *Mammal Review*, *50*(1), 91–100. https://doi.org/10.1111/mam.12181

Brack Jr., V., & Twente, J. (1985). The duration of the period of hibernation of three species of vespertilionid bats. I. Field studies. *Canadian Journal of Zoology*, *63*, 2952–2954. https://doi.org/10.1139/z85-442

Bradley, W. G., & O'Farrell, M. J. (1969). Temperature Relationships of the Western Pipistrelle (*Pipistrellus hesperus*). *Physiological Systems in Semi-Arid Environments*, 85–96.

Bure, C. M., & Moore, M. S. (2019). White-nose syndrome: A fungal disease of North American hibernating bats. In *Encyclopedia of Caves* (pp. 1165–1174). Elsevier. https://doi.org/10.1016/B978-0-12-814124-3.00136-9

Campbell, L. J., Walsh, D. P., Blehert, D. S., & Lorch, J. M. (2020). Long-term survival of *Pseudogymnoascus destructans* at elevated temperatures. *Journal of Wildlife Diseases*, *56*(2), 278–287. https://doi.org/10.7589/2019-04-106

Carpenter, R. E. (1969). Structure and function of the kidney and the water balance of desert bats. *Physiological Zoology*, *42*(3), 288–302.

Cheng, T. L., Reichard, J. D., Coleman, J. T. H., Weller, T. J., Thogmartin, W. E., Reichert, B. E., Bennett, A. B., Broders, H. G., Campbell, J., Etchison, K., Feller, D. J., Geboy, R., Hemberger, T., Herzog, C., Hicks, A. C., Houghton, S., Humber, J., Kath, J. A., King, R. A., … Frick, W. F. (2021). The scope and severity of white-nose syndrome on hibernating bats in North America. *Conservation Biology*, *35*(5), 1586–1597. https://doi.org/10.1111/cobi.13739

Cockrum, E. L., Musgrove, Bill., & Petryszyn, Yar. (1996). *Bats of Mohave County, Arizona: Populations and movements*. Museum of Texas Tech University. https://doi.org/10.5962/bhl.title.143249

Coleman, J. (2015). *White-Nose Syndrome, The devastating disease of hibernating bats in North America*. U.S. Fish and Wildlife Service.

Conenna, I., Santini, L., Rocha, R., Monadjem, A., Cabeza, M., & Russo, D. (2021). Global patterns of functional trait variation along aridity gradients in bats. *Global Ecology and Biogeography*, *30*(5), 1014–1029. https://doi.org/10.1111/geb.13278

Corbett, J., Gillies, K., Monfeli, J., & Gilleland, T. (2017). *Surveys of bat hibernacula sites in Eastern, Southeastern, and North Central Arizona*. Arizona Game and Fish Department; Bat Conservation International.

Cross, S. P. (1965). Roosting Habits of *Pipistrellus hesperus*. *Journal of Mammalogy*, *46*(2), 270. https://doi.org/10.2307/1377847

Cryan, P. M., Meteyer, C. U., Blehert, D. S., Lorch, J. M., Reeder, D. M., Turner, G. G., Webb, J., Behr, M., Verant, M., Russell, R. E., & Castle, K. T. (2013). Electrolyte depletion in white-nose syndrome bats. *Journal of Wildlife Diseases*, *49*(2), 398–402. https://doi.org/10.7589/2012-04-121

Davis, W. H., & Hitchcock, H. B. (1965). Biology and migration of the bat, *Myotis lucifugus*, in New England. *Journal of Mammalogy*, *46*(2), 296–313. https://doi.org/10.2307/1377850

Drees, K. P., Lorch, J. M., Puechmaille, S. J., Parise, K. L., Wibbelt, G., Hoyt, J. R., Sun, K., Jargalsaikhan, A., Dalannast, M., Palmer, J. M., Lindner, D. L., Marm Kilpatrick, A., Pearson, T., Keim, P. S., Blehert, D. S., & Foster, J. T. (2017). Phylogenetics of a fungal invasion: Origins and widespread dispersal of white-nose syndrome. *mBio*, *8*(6), e01941-17. https://doi.org/10.1128/mBio.01941-17

Fenton, B. (1982). Echolocation, insect hearing, and feeding ecology of insectivoroous bats. In T. H. Kunz (Ed.), *Ecology of Bats* (pp. 261–285). Springer. https://doi-org.ezproxy1.lib.asu.edu/10.1007/978-1-4613-3421-7_7

Festa, F., Ancillotto, L., Santini, L., Pacifici, M., Rocha, R., Toshkova, N., Amorim, F., Benítez-López, A., Domer, A., Hamidović, D., Kramer-Schadt, S., Mathews, F., Radchuk, V., Rebelo, H., Ruczynski, I., Solem, E., Tsoar, A., Russo, D., & Razgour, O. (2023). Bat responses to climate change: A systematic review. *Biological Reviews*, *98*(1), 19–33. https://doi.org/10.1111/brv.12893

Field, K. A., Johnson, J. S., Lilley, T. M., Reeder, S. M., Rogers, E. J., Behr, M. J., & Reeder, D. M. (2015). The white-nose syndrome transcriptome: Activation of anti-fungal host responses in wing tissue of hibernating little brown myotis. *PLOS Pathogens*, *11*(10), e1005168. https://doi.org/10.1371/journal.ppat.1005168

Frank, C. L., Michalski, A., McDonough, A. A., Rahimian, M., Rudd, R. J., & Herzog, C. (2014). The resistance of a North American bat species (Eptesicus fuscus) to white-nose syndrome (WNS). *PLoS ONE*, *9*(12), e113958. https://doi.org/10.1371/journal.pone.0113958

Frick, W. F., Kingston, T., & Flanders, J. (2020). A review of the major threats and challenges to global bat conservation. *Annals of the New York Academy of Sciences*, *1469*(1), 5–25. https://doi.org/10.1111/nyas.14045

Frick, W. F., Pollock, J. F., Hicks, A. C., Langwig, K. E., Reynolds, D. S., Turner, G. G., Butchkoski, C. M., & Kunz, T. H. (2010). An emerging disease causes regional population collapse of a common North American bat species. *Science*, *329*(5992), 679–682.

Frick, W. F., Puechmaille, S. J., Hoyt, J. R., Nickel, B. A., Langwig, K. E., Foster, J. T., Barlow, K. E., Bartonička, T., Feller, D., Haarsma, A.-J., Herzog, C., Horáček, I., van der Kooij, J., Mulkens, B., Petrov, B., Reynolds, R., Rodrigues, L., Stihler, C. W., Turner, G. G., & Kilpatrick, A. M. (2015). Disease alters macroecological patterns of North American bats. *Global Ecology and Biogeography*, *24*(7), 741–749. https://doi.org/10.1111/geb.12290

Frick, W. F., Puechmaille, S. J., & Willis, C. K. R. (2016). White-nose syndrome in bats. In C. C. Voigt & T. Kingston (Eds.), *Bats in the Anthropocene: Conservation of Bats in a Changing World* (pp. 245–262). Springer International Publishing. https://doi.org/10.1007/978-3-319-25220-9_9

Gargas, A., Trest, M. T., Christensen, M., Volk, T. J., & Blehert, D. S. (2009). Geomyces destructans sp. nov. associated with bat white-nose syndrome. *Mycotaxon*, *108*(1), 147–154. https://doi.org/10.5248/108.147

Geiser, F. (2013). Hibernation. *Current Biology*, *23*(5), R188–R193. https://doi.org/10.1016/j.cub.2013.01.062

Geiser, F., Bondarenco, A., Currie, S. E., Doty, A. C., Körtner, G., Law, B. S., Pavey, C. R., Riek, A., Stawski, C., Turbill, C., Willis, C. K. R., & Brigham, R. M. (2019). Hibernation and daily torpor in Australian and New Zealand bats: Does the climate zone matter? *Australian Journal of Zoology*, *67*(6), 316. https://doi.org/10.1071/ZO20025

Geiser, F., & Ruf, T. (1995). Hibernation versus daily torpor in mammals and birds: Physiological variables and classification of torpor patterns. *Physiological Zoology*, *68*(6), 935–966.

Geluso, K. N. (1978). Urine concentrating ability and renal structure of insectivorous bats. *Journal of Mammalogy*, *59*(2), 312–323. https://doi.org/10.2307/1379915

Genter, D. L. (1986). Wintering bats of the Upper Snake River Plain: Occurrence in lava-tube caves. *The Great Basin Naturalist*, *46*(2), 241–244.

Gillies, K. E., Murphy, P. J., & Matocq, M. D. (2014). Hibernacula characteristics of Townsend's big-eared bats in southeastern Idaho. *Natural Areas Journal*, *34*(1), 24–30.

Griffith, G. E., Omernik, J. M., Johnson, C. B., & Turner, D. S. (2014). *Ecoregions of Arizona*. U.S. Geological Survey. http://dx.doi.org/10.3133/ofr20141141

Haase, C. G., Fuller, N. W., Dzal, Y. A., Hranac, C. R., Hayman, D. T. S., Lausen, C. L., Silas, K. A., Olson, S. H., & Plowright, R. K. (2021). Body mass and hibernation microclimate may predict bat susceptibility to white-nose syndrome. *Ecology and Evolution*, *11*(1), 506–515. https://doi.org/10.1002/ece3.7070

Hammer, G. R. (2006). *Climate of Arizona*. National Climatic Data Center.

Harrell Jr, F. E. (2022). *Hmisc: Harrell Miscellaneous*. https://CRAN.R-project.org/package=Hmisc

Hartig, F. (2022). *DHARMa: Residual Diagnostics for Hierarchical (Multi-Level / Mixed) Regression Models*. https://CRAN.R-project.org/package=DHARMa

Harvey, J. A., Tougeron, K., Gols, R., Heinen, R., Abarca, M., Abram, P. K., Basset, Y., Berg, M., Boggs, C., Brodeur, J., Cardoso, P., de Boer, J. G., De Snoo, G. R., Deacon, C., Dell, J. E., Desneux, N., Dillon, M. E., Duffy, G. A., Dyer, L. A., … Chown, S. L. (2023). Scientists' warning on climate change and insects. *Ecological Monographs*, *93*(1), e1553. https://doi.org/10.1002/ecm.1553

Hayes, M. A., Schorr, R. A., & Navo, K. W. (2011). Hibernacula selection by Townsend's big-eared bat in southwestern Colorado. *The Journal of Wildlife Management*, *75*(1), 137–143.

Hayman, D. T. S., Cryan, P. M., Fricker, P. D., & Dannemiller, N. G. (2017). Long-term video surveillance and automated analyses reveal arousal patterns in groups of hibernating bats. *Methods in Ecology and Evolution*, *8*(12), 1813–1821. https://doi.org/10.1111/2041-210X.12823

Hayward, B. J. (1961). *The natural history of the cave bat, Myotis velifer.* [Ph.D., The University of Arizona]. https://www.proquest.com/docview/302065007/citation/267BFA9DBA774F16PQ/1

Herreid, C., & Schmidt-Nielsen, K. (1966). Oxygen consumption, temperature, and water loss in bats from different environments. *American Journal of Physiology-Legacy Content*, *211*(5), 1108–1112. https://doi.org/10.1152/ajplegacy.1966.211.5.1108

Hoffmeister, D. F. (1970). The seasonal distribution of bats in Arizona: A case for improving mammalian range maps. *The Southwestern Naturalist*, *15*(1), 11–22. https://doi.org/10.2307/3670197

Hope, P. R., & Jones, G. (2012). Warming up for dinner: Torpor and arousal in hibernating Natterer's bats (*Myotis nattereri*) studied by radio telemetry. *Journal of Comparative Physiology. B, Biochemical, Systemic, and Environmental Physiology*, *182*(4), 569–578. https://doi.org/10.1007/s00360-011-0631-x

Hoyt, J. R., Kilpatrick, A. M., & Langwig, K. E. (2021). Ecology and impacts of white-nose syndrome on bats. *Nature Reviews Microbiology*, *19*(3), Article 3. https://doi.org/10.1038/s41579-020-00493-5

Hoyt, J. R., Langwig, K. E., Okoniewski, J., Frick, W. F., Stone, W. B., & Kilpatrick, A. M. (2015). Long-term persistence of *Pseudogymnoascus destructans*, the causative agent of white-nose syndrome, in the absence of bats. *EcoHealth*, *12*(2), 330–333. https://doi.org/10.1007/s10393-014-0981-4

Hranac, C. R., Haase, C. G., Fuller, N. W., McClure, M. L., Marshall, J. C., Lausen, C. L., McGuire, L. P., Olson, S. H., & Hayman, D. T. S. (2021). What is winter? Modeling spatial variation in bat host traits and hibernation and their implications for overwintering energetics. *Ecology and Evolution*, *11*(17), 11604–11614. https://doi.org/10.1002/ece3.7641

Humphries, M. M., Thomas, D. W., & Speakman, J. R. (2002). Climate-mediated energetic constraints on the distribution of hibernating mammals. *Nature*, *418*(6895), 313–316. https://doi.org/10.1038/nature00828

Jackson, R. T., Willcox, E. V., & Bernard, R. F. (2022). Winter torpor expression varies in four bat species with differential susceptibility to white-nose syndrome. *Scientific Reports*, *12*(1), Article 1. https://doi.org/10.1038/s41598-022-09692-x

Jagnow, D. H. (1998). Bat usage and cave management of Torgac Cave, New Mexico. Journal of Cave and Karst Studies, 60(1), 33–38.

Johnson, J. S., Treanor, J. J., Lacki, M. J., Baker, M. D., Falxa, G. A., Dodd, L. E., Waag, A. G., & Lee, E. H. (2017). Migratory and winter activity of bats in Yellowstone National Park. *Journal of Mammalogy*, *98*(1), 211–221. https://doi.org/10.1093/jmammal/gyw175

Kitchell, M. (2021). *State and federal partners in California and Arizona ask public to help detect and prevent spread of fungus deadly to bats*. White-Nose Syndrome Response Team. https://www.whitenosesyndrome.org/press-release/state-and-federal-partners-in-california-and-arizona-ask-public-to-help-detect-and-prevent-spread-of-fungus-deadly-to-bats

Klüg-Baerwald, B. J., & Brigham, R. M. (2017). Hung out to dry? Intraspecific variation in water loss in a hibernating bat. *Oecologia*, *183*(4), 977–985. https://doi.org/10.1007/s00442-017-3837-0

Klüg-Baerwald, B. J., Lausen, C. L., Wissel, B., & Brigham, R. M. (2022). Meet you at the local watering hole? No use of an artificial water resource, and evidence of dehydration in hibernating bats in the prairies. *Acta Chiropterologica*, *23*(2). https://doi.org/10.3161/15081109ACC2021.23.2.010

Kurta, A. (2014). The misuse of relative humidity in ecological studies of hibernating bats. *Acta Chiropterologica*, *16*(1), 249–254. https://doi.org/10.3161/150811014X683444

Kurta, A., & Smith, S. M. (2014). Hibernating bats and abandoned mines in the Upper Peninsula of Michigan. *Northeastern Naturalist*, *21*(4), 587–605. https://doi.org/10.1656/045.021.0407

Langwig, K. E., Frick, W. F., Bried, J. T., Hicks, A. C., Kunz, T. H., & Marm Kilpatrick, A. (2012). Sociality, density-dependence and microclimates determine the persistence of populations suffering from a novel fungal disease, white-nose syndrome. *Ecology Letters*, *15*(9), 1050–1057. https://doi.org/10.1111/j.1461-0248.2012.01829.x

Lesiński, G. (1986). Ecology of bats hibernating underground in Central Poland. *Acta Theriologica*, *31*, 507–521. https://doi.org/10.4098/AT.arch.86-45

Lorch, J. M., Meteyer, C. U., Behr, M. J., Boyles, J. G., Cryan, P. M., Hicks, A. C., Ballmann, A. E., Coleman, J. T. H., Redell, D. N., Reeder, D. M., & Blehert, D. S. (2011). Experimental infection of bats with Geomyces destructans causes white-nose syndrome. *Nature*, *480*(7377), 376–378. https://doi.org/10.1038/nature10590

Lorch, J. M., Muller, L. K., Russell, R. E., O'Connor, M., Lindner, D. L., & Blehert, D. S. (2013). Distribution and environmental persistence of the causative agent of white-nose syndrome, *Geomyces destructans*, in bat hibernacula of the eastern United States. *Applied and Environmental Microbiology*, *79*(4), 1293–1301. https://doi.org/10.1128/AEM.02939-12

Lundy, M., Montgomery, I., & Russ, J. (2010). Climate change-linked range expansion of Nathusius' pipistrelle bat, *Pipistrellus nathusii* (Keyserling & Blasius, 1839). *Journal of Biogeography*, *37*(12), 2232–2242. https://doi.org/10.1111/j.1365-2699.2010.02384.x

Maestre, F. T., Salguero-Gómez, R., & Quero, J. L. (2012). It is getting hotter in here: Determining and projecting the impacts of global environmental change on drylands. Philosophical Transactions of the Royal Society B: Biological Sciences, 367(1606), 3062–3075. https://doi.org/10.1098/rstb.2011.0323

Mallinger, E. C., Goodwin, K. R., Kirschbaum, A., Shen, Y., Gillam, E. H., & Olson, E. R. (2023). Species-specific responses to white-nose syndrome in the Great Lakes region. Ecology and Evolution, 13(7), e10267. https://doi.org/10.1002/ece3.10267

Marroquin, C. M., Lavine, J. O., & Windstam, S. T. (2017). Effect of humidity on development of *Pseudogymnoascus destructans*, the causal agent of bat white-nose syndrome. *Northeastern Naturalist*, *24*(1), 54–64. https://doi.org/10.1656/045.024.0105

McGuire, L. P., Mayberry, H. W., & Willis, C. K. R. (2017). White-nose syndrome increases torpid metabolic rate and evaporative water loss in hibernating bats. *American Journal of Physiology-Regulatory, Integrative and Comparative Physiology*, *313*(6), R680–R686. https://doi.org/10.1152/ajpregu.00058.2017

Meteyer, C. U., Barber, D., & Mandl, J. N. (2012). Pathology in euthermic bats with white nose syndrome suggests a natural manifestation of immune reconstitution inflammatory syndrome. *Virulence*, *3*(7), 583–588. https://doi.org/10.4161/viru.22330

Meteyer, C. U., Buckles, E. L., Blehert, D. S., Hicks, A. C., Green, D. E., Shearn-Bochsler, V., Thomas, N. J., Gargas, A., & Behr, M. J. (2009). Histopathologic criteria to confirm white-nose syndrome in bats. *Journal of Veterinary Diagnostic Investigation*, *21*(4), 411–414. https://doi.org/10.1177/104063870902100401

Meyer, G. A., Senulis, J. A., & Reinartz, J. A. (2016). Effects of temperature and availability of insect prey on bat emergence from hibernation in spring. *Journal of Mammalogy*, *97*(6), 1623–1633. https://doi.org/10.1093/jmammal/gyw126

Mickleburgh, S. P., Hutson, A. M., & Racey, P. A. (2002). A review of the global conservation status of bats. *Oryx*, *36*(1), 18–34. https://doi.org/10.1017/S0030605302000054

Minnis, A. M., & Lindner, D. L. (2013). Phylogenetic evaluation of *Geomyces* and allies reveals no close relatives of Pseudogymnoascus destructans, comb. Nov., in bat hibernacula of eastern North America. *Fungal Biology*, *117*(9), 638–649. https://doi.org/10.1016/j.funbio.2013.07.001

Moore, M. S., Field, K. A., Behr, M. J., Turner, G. G., Furze, M. E., Stern, D. W. F., Allegra, P. R., Bouboulis, S. A., Musante, C. D., Vodzak, M. E., Biron, M. E., Meierhofer, M. B., Frick, W. F., Foster, J. T., Howell, D., Kath, J. A., Kurta, A., Nordquist, G., Johnson, J. S., … Reeder, D. M. (2018). Energy conserving thermoregulatory patterns and lower disease severity in a bat resistant to the impacts of white-nose syndrome. *Journal of Comparative Physiology B*, *188*(1), 163–176. https://doi.org/10.1007/s00360-017-1109-2

Moore, M. S., Reichard, J. D., Murtha, T. D., Nabhan, M. L., Pian, R. E., Ferreira, J. S., & Kunz, T. H. (2013). Hibernating little brown myotis (*Myotis lucifugus*) show variable immunological responses to white-nose syndrome. *PLoS ONE*, *8*(3), e58976. https://doi.org/10.1371/journal.pone.0058976

Moore, M. S., Reichard, J. D., Murtha, T. D., Zahedi, B., Fallier, R. M., & Kunz, T. H. (2011). Specific Alterations in Complement Protein Activity of Little Brown Myotis (*Myotis lucifugus*) Hibernating in White-Nose Syndrome Affected Sites. *PLOS ONE*, *6*(11), e27430. https://doi.org/10.1371/journal.pone.0027430

Nagorsen, D. W., Bryant, A. A., Kerridge, D., Roberts, G., Roberts, A., & Sarell, M. J. (1993). Winter bat records for British Columbia. *Northwestern Naturalist*, *74*(3), 61–66. https://doi.org/10.2307/3536599

Norquay, K. J. O., & Willis, C. K. R. (2014). Hibernation phenology of *Myotis lucifugus*. *Journal of Zoology*, *294*(2), 85–92. https://doi.org/10.1111/jzo.12155

O'Donoghue, A. J., Knudsen, G. M., Beekman, C., Perry, J. A., Johnson, A. D., DeRisi, J. L., Craik, C. S., & Bennett, R. J. (2015). Destructin-1 is a collagen-degrading endopeptidase secreted by *Pseudogymnoascus destructans*, the causative agent of white-nose syndrome. *Proceedings of the National Academy of Sciences*, *112*(24), 7478–7483. https://doi.org/10.1073/pnas.1507082112

O'Farrell, M. J., & Bradley, W. G. (1970). Activity patterns of bats over a desert spring. *Journal of Mammalogy*, *51*(1), 18–26. https://doi.org/10.2307/1378527

Olival, K. J., Cryan, P. M., Amman, B. R., Baric, R. S., Blehert, D. S., Brook, C. E., Calisher, C. H., Castle, K. T., Coleman, J. T. H., Daszak, P., Epstein, J. H., Field, H., Frick, W. F., Gilbert, A. T., Hayman, D. T. S., Ip, H. S., Karesh, W. B., Johnson, C. K., Kading, R. C., … Wang, L.-F. (2020). Possibility for reverse zoonotic transmission of SARS-CoV-2 to free-ranging wildlife: A case study of bats. *PLOS Pathogens*, *16*(9), e1008758. https://doi.org/10.1371/journal.ppat.1008758

Palmer, J. M., Kubatova, A., Novakova, A., Minnis, A. M., Kolarik, M., & Lindner, D. L. (2014). Molecular characterization of a heterothallic mating system in *Pseudogymnoascus destructans*, the fungus causing white-nose syndrome of bats. *G3 Genes|Genomes|Genetics*, *4*(9), 1755–1763. https://doi.org/10.1534/g3.114.012641

Pérez, N. E. M., Moore, M. S., DeNardo, D., Deviche, P., & Smith, B. (2020). *Hibernation ecology of bats using three high-elevation caves in northern Arizona: Implications for potential white-nose syndrome impacts on desert southwest species* [Master's thesis]. Arizona State University.

Perry, R. W. (2013). A review of factors affecting cave climates for hibernating bats in temperate North America. *Environmental Reviews*, *21*(1), 28–39.

Prăvălie, R. (2016). Drylands extent and environmental issues. A global approach. Earth-Science Reviews, 161, 259–278. https://doi.org/10.1016/j.earscirev.2016.08.003

Puechmaille, S. J., Verdeyroux, P., Fuller, H., Gouilh, M. A., Bekaert, M., & Teeling, E. C. (2010). White-nose syndrome fungus (*Geomyces destructans*) in bat, France. *Emerging Infectious Diseases*, *16*(2). https://doi.org/10.3201/eid1602.091391

Puechmaille, S. J., Wibbelt, G., Korn, V., Fuller, H., Forget, F., Mühldorfer, K., Kurth, A., Bogdanowicz, W., Borel, C., Bosch, T., Cherezy, T., Drebet, M., Görföl, T., Haarsma, A.-J., Herhaus, F., Hallart, G., Hammer, M., Jungmann, C., Le Bris, Y., … Teeling, E. C. (2011). Pan-European distribution of white-nose syndrome fungus (*Geomyces destructans*) not associated with mass mortality. *PLoS ONE*, *6*(4), e19167. https://doi.org/10.1371/journal.pone.0019167

R Core Team. (2022). *R: A language and environment for statistical computing* [Computer software]. R Foundation for Statistical Computing. https://www.R-project.org/

Rajkumar, S. S., Li, X., Rudd, R. J., Okoniewski, J. C., Xu, J., Chaturvedi, S., & Chaturvedi, V. (2011). Clonal genotype of *Geomyces destructans* among bats with white nose syndrome, New York, USA. *Emerging Infectious Diseases*, *17*(7), 1273–1276. https://doi.org/10.3201/eid1707.102056

Reeder, D. M., Frank, C. L., Turner, G. G., Meteyer, C. U., Kurta, A., Britzke, E. R., Vodzak, M. E., Darling, S. R., Stihler, C. W., Hicks, A. C., Jacob, R., Grieneisen, L. E., Brownlee, S. A., Muller, L. K., & Blehert, D. S. (2012). Frequent arousal from

hibernation linked to severity of infection and mortality in bats with white-nose syndrome. *PLOS ONE*, *7*(6), e38920. https://doi.org/10.1371/journal.pone.0038920

Reynolds, H. T., Ingersoll, T., & Barton, H. A. (2015). Modeling the environmental growth of *Pseudogymnoascus destructans* and its impact on the white-nose syndrome epidemic. *Journal of Wildlife Diseases*, *51*(2), 318. https://doi.org/10.7589/2014-06-157

RStudio Team. (2020). *RStudio: Integrated development for R* [Computer software]. http://www.rstudio.com/

Schmidt, S. L. (1995). *Bat/mine survey, Dragoon and Chiricahua Mountains* (p. 18). Arizona Game and Fish Department.

Speakman, J. R., & Thomas, D. W. (2003). Physiological ecology and energetics of bats. In T. H. Kunz & M. B. Fenton (Eds.), *Bat Ecology* (pp. 430–492). University of Chicago Press.

Stawski, C., Willis, C. K. R., & Geiser, F. (2014). The importance of temporal heterothermy in bats. *Journal of Zoology*, *292*(2), 86–100. https://doi.org/10.1111/jzo.12105

Strong, T. R. (2010). Vertebrate species in desert caves and mines—A comparison between the Chihuahuan and Sonoran deserts. In W. Halvorson, C. Schwalbe, & C. van Riper (Eds.), *Southwestern Desert Resources* (pp. 93–106). University of Arizona Press. https://www.jstor.org/stable/j.ctv34h09n5.11

Szewczak, J. (2017). *SonoBat* (4.4.5) [Computer software]. SonoBat.

Thomas, D. W., Dorais, M., & Bergeron, J.-M. (1990). Winter energy budgets and cost of arousals for hibernating little brown bats, *Myotis lucifugus*. *Journal of Mammalogy*, *71*(3), 475–479. https://doi.org/10.2307/1381967

Thomas, D. W., & Geiser, F. (1997). Periodic arousals in hibernating mammals: Is evaporative water loss involved? *Functional Ecology*, *11*(5), 585–591.

Tim K. Snow. (1996). *Bat inventory of abandoned mines: Bureau of Land Management - Tucson Resource Area, Pima County, Arizona*. Arizona Game and Fish Department.

Tim K. Snow. (1998). *Bat inventory of the Kofa National Wildlife Refuge*. Arizona Game and Fish Department.

Tuttle, M., & Stevenson, D. (1978). Variation in the cave environment and its biological implications. *1977 National Cave Management Symposium Proceedings*, 108–121.

Twente, J., Twente, J., & Brack, V. (1985). The duration of the period of hibernation of three species of vespertilionid bats. II. Laboratory studies. *Canadian Journal of Zoology*, *63*, 2955–2961. https://doi.org/10.1139/z85-443

Twente, J. W. (1955a). Aspects of a population study of cavern-dwelling bats. *Journal of Mammalogy*, *36*(3), 379–390. https://doi.org/10.2307/1375680

Twente, J. W. (1955b). Some aspects of habitat selection and other behavior of cavern-dwelling bats. *Ecology*, *36*(4), 706–732. https://doi.org/10.2307/1931308

University of Arizona. (n.d.). *Temperature and precipitation*. CLIMAS. Retrieved August 30, 2023, from https://climas.arizona.edu/sw-climate/temperature-and-precipitation

U.S. National Park Service. (2019). *Bat fungus potentially detected at Grand Canyon*. U.S. National Park Service. https://www.nps.gov/grca/learn/news/bat-fungus-potentially-detected-at-grand-canyon-20191204.htm

Vaccarelli, I., Colado, R., Pallarés, S., Galassi, D. M. P., Sánchez-Fernández, D., Di Cicco, M., Meierhofer, M. B., Piano, E., Di Lorenzo, T., & Mammola, S. (2023). A global meta-analysis reveals multilevel and context-dependent effects of climate change on subterranean ecosystems. *One Earth*, S2590332223004050. https://doi.org/10.1016/j.oneear.2023.09.001

Verant, M. L., Boyles, J. G., Waldrep, W., Wibbelt, G., & Blehert, D. S. (2012). Temperature-dependent growth of *Geomyces destructans*, the fungus that causes bat white-nose syndrome. *PLoS ONE*, *7*(9), e46280. https://doi.org/10.1371/journal.pone.0046280

Verant, M. L., Meteyer, C. U., Speakman, J. R., Cryan, P. M., Lorch, J. M., & Blehert, D. S. (2014). *White-nose syndrome initiates a cascade of physiologic disturbances in the hibernating bat host*. 11.

Warnecke, L., Turner, J. M., Bollinger, T. K., Lorch, J. M., Misra, V., Cryan, P. M., Wibbelt, G., Blehert, D. S., & Willis, C. K. R. (2012). Inoculation of bats with European *Geomyces destructans* supports the novel pathogen hypothesis for the origin of white-nose syndrome. *Proceedings of the National Academy of Sciences*, *109*(18), 6999–7003. https://doi.org/10.1073/pnas.1200374109

Webb, P. I., Speakman, J. R., & Racey, P. A. (1996). How hot is a hibernaculum? A review of the temperatures at which bats hibernate. *Canadian Journal of Zoology*, *74*(4), 761–765. https://doi.org/10.1139/z96-087

Weller, T. J., Rodhouse, T. J., Neubaum, D. J., Ormsbee, P. C., Dixon, R. D., Popp, D. L., Williams, J. A., Osborn, S. D., Rogers, B. W., Beard, L. O., McIntire, A. M., Hersey, K. A., Tobin, A., Bjornlie, N. L., Foote, J., Bachen, D. A., Maxell, B. A., Morrison, M. L., Thomas, S. C., … Navo, K. W. (2018). A review of bat

hibernacula across the western United States: Implications for white-nose syndrome surveillance and management. *PLOS ONE*, *13*(10), e0205647. https://doi.org/10.1371/journal.pone.0205647

White-nose syndrome. (n.d.). Retrieved September 9, 2023, from https://www.whitenosesyndrome.org/static-page/bats-affected-by-wns

White-Nose Syndrome. (2023). https://www.whitenosesyndrome.org/where-is-wns

White-Nose Syndrome Disease Management Working Group. (2020). *National white-nose syndrome decontamination protocol*. White-Nose Syndrome Response Team.

White-nose syndrome research for conservation grants. (2021). U.S. Fish and Wildlife Service.

Whitford, W., & Wade, E. L. (2002). Chapter 3—Characterization of desert climates. In W. Whitford & E. L. Wade (Eds.), *Ecology of Desert Systems* (pp. 43–63). Academic Press. https://doi.org/10.1016/B978-012747261-4/50004-3

Whiting, J. C., Doering, B., Aho, K., & Rich, J. (2021). Long-term patterns of cave-exiting activity of hibernating bats in western North America. *Scientific Reports*, *11*(1), 8175. https://doi.org/10.1038/s41598-021-87605-0

Wibbelt, G., Puechmaille, S. J., Ohlendorf, B., Mühldorfer, K., Bosch, T., Görföl, T., Passior, K., Kurth, A., Lacremans, D., & Forget, F. (2013). Skin lesions in European hibernating bats associated with *Geomyces destructans*, the etiologic agent of white-nose syndrome. *PLoS ONE*, *8*(9), e74105. https://doi.org/10.1371/journal.pone.0074105

Willis, C. K. R., Menzies, A. K., Boyles, J. G., & Wojciechowski, M. S. (2011). Evaporative water loss is a plausible explanation for mortality of bats from white-nose syndrome. *Integrative and Comparative Biology*, *51*(3), 364–373. https://doi.org/10.1093/icb/icr076

Zomer, R. J., Xu, J., & Trabucco, A. (2022). Version 3 of the global aridity index and potential evapotranspiration database. *Scientific Data*, *9*(1), Article 1. https://doi.org/10.1038/s41597-022-01493-1

APPENDIX A

SUPPLEMENTAL TABLES AND FIGURES

Table A1. Internal survey schedule across all caves in 2018-2023. **X** indicates a month when an internal survey occurred.

	August	September	October	November	December	January	February	March	April	May
Cave 1										
2018-2019	X						X	X	X	
2019-2020		X	X	X	X	X	X	X	X	
2021-2022		X	X	X		X	X	X		
2022-2023				X		X	X			
Cave 2										
2018-2019					X			X	X	
2019-2020		X		X	X	X	X	X	X	
2021-2022		X	X	X		X	X	X	X	
2022-2023				X			X			
Cave 3										
2018-2019		X		X		X	X	X	X	
2019-2020		X	X	X	X	X	X	X	X	
2021-2022			X	X		X	X	X	X	
2022-2023				X		X	X			
Cave 4										
2021-2022							X			
Cave 5										
2021-2022							X			
Cave 6										
2021-2022							X			
Cave 7										
2021-2022							X			
2022-2023						X				X
Cave 8										
2022-2023				X		X				X
Cave 9										
2022-2023				X		X				
Cave 10										
2022-2023				X		X				
Cave 11										
2022-2023							X			
Cave 12										
2022-2023							X			

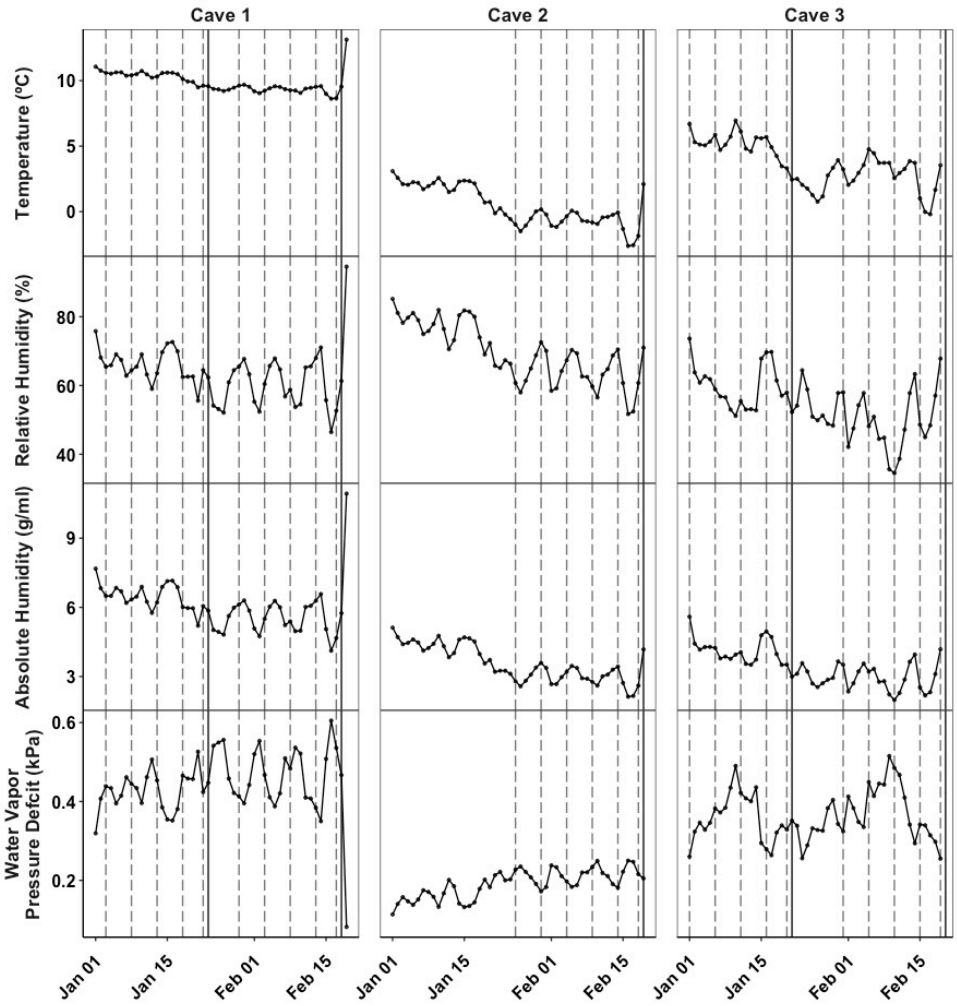

Figure A1. The variation of conditions over time at each cave site in January-February 2023. Solid grey vertical lines indicate survey dates (days when bat roost conditions were measured). Dashed lines indicate 1, 5, 10, 15, 20, and 25 days prior to each survey date, which were used to compare to measured bat roost conditions. Black lines horizontally indicate the trend of daily average for each condition over time. I did not complete a survey at Cave 2 in January 2023 which is why dashed lines are not used at that site in January.

Table A2. Species Detections from Acoustic Recording Units from 2021-2023. An X represents at least one confirmed call by that species at each site in either Year 4 or Year 5. Species codes are as follows: MYTH=*M. thysanodes*; 40KMYO=40 kHz *Myotis* group; COTO= *Corynorhinus townsendii*; 50KMYO=50 kHz *Myotis* group; EPFU=*Eptesicus fuscus*; LACI=*Lasiurus cinereus*; LANO=*Lasionycteris noctivagans*; TABR=*Tadarida brasiliensis*; EUPE=*Eumops perotis*; IDPH=*Idionycteris phyllotis*; PAHE=*P. hesperus*; ANPA=*Antrozous pallidus*; NYSP=*Nyctinomops* spp.; LABL=*L. blossevillii*.

	MYTH	40KMYO	COTO	50KMYO	EPFU	LACI	LANO	TABR	EUPE	IDPH	PAHE	ANPA	NYSP	LABL
Cave 1	X	X	X	X	X	X	X	X	X		X	X	X	X
Cave 2	X	X	X	X	X	X	X	X	X	X	X	X		
Cave 3	X	X	X	X	X	X		X	X		X	X		

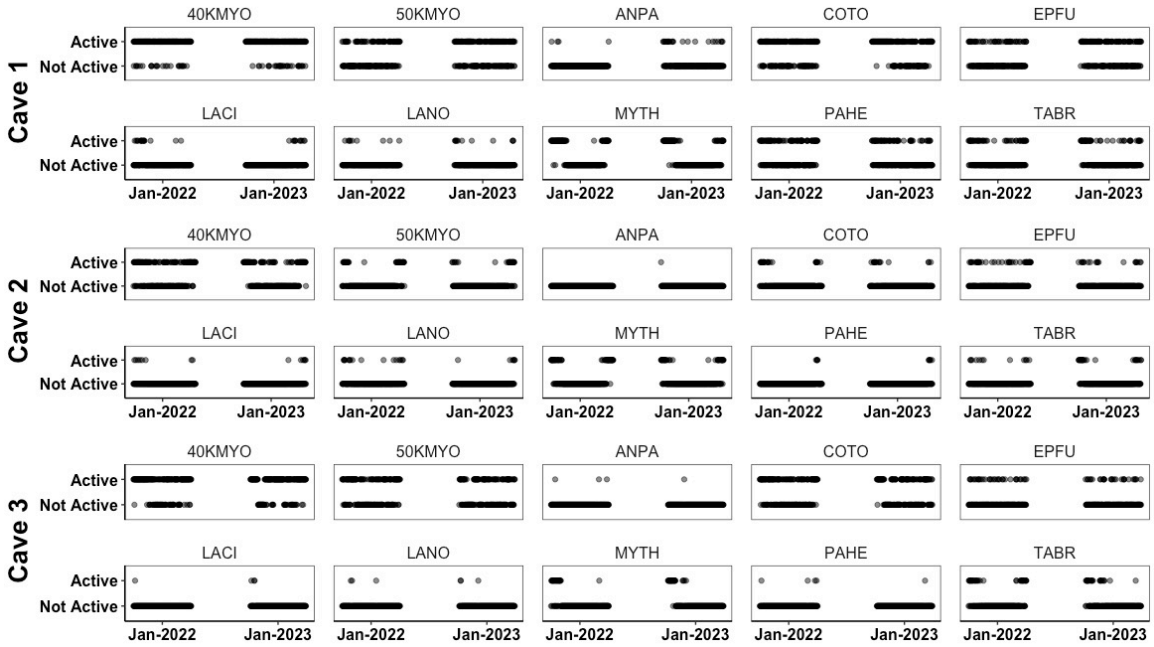

Figure A2. Seasonality in calls from many species detected on acoustic recorders. Acoustic activity by species at Cave 1, Cave 2, and Cave 3 between October and April in Years 4 and 5. Circles represent each acoustic-night. "Active" indicates at least one confirmed call from that species in a night. "Not Active" indicates no calls from that species in a night. Species codes are as follows: 40KMYO= 40 kHz *Myotis*; 50KMYO= 50 kHz *Myotis*; ANPA=*A. pallidus*; COTO=*C. townsendii*; EPFU=*E. fuscus*; LACI=*L. cinereus*; LANO=*Lasionycteris noctivagans*; MYTH=*M. thysanodes*; PAHE=*P. hesperus*; TABR=*Tadarida brasiliensis.*

APPENDIX B

SUPPLEMENTAL MODELING MATERIAL

Table B1. All measured environmental variables initially considered for modeling. "Correlation with bat activity" is the rho value (ρ) calculated by the Spearman correlation. Variables with ρ ≥|0.3| were selected to be evaluated in the next step of modeling.

Variable Tested	Correaltion with Bat Activity	p-value	Selected for next step of modeling
daily_avg_temp	0.56	< .001	yes
daily_avg_rel_hum	-0.24	< .001	no
daily_avg_abs_hum	0.11	0.851	no
daily_avg_vpd	0.41	< .001	yes
daily_min_temp	0.37	< .001	yes
daily_min_rel_hum	-0.1	> .999	no
daily_min_abs_hum	0.28	< .001	no
daily_min_vpd	0.3	< .001	yes
daily_max_temp	0.38	< .001	yes
daily_max_rel_hum	-0.19	0.024	no
daily_max_abs_hum	0.2	0.008	no
daily_max_vpd	0.25	< .001	no
daily_avg_pressure_noaa	0.56	< .001	yes
daily_avg_wind_speed_noaa	-0.2	< .001	no
daily_max_wind_speed_noaa	-0.31	< .001	yes
daily_total_precip_noaa	-0.28	< .001	no
lunar_illumuniation	4.77E-03	> .999	no
daily_avg_temp_interior	0.6	< .001	yes
daily_min_temp_interior	0.62	< .001	yes
daily_max_temp_interior	0.54	< .001	yes
daily_avg_rel_hum_interior	-0.32	< .001	yes
daily_min_rel_hum_interior	-0.34	< .001	yes
daily_max_rel_hum_interior	-0.17	0.007	no
daily_avg_abs_hum_interior	0.17	0.005	no
daily_min_abs_hum_interior	0.21	< .001	no
daily_max_abs_hum_interior	0.16	0.009	no
daily_avg_vpd_interior	0.56	< .001	yes
daily_min_vpd_interior	0.33	< .001	yes
daily_max_vpd_interior	0.49	< .001	yes

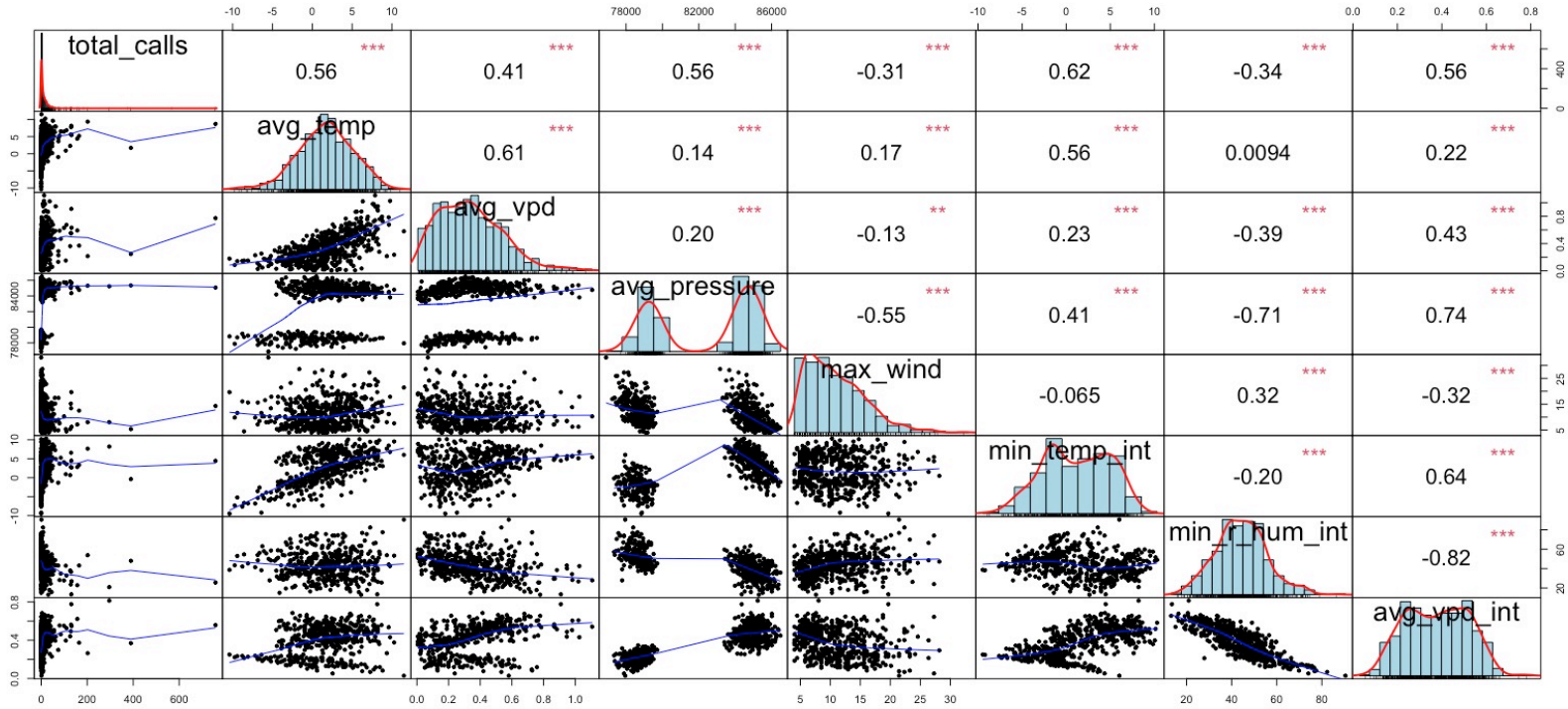

Figure B1. Correlations between bat activity and selected environmental variables using the Spearman correlation method. Variables with ρ ≥0.6 were not included in the same model.

Table B2. Environmental variables that I selected to use in modeling. "Correlation with bat activity" is the rho value (ρ) calculated by the Spearman correlation.

Variable	Correaltion with Bat Activity	p-value
daily_avg_temp	0.56	< .001
daily_avg_vpd	0.41	< .001
daily_avg_pressure_noaa	0.56	< .001
daily_max_wind_speed_noaa	-0.31	< .001
daily_min_temp_interior	0.62	< .001
daily_min_rel_hum_interior	-0.34	< .001
daily_avg_vpd_interior	0.56	< .001

Table B3. *A priori* models that I tested and that included only uncorrelated variables. All possible model combinations within each model "suite" were tested. WVPD=water vapor pressure deficit.

a priori Models	Variables Included in Models			
Suite 1	Daily Average Temperature	Daily Average Pressure	Daily Maximum Wind Speed	Daily Minimum Internal Cave Temperature
Suite 2	Daily Average WVPD	Daily Average Pressure	Daily Maximum Wind Speed	Daily Minimum Internal Cave Temperature
Suite 3	Daily Average Temperature	Daily Maximum Wind Speed	Daily Minimum Internal Cave Temperature	Daily Average Internal Cave WVPD
Suite 4	Daily Average Temperature	Daily Maximum Wind Speed	Daily Minimum Internal Cave Temperature	Daily Minimum Internal Cave Relative Humidity
Suite 5	Daily Average WVPD	Daily Maximum Wind Speed	Daily Minimum Internal Cave Temperature	Daily Average Internal Cave WVPD
Suite 6	Daily Average WVPD	Daily Maximum Wind Speed	Daily Minimum Internal Cave Temperature	Daily Minimum Internal Cave Relative Humidity

Table B4. Overdispersion results for each type of model tested. GLM=generalized linear model, GLMM=generalized linear mixed model, NB=negative binomial. P-value in bold typeface indicated model was over dispersed.

Suite	Model Type	Family	Dispersion Ratio	Pearson's Chi-Squared	Overdispersion p-value
1	GLM	Poisson	38.553	18120.112	**<0.001**
1	GLM	NB	1.846	867.422	0.096
1	GLMM	Poisson	33.682	15796.803	0.888
1	GLMM	NB	1.853	867.424	0.08
2	GLM	Poisson	69.988	32894.302	**<0.001**
2	GLM	NB	2.559	1205.303	**0.04**
2	GLMM	Poisson	46.666	21886.25	0.768
2	GLMM	NB	2.279	1068.97	0.6
3	GLM	Poisson	49.993	23496.797	**<0.001**
3	GLM	NB	2.404	1132.448	0.464
3	GLMM	Poisson	35.188	16503.33	0.176
3	GLMM	NB	1.686	790.651	0.44
4	GLM	Poisson	53.669	25224.53	**<0.001**
4	GLM	NB	2.943	1383.204	0.432
4	GLMM	Poisson	35.719	16752.153	0.152
4	GLMM	NB	1.786	837.583	0.48
5	GLM	Poisson	96.246	45235.407	**<0.001**
5	GLM	NB	3.762	1768.17	0.528
5	GLMM	Poisson	43.333	20323.053	0.448
5	GLMM	NB	2.004	938.065	0.8
6	GLM	Poisson	97.493	45821.94	**<0.001**
6	GLM	NB	4.204	1976.038	0.32
6	GLMM	Poisson	41.859	19631.638	0.352
6	GLMM	NB	1.834	858.104	0.888

Table B5. Akaike Information Criterion (AIC) values for a series of Generalized Linear Models (GLMs) with a negative binomial distribution with the response variable "total nightly bat activity" in relation to cave as a fixed effect and seven environmental variables (ET=daily average external temperature, IT=daily minimum internal temperature, W=daily maximum wind speed, P=daily average atmospheric pressure, IVPD=daily average internal water vapor pressure deficit (VPD), EVPD=daily average external VPD, and IRH=daily minimum internal relative humidity). K is the number of parameters. AIC is the AIC for each model, *Δ*AIC is the difference between the AIC of the best fitting model and the AIC of that model, AICWt is the weight of each model, Cum.Wt is the cumulative weight of models combined, and LL is the log-likelihood. The table is truncated and does not include all models tested.

	K	AIC	Delta_AIC	AICWt	Cum.Wt	LL
ET + W + IT + Cave	7	2963.6	0.0	0.3	0.3	-1474.8
ET + P + W + IT + Cave	8	2964.4	0.8	0.2	0.5	-1474.2
ET + W + IRH + Cave	7	2964.9	1.3	0.2	0.6	-1475.5
ET + W + IVPD + Cave	7	2965.0	1.4	0.1	0.8	-1475.5
ET + W + IT + IVPD + Cave	8	2965.5	1.9	0.1	0.9	-1474.8
ET + W + IT + IRH + Cave	8	2965.5	1.9	0.1	1.0	-1474.8
ET + P + W + IT	6	2973.7	10.1	0.0	1.0	-1480.8
EVPD + W + IT + IRH + Cave	8	2986.0	22.4	0.0	1.0	-1485.0
ET + P + IT	5	2988.9	25.3	0.0	1.0	-1489.5
EVPD + W + IT + IVPD + Cave	8	2990.3	26.7	0.0	1.0	-1487.2
ET + P + IT + Cave	7	2992.0	28.3	0.0	1.0	-1489.0
EVPD + P + W + IT + Cave	8	3012.2	48.6	0.0	1.0	-1498.1
EVPD + W + IT + Cave	7	3012.4	48.8	0.0	1.0	-1499.2
EVPD + W + IRH + Cave	7	3016.9	53.3	0.0	1.0	-1501.5
EVPD + P + IT + Cave	7	3033.3	69.7	0.0	1.0	-1509.7
EVPD + W + IVPD + Cave	7	3045.1	81.4	0.0	1.0	-1515.5
ET + W + IVPD	5	3047.7	84.1	0.0	1.0	-1518.9
ET + W + IT + IVPD	6	3049.4	85.8	0.0	1.0	-1518.7
ET + W + IT + IRH	6	3053.6	90.0	0.0	1.0	-1520.8
ET + W + IRH	5	3068.6	105.0	0.0	1.0	-1529.3
EVPD + P + IT	5	3073.2	109.6	0.0	1.0	-1531.6
EVPD + P + W + IT	6	3074.0	110.4	0.0	1.0	-1531.0
ET + W + IT	5	3082.8	119.2	0.0	1.0	-1536.4
ET + IT + Cave	6	3114.9	151.3	0.0	1.0	-1551.5
ET + IVPD + Cave	6	3115.4	151.8	0.0	1.0	-1551.7
ET + IRH + Cave	6	3115.5	151.9	0.0	1.0	-1551.7
ET + IT + IVPD + Cave	7	3116.7	153.1	0.0	1.0	-1551.4
ET + IT + IRH + Cave	7	3116.9	153.3	0.0	1.0	-1551.4
EVPD + IT + IRH + Cave	7	3129.3	165.7	0.0	1.0	-1557.7
EVPD + IT + IVPD + Cave	7	3137.2	173.6	0.0	1.0	-1561.6
EVPD + IRH + Cave	6	3144.3	180.7	0.0	1.0	-1566.1
EVPD + IT + Cave	6	3154.5	190.9	0.0	1.0	-1571.3
EVPD + IVPD + Cave	6	3169.8	206.1	0.0	1.0	-1578.9
EVPD + W + IT + IRH	6	3179.7	216.1	0.0	1.0	-1583.9
EVPD + W + IT + IVPD	6	3182.8	219.1	0.0	1.0	-1585.4
EVPD + W + IT	5	3192.9	229.3	0.0	1.0	-1591.4
ET + IT + IVPD	5	3215.6	252.0	0.0	1.0	-1602.8
ET + IVPD	4	3215.7	252.1	0.0	1.0	-1603.9
EVPD + W + IVPD	5	3222.3	258.7	0.0	1.0	-1606.2
ET + IT + IRH	5	3232.1	268.5	0.0	1.0	-1611.0
ET + IRH	4	3237.2	273.6	0.0	1.0	-1614.6
EVPD + W + IRH	5	3249.7	286.0	0.0	1.0	-1619.8
ET + IT	4	3273.0	309.4	0.0	1.0	-1632.5
EVPD + IT + IVPD	5	3325.4	361.8	0.0	1.0	-1657.7
EVPD + IT + IRH	5	3327.1	363.5	0.0	1.0	-1658.6
EVPD + IT	4	3345.9	382.2	0.0	1.0	-1668.9
EVPD + IVPD	4	3349.8	386.1	0.0	1.0	-1670.9
ET + P + W + Cave	7	3370.4	406.8	0.0	1.0	-1678.2
ET + W + Cave	6	3371.0	407.4	0.0	1.0	-1679.5
EVPD + IRH	4	3379.1	415.5	0.0	1.0	-1685.5
ET + P + W	5	3380.4	416.8	0.0	1.0	-1685.2
ET + P	4	3393.3	429.7	0.0	1.0	-1692.6
ET + P + Cave	6	3396.4	432.8	0.0	1.0	-1692.2
P + W + IT + Cave	7	3443.9	480.2	0.0	1.0	-1714.9
W + IT + IRH + Cave	7	3447.1	483.5	0.0	1.0	-1716.6

Table B6. Akaike Information Criterion (AIC) values for a series of Generalized Linear Models (GLMs) with a Poisson distribution with the response variable "total nightly bat activity" in relation to seven environmental variables (ET=daily average external temperature, IT=daily minimum internal temperature, W=daily maximum wind speed, P=daily average atmospheric pressure, IVPD=daily average internal water vapor pressure deficit (VPD), EVPD=daily average external VPD, and IRH=daily minimum internal relative humidity). K is the number of parameters. AIC is the AIC for each model, *Δ*AIC is the difference between the AIC of the best fitting model and the AIC of that model, AICWt is the weight of each model, Cum.Wt is the cumulative weight of models combined, and LL is the log-likelihood. Coefficients for each predictor variable in the top model are listed in Table B9.

	K	AIC	Delta_AIC	AICWt	Cum.Wt	LL
ET + P + W + IT	5	11565.2	0.0	1	1	-5777.6
ET + P + IT	4	11713.0	147.8	0	1	-5852.5
ET + W + IT + IRH	5	12568.7	1003.5	0	1	-6279.3
ET + W + IRH	4	12591.6	1026.4	0	1	-6291.8
ET + W + IT + IVPD	5	12687.7	1122.5	0	1	-6338.9
ET + P + W	4	12935.3	1370.1	0	1	-6463.7
ET + W + IVPD	4	12999.0	1433.8	0	1	-6495.5
ET + P	3	13106.4	1541.2	0	1	-6550.2
ET + IT + IRH	4	13455.0	1889.7	0	1	-6723.5
ET + IRH	3	13461.0	1895.8	0	1	-6727.5
ET + IT + IVPD	4	13570.7	2005.5	0	1	-6781.4
ET + W + IT	4	13826.0	2260.8	0	1	-6909.0
ET + IVPD	3	13868.5	2303.3	0	1	-6931.2
EVPD + P + W + IT	5	14297.4	2732.2	0	1	-7143.7
EVPD + P + IT	4	14329.3	2764.1	0	1	-7160.7
ET + IT	3	15171.2	3605.9	0	1	-7582.6
ET + W	3	15194.4	3629.2	0	1	-7594.2
EVPD + P + W	4	15436.9	3871.7	0	1	-7714.4
EVPD + P	3	15482.3	3917.0	0	1	-7738.1
EVPD + W + IT + IRH	5	15913.9	4348.7	0	1	-7952.0
EVPD + W + IT + IVPD	5	16065.1	4499.9	0	1	-8027.6
EVPD + IT + IRH	4	16242.3	4677.1	0	1	-8117.2
EVPD + W + IVPD	4	16271.2	4706.0	0	1	-8131.6
EVPD + W + IT	4	16343.4	4778.2	0	1	-8167.7
EVPD + IT + IVPD	4	16402.2	4837.0	0	1	-8197.1
EVPD + IVPD	3	16589.8	5024.6	0	1	-8291.9
EVPD + W + IRH	4	16599.9	5034.6	0	1	-8295.9
ET	2	16746.7	5181.5	0	1	-8371.3
EVPD + IT	3	16770.8	5205.6	0	1	-8382.4
EVPD + IRH	3	16925.8	5360.6	0	1	-8459.9
P + W + IT	4	17155.8	5590.6	0	1	-8573.9
P + IT	3	17157.3	5592.1	0	1	-8575.6
W + IT + IRH	4	18040.6	6475.4	0	1	-9016.3
IT + IRH	3	18425.9	6860.7	0	1	-9210.0
W + IT + IVPD	4	18470.6	6905.4	0	1	-9231.3
EVPD + W	3	18695.1	7129.9	0	1	-9344.5
IT + IVPD	3	18860.5	7295.3	0	1	-9427.2
W + IVPD	3	18900.8	7335.6	0	1	-9447.4
EVPD	2	19221.3	7656.1	0	1	-9608.7
IVPD	2	19264.4	7699.2	0	1	-9630.2
W + IT	3	19763.0	8197.7	0	1	-9878.5
P + W	3	20113.7	8548.5	0	1	-10053.9
P	2	20140.3	8575.1	0	1	-10068.1
W + IRH	3	20426.9	8861.7	0	1	-10210.4
IT	2	20522.7	8957.5	0	1	-10259.4
IRH	2	20870.3	9305.1	0	1	-10433.1
W	2	26030.7	14465.4	0	1	-13013.3
Intercept	1	27218.0	15652.8	0	1	-13608.0

Table B7. Akaike Information Criterion (AIC) values for a series of Generalized Linear Mixed Models (GLMMs) with a negative binomial distribution, "cave" set as a random intercept, and with the response variable "total nightly bat activity" in relation to seven environmental variables (ET=daily average external temperature, IT=daily minimum internal temperature, W=daily maximum wind speed, P=daily average atmospheric pressure, IVPD=daily average internal water vapor pressure deficit (VPD), EVPD=daily average external VPD, and IRH=daily minimum internal relative humidity). K is the number of parameters. AIC is the AIC for each model, *Δ*AIC is the difference between the AIC of the best fitting model and the AIC of that model, AICWt is the weight of each model, Cum.Wt is the cumulative weight of models combined, and LL is the log-likelihood. Coefficients for each predictor variable in the top model are listed in Table B10.

	K	AIC	Delta_AIC	AICWt	Cum.Wt	LL
ET + P + W + IT	7	2975.68	0	0.55	0.55	-1480.84
ET + W + IT	6	2977.91	2.23	0.18	0.74	-1482.95
ET + W + IT + IVPD	7	2979.9	4.23	0.07	0.87	-1482.95
ET + W + IT + IRH	7	2979.9	4.23	0.07	0.8	-1482.95
ET + W + IRH	6	2979.93	4.25	0.07	0.93	-1483.96
ET + W + IVPD	6	2979.97	4.29	0.06	1	-1483.98
ET + P + IT	6	2990.9	15.23	0	1	-1489.45
EVPD + W + IT + IRH	7	3002.14	26.47	0	1	-1494.07
EVPD + W + IT + IVPD	7	3006.41	30.74	0	1	-1496.21
EVPD + W + IT	6	3026.23	50.56	0	1	-1507.12
EVPD + P + W + IT	7	3028.13	52.45	0	1	-1507.06
EVPD + W + IRH	6	3035.08	59.4	0	1	-1511.54
EVPD + P + IT	6	3044.15	68.48	0	1	-1516.08
EVPD + W + IVPD	6	3063.35	87.68	0	1	-1525.68
ET + IVPD	5	3130.64	154.96	0	1	-1560.32
ET + IT	5	3130.7	155.02	0	1	-1560.35
ET + IRH	5	3130.86	155.18	0	1	-1560.43
ET + IT + IVPD	6	3132.2	156.52	0	1	-1560.1
ET + IT + IRH	6	3132.54	156.86	0	1	-1560.27
EVPD + IT + IRH	6	3146.16	170.48	0	1	-1567.08
EVPD + IT + IVPD	6	3153.96	178.29	0	1	-1570.98
EVPD + IRH	5	3162.46	186.78	0	1	-1576.23
EVPD + IT	5	3169.03	193.35	0	1	-1579.51
EVPD + IVPD	5	3188.05	212.37	0	1	-1589.02
ET + P + W	6	3382.39	406.71	0	1	-1685.19
ET + W	5	3385.69	410.01	0	1	-1687.84
ET + P	5	3395.28	419.6	0	1	-1692.64
P + W + IT	6	3458.3	482.62	0	1	-1723.15
W + IT + IRH	6	3459.9	484.22	0	1	-1723.95
W + IT	5	3461.76	486.08	0	1	-1725.88
W + IT + IVPD	6	3461.78	486.11	0	1	-1724.89
P + IT	5	3468.2	492.52	0	1	-1729.1
EVPD + W	5	3487.38	511.71	0	1	-1738.69
EVPD + P	5	3488.68	513	0	1	-1739.34
EVPD + P + W	6	3490.66	514.99	0	1	-1739.33
ET	4	3534.96	559.28	0	1	-1763.48
W + IVPD	5	3540.15	564.47	0	1	-1765.07
W + IRH	5	3543.93	568.26	0	1	-1766.97
EVPD	4	3609.2	633.52	0	1	-1800.6
IT + IVPD	5	3610.34	634.66	0	1	-1800.17
IT + IRH	5	3610.55	634.87	0	1	-1800.27
IT	4	3612.02	636.34	0	1	-1802.01
IVPD	4	3668.71	693.04	0	1	-1830.36
IRH	4	3674.67	698.99	0	1	-1833.33
P	4	4646.48	1670.8	0	1	-2319.24
P + W	5	4648.25	1672.58	0	1	-2319.13
W	4	4659.94	1684.26	0	1	-2325.97
Intercept	3	4802.36	1826.68	0	1	-2398.18

Table B8. Akaike Information Criterion (AIC) values for a series of Generalized Linear Mixed Models (GLMMs) with a Poisson distribution, "cave" set as a random intercept, and with the response variable "total nightly bat activity" in relation to seven environmental variables (ET=daily average external temperature, IT=daily minimum internal temperature, W=daily maximum wind speed, P=daily average atmospheric pressure, IVPD=daily average internal water vapor pressure deficit (VPD), EVPD=daily average external VPD, and IRH=daily minimum internal relative humidity). K is the number of parameters. AIC is the AIC for each model, *Δ*AIC is the difference between the AIC of the best fitting model and the AIC of that model, AICWt is the weight of each model, Cum.Wt is the cumulative weight of models combined, and LL is the log-likelihood. Coefficients for each predictor variable in the top model are listed in Table B11.

	K	AIC	Delta_AIC	AICWt	Cum.Wt	LL
ET + P + W + IT	6	10946.15	0	1	1	-5467.08
ET + W + IT + IRH	6	11018.65	72.49	0	1	-5503.32
ET + W + IRH	5	11027.95	81.79	0	1	-5508.97
ET + W + IT + IVPD	6	11039.4	93.24	0	1	-5513.7
ET + W + IT	5	11047.67	101.51	0	1	-5518.83
ET + W + IVPD	5	11063.96	117.8	0	1	-5526.98
EVPD + W + IT + IVPD	6	11581.65	635.49	0	1	-5784.82
ET + P + IT	5	11603.91	657.76	0	1	-5796.96
EVPD + W + IT + IRH	6	11709.2	763.05	0	1	-5848.6
EVPD + P + W + IT	6	11956.47	1010.32	0	1	-5972.24
ET + P + W	5	12015.57	1069.41	0	1	-6002.78
ET + W	4	12068.84	1122.69	0	1	-6030.42
EVPD + W + IT	5	12088.63	1142.48	0	1	-6039.32
ET + IT + IRH	5	12096.24	1150.08	0	1	-6043.12
ET + IT + IVPD	5	12125.72	1179.57	0	1	-6057.86
ET + IT	4	12166.25	1220.1	0	1	-6079.13
ET + IRH	4	12196.01	1249.85	0	1	-6094
ET + IVPD	4	12299.91	1353.76	0	1	-6145.95
EVPD + W + IRH	5	12424.44	1478.28	0	1	-6207.22
EVPD + P + IT	5	12515.08	1568.92	0	1	-6252.54
EVPD + IT + IVPD	5	12594.1	1647.94	0	1	-6292.05
ET + P	4	12667.9	1721.75	0	1	-6329.95
EVPD + IT + IRH	5	12674.51	1728.36	0	1	-6332.26
EVPD + IT	4	12932.85	1986.69	0	1	-6462.42
EVPD + W + IVPD	5	12945.2	1999.04	0	1	-6467.6
EVPD + IRH	4	13067.83	2121.68	0	1	-6529.92
ET	3	13408.06	2461.9	0	1	-6701.03
EVPD + IVPD	4	13453.36	2507.2	0	1	-6722.68
EVPD + P + W	5	14072.43	3126.28	0	1	-7031.22
W + IT + IRH	5	14335.13	3388.98	0	1	-7162.57
EVPD + W	4	14374.29	3428.14	0	1	-7183.15
EVPD + P	4	14388.44	3442.29	0	1	-7190.22
W + IT + IVPD	5	14436.17	3490.02	0	1	-7213.09
W + IT	4	14583.71	3637.55	0	1	-7287.85
P + W + IT	5	14585.12	3638.97	0	1	-7287.56
EVPD	3	14801.03	3854.87	0	1	-7397.51
P + IT	4	14978.32	4032.16	0	1	-7485.16
IT + IRH	4	15432.49	4486.34	0	1	-7712.25
IT + IVPD	4	15541.63	4595.47	0	1	-7766.81
IT	3	15946.36	5000.2	0	1	-7970.18
W + IVPD	4	16486.47	5540.31	0	1	-8239.23
IVPD	3	17002.31	6056.15	0	1	-8498.15
W + IRH	4	17003.99	6057.84	0	1	-8498
IRH	3	17640.15	6694	0	1	-8817.08
P + W	4	19579.55	8633.4	0	1	-9785.78
W	3	19599.75	8653.6	0	1	-9796.87
P	3	19660.96	8714.8	0	1	-9827.48
Intercept	2	20344.68	9398.52	0	1	-10170.34

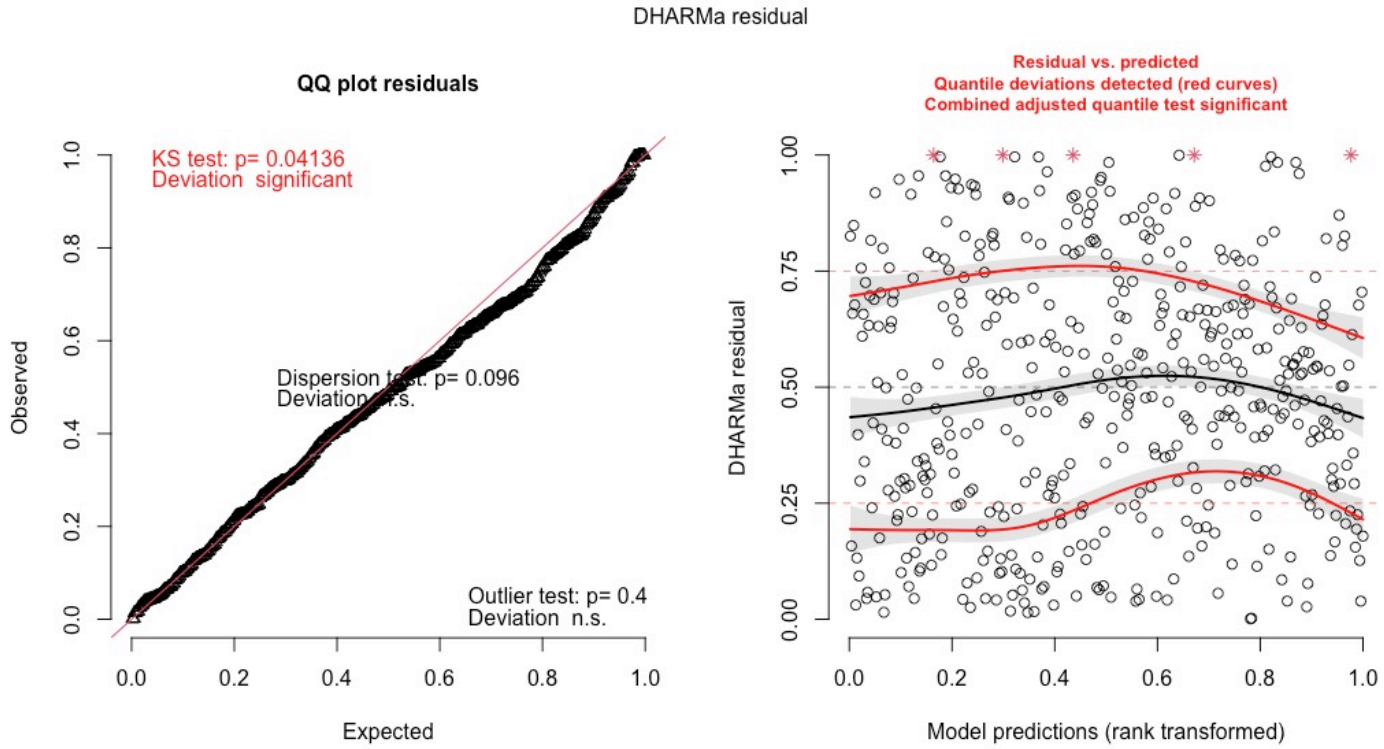

Figure B2. Q-Qplot (left) to test for goodness of fit for the top performing generalized linear model with a negative binomial distribution, as determined by AIC (Table 7). Residual versus predicted plot on the right.

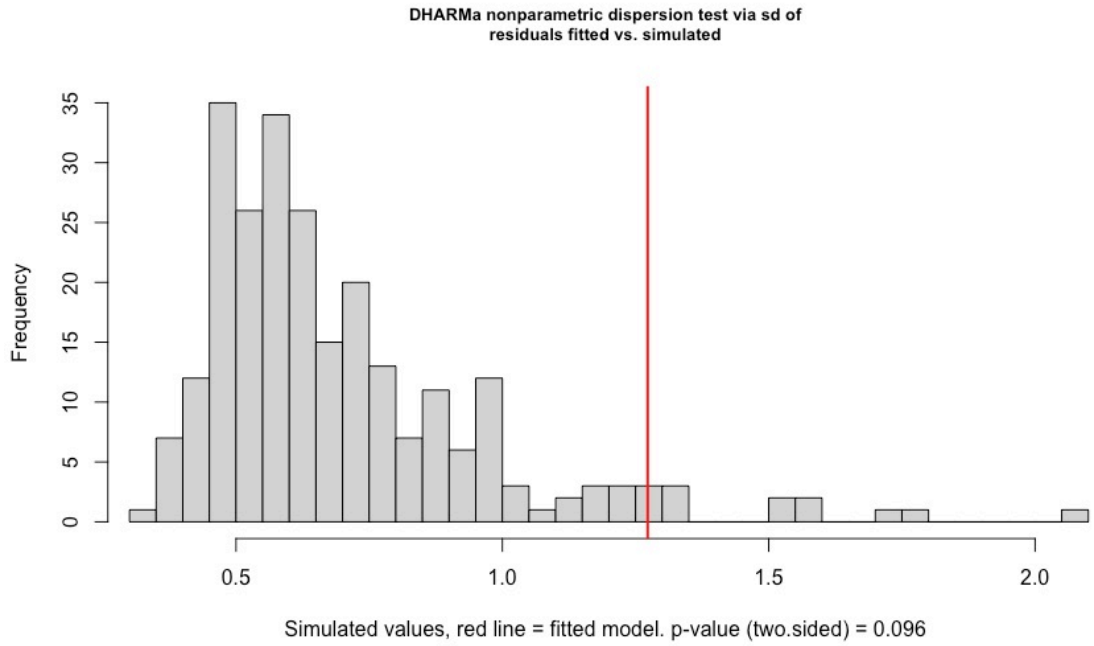

Figure B3. Nonparametric dispersion histogram to test for goodness of fit for the top performing generalized linear model with a negative binomial distribution, as determined by AIC (Table 7).

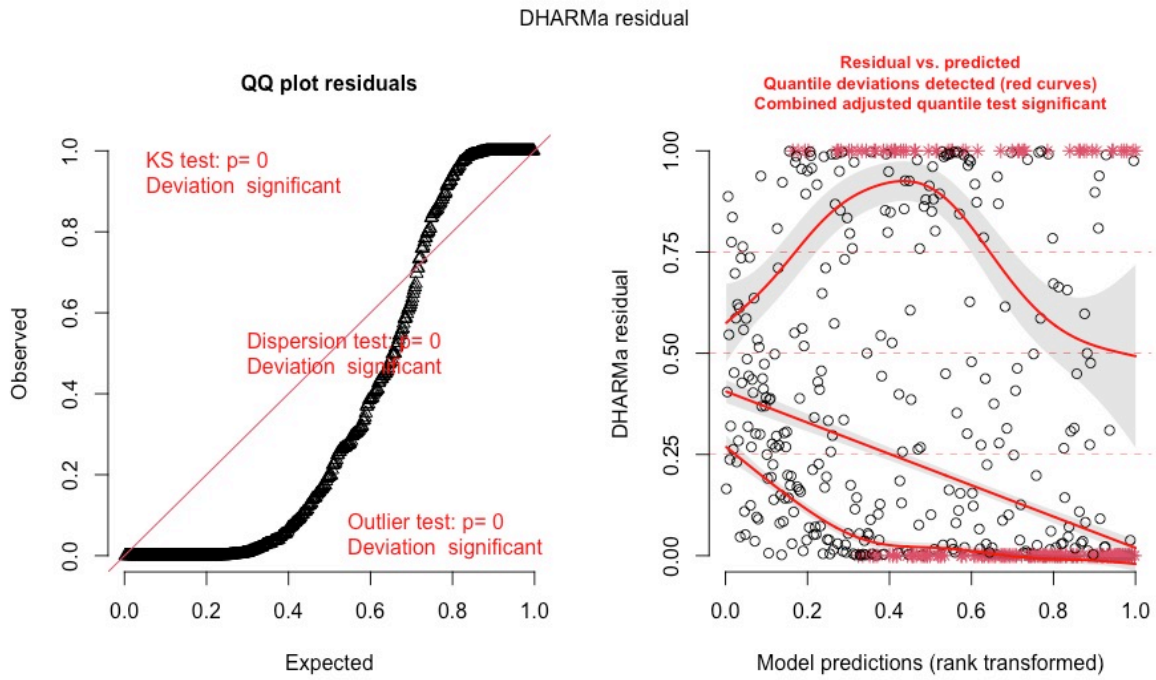

Figure B4. Q-Qplot (left) to test for goodness of fit for the top performing generalized linear model with a Poisson distribution, as determined by AIC (Table B6). Residual versus predicted plot on the right.

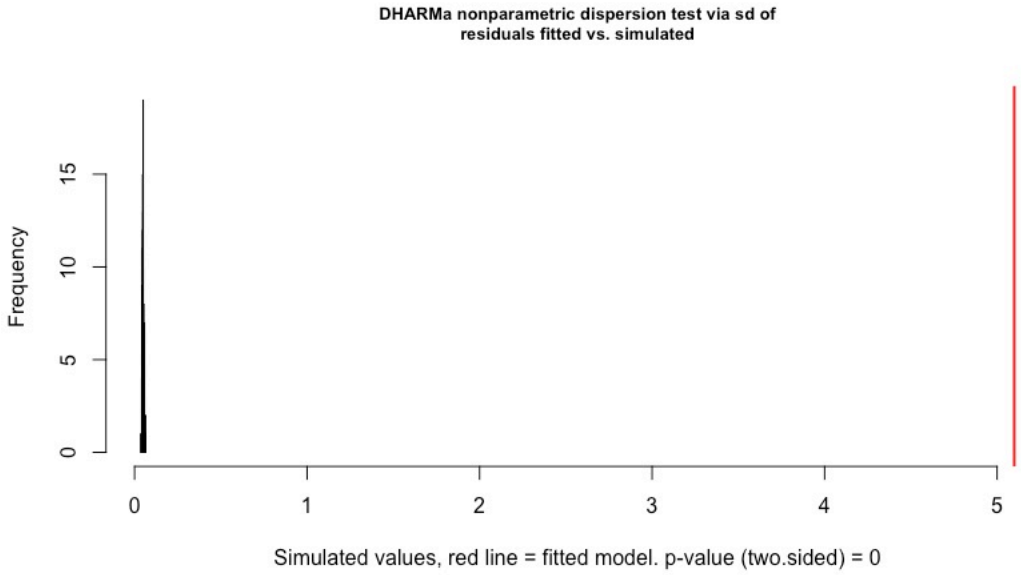

Figure B5. Nonparametric dispersion histogram to test for goodness of fit for the top performing generalized linear model with a Poisson distribution, as determined by AIC (Table B6).

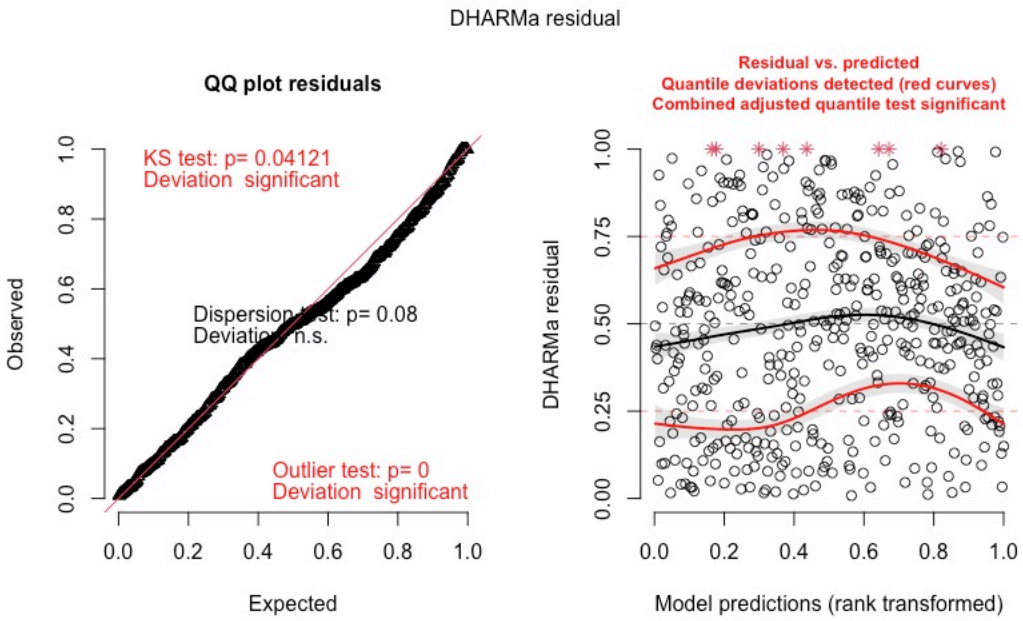

Figure B6. Q-Qplot (left) to test for goodness of fit for the top performing generalized linear mixed model with a negative binomial distribution and cave as a random intercept, as determined by AIC (Table B7). Residual versus predicted plot on the right.

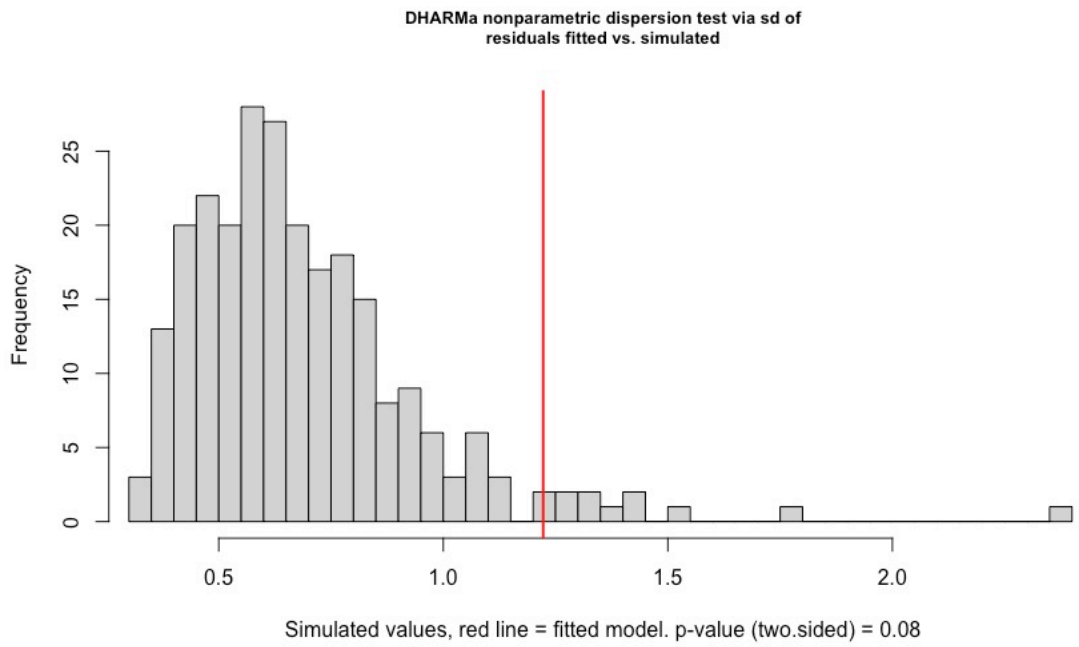

Figure B7. Nonparametric dispersion histogram to test for goodness of fit for the top performing generalized linear mixed model with a negative binomial distribution and cave as a random intercept, as determined by AIC (Table B7).

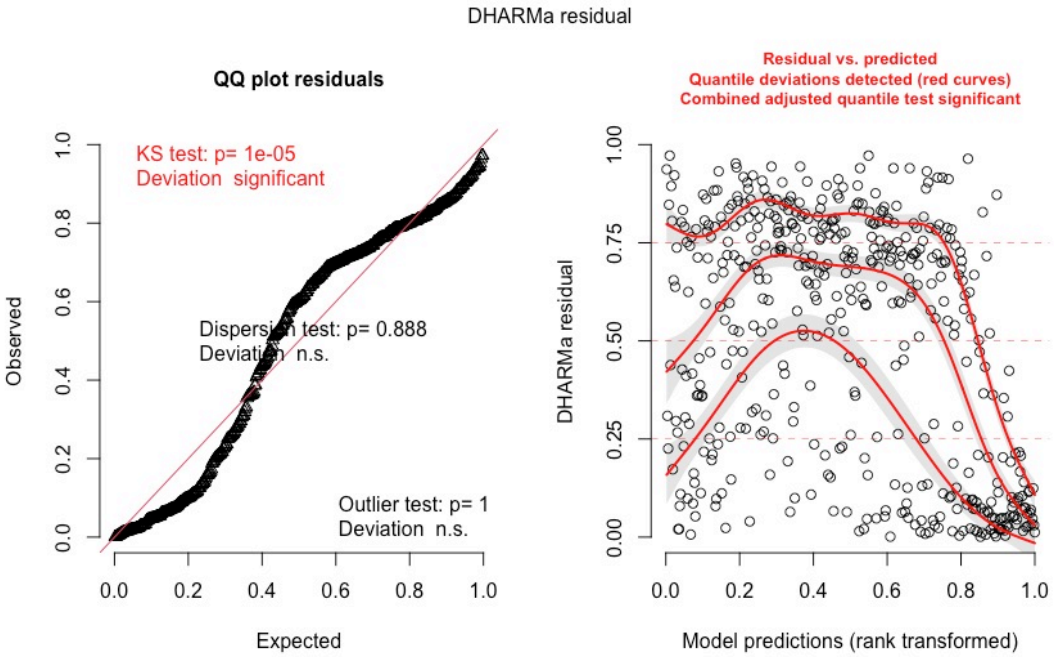

Figure B8. Q-Qplot (left) to test for goodness of fit for the top performing generalized linear mixed model with a Poisson distribution and cave as a random intercept, as determined by AIC (Table B8). Residual versus predicted plot on the right.

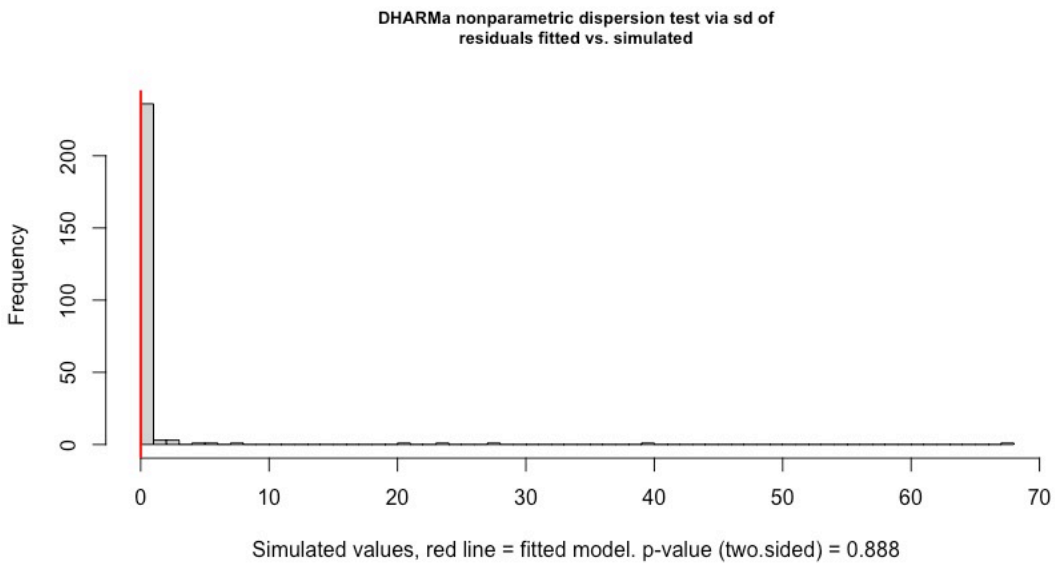

Figure B9. Nonparametric dispersion histogram to test for goodness of fit for the top performing generalized linear mixed model with a Poisson distribution and cave as a random intercept, as determined by AIC (Table B8).

Table B9. Beta estimates for predictor variables included in the top generalized linear model with a Poisson distribution (Table B6).

	β Estimate	Std. Error	z value	p-value
(Intercept)	1.67	0.03	53.52	<0.001
Daily Average External Temperature	1.10	0.02	59.18	<0.001
Daily Average Pressure	1.20	0.03	36.32	<0.001
Daily Maximum Wind Speed	-0.16	0.01	-11.94	<0.001
Daily Minimum Internal Cave Temperature	-0.40	0.02	-18.63	<0.001

Table B10. Beta estimates for predictor variables included in the top generalized linear mixed model with a negative binomial distribution and cave set as a random intercept (Table B7).

	β Estimate	Std. Error	z value	p-value
(Intercept)	1.52	0.07	20.48	<0.001
Daily Average External Temperature	1.02	0.08	13.09	<0.001
Daily Average Pressure	1.10	0.10	11.51	<0.001
Daily Maximum Wind Speed	-0.32	0.07	-4.28	<0.001
Daily Minimum Internal Cave Temperature	0.07	0.08	0.78	0.44

Table B11. Beta estimates for predictor variables included in the top generalized linear mixed model with a Poisson distribution and cave set as a random intercept (Table B8).

	β Estimate	Std. Error	z value	p-value
(Intercept)	1.90	1.30	1.46	0.14
Daily Average External Temperature	1.08	0.02	51.68	<0.001
Daily Average Pressure	-1.12	0.11	-10.22	<0.001
Daily Maximum Wind Speed	-0.46	0.02	-24.86	<0.001
Daily Minimum Internal Cave Temperature	-0.27	0.03	-7.64	<0.001

APPENDIX C

SUPPLEMENTAL PHOTOS FROM FIELD WORK 2021-2023

Figure C1. An internal survey at Cave 3 in January 2022. Note significant amounts of light in the cave.

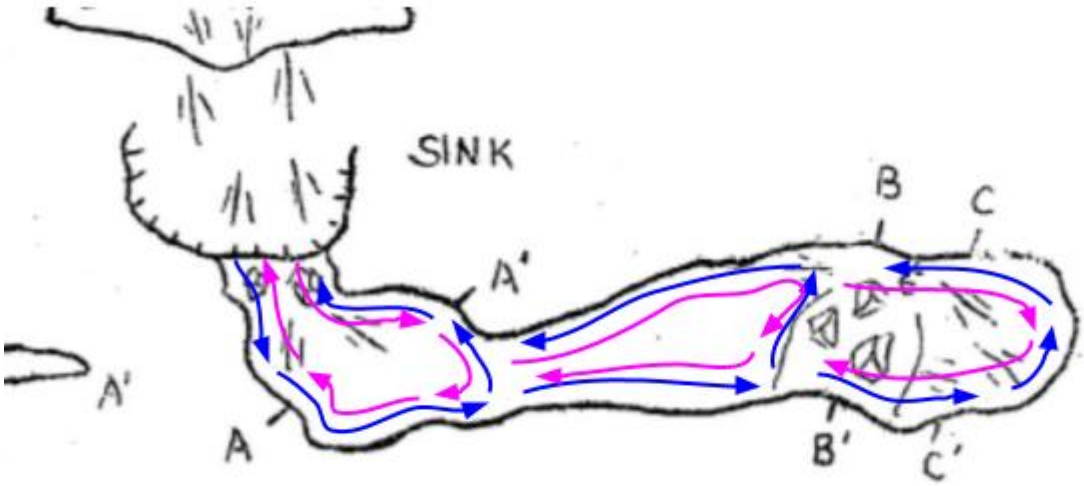

Figure C2. A simplified diagram of the double-observer technique used to survey caves. The pink line indicates the route Observer 1 would take, and the blue line indicates the route Observer 2 would take in each room.

Figure C3. Using a telescoping pole with two Kestrel 3000s, one Kestrel Professional, and one HOBO data logger attached to record bat roost humidity for five consecutive minutes as part of the validation study of humidity-measuring devices. Cave 1 in January 2023.

Figure C4. A HOBO data logger partially concealed in the ceiling of Cave 1 with camouflaged duct tape.

Figure C5. Acoustic monitor set up at Cave 1. Note the solar panel (left) and microphone attached to a telescoping pole in the tree (right).

Figure C6. Acoustic monitor set up at Cave 2. Note the solar panel, ARU next to the solar panel, and microphone attached to a telescoping pole in the tree.

Figure C7. Acoustic monitor set up at Cave 3. Note the solar panel at ground level and microphone attached to a telescoping pole secured in rocks.

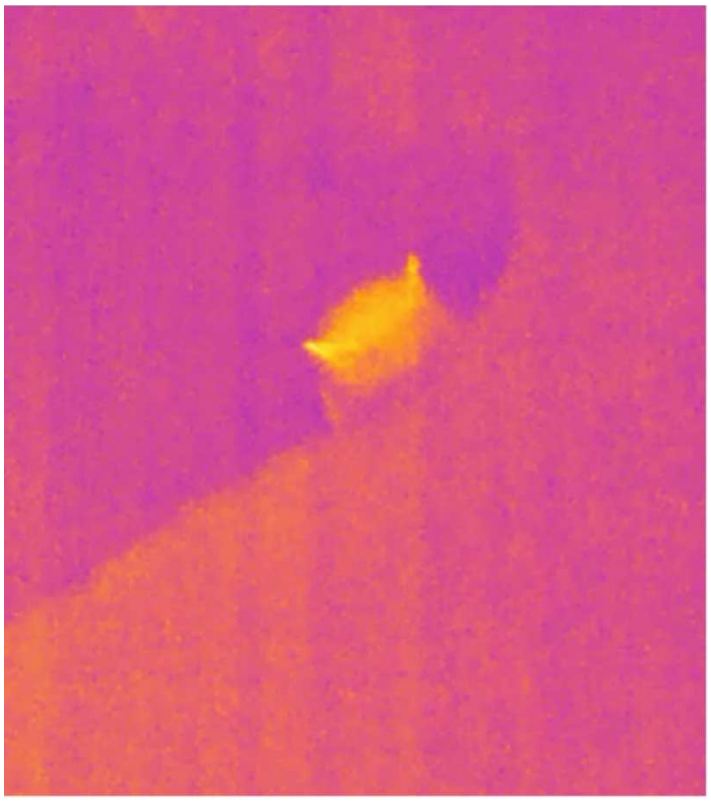

Figure C8. Thermal image of a roosting *Myotis* spp. near the cave entrance at Cave 1 in January 2022. Although appearing "hot" in the image, it had an external body temperature of 2.6°C, which approached the ambient temperature of -1.9°C (scale not shown). Thermal image was taken within 10 minutes of researchers entering the cave. These findings suggest deep torpor at time of first observation.

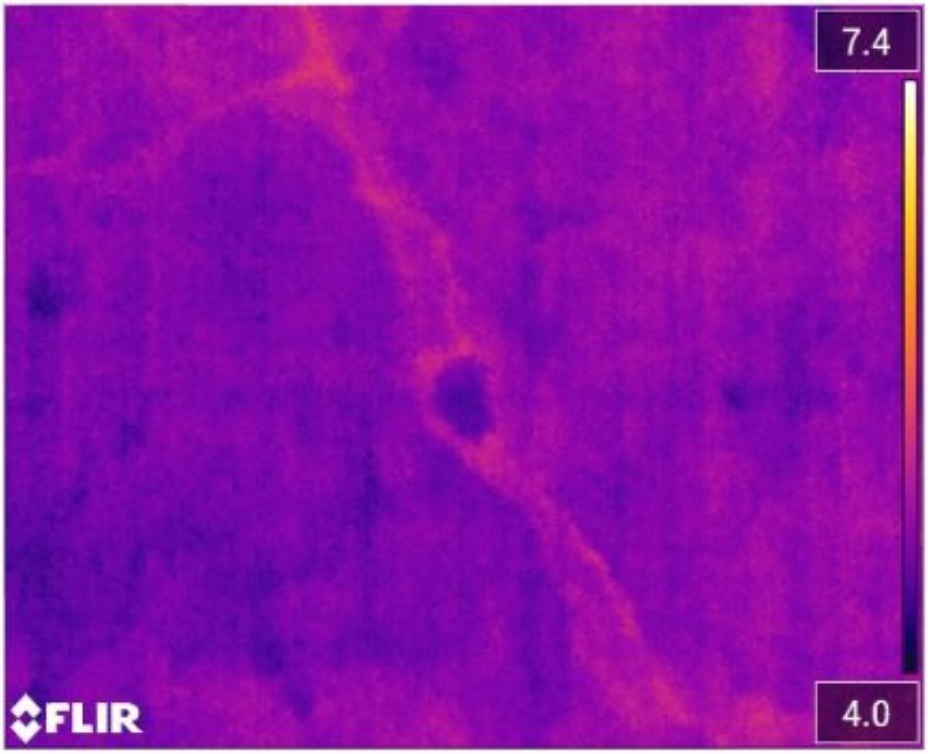

Figure C9. Thermal image of a roosting *C. townsendii* in Cave 2 in November 2021. The bat (middle) had an external body temperature near ambient at 4.0°C. The surrounding hibernacula temperature was 4.0°C-6.0°C. This image was taken after several hours of internal surveys being conducted. The bat maintained torpid temperatures throughout the extended survey.

APPENDIX D

ETHICAL STATEMENT & IACUC APPROVAL

This project was approved by the Arizona Game and Fish Department (Scientific Activity License # SP403931), the Institutional Animal Care and Use Committee at ASU (protocol #16-1517R) and ASU's Biosafety Committee (disclosure # SPROTO202100000100). Live bats were not handled during the hibernation period. To minimize disturbance to hibernating bats, cave entries were strictly task-oriented, limited in frequency, and all persons entering hibernacula were trained to minimize time spent collecting data. To reduce the risk of introducing *Pseudogymnoascus destructans* to any cave in this study, we adhered to the National White-nose Syndrome Decontamination protocols following each cave visit. To reduce risk of introducing SARS-CoV-2 into North American bat populations, each participant was fully vaccinated, completed PCR tests within 72 hours prior to entering hibernacula, completed rapid antigen tests the day of internal surveys, and always wore N95 masks within caves.

Institutional Animal Care and Use Committee (IACUC)
Office of Research Integrity and Assurance
Arizona State University
660 South Mill Avenue, Suite 312
Tempe, Arizona 85287-6111
Phone: (480) 965-6788 *FAX:* (480) 965-7772

Animal Protocol Review

ASU Protocol Number:	**19-1725R**
Protocol Title:	**Ecology, Immunology & Disease Risk in Arizona Bats**
Principal Investigator:	**Marianne Moore**
Date of Action:	**6/27/2019**

The animal protocol review was considered by the Committee and the following decisions were made:

The protocol was approved.

If you have not already done so, documentation of Level III Training (i.e., procedure-specific training) will need to be provided to the IACUC office before participants can perform procedures independently. For more information on Level III requirements see https://researchintegrity.asu.edu/animals/training.

Total # of Animals:	**3420**	
Species:	**Bats**	**Pain Category: C**

Protocol Approval Period:	**6/27/2019 – 6/26/2022**
Sponsor:	**US Fish & Wildlife Service**
ASU Proposal/Award #:	**FP00014144**
Title:	**Exploring the winter ecology and physiology of desert southwest bats to help predict their risk to white-nose syndrome**

Signature: _____ for C. Shalley _____ Date: 7/8/2019
IACUC Chair or ***Designee***

Cc: IACUC Office
IACUC Chair

Institutional Animal Care and Use Committee (IACUC)
Office of Research Integrity and Assurance
Arizona State University
660 South Mill Avenue, Suite 312
Tempe, Arizona 85287-6111
Phone: (480) 965-6788 *FAX:* (480) 965-7772

Animal Protocol Review

ASU Protocol Number:	**22-1936R**
Protocol Title:	**Investigating the winter ecology and physiology of hibernating desert southwest bats across expanded temporal and geographic scales**
ASU Principal Investigator:	**Marianne Moore**
Date of Action:	**5/26/2022**

The animal protocol review was considered by the Committee and the following decisions were made:

The protocol was approved.

NOTE: If you have not already done so, documentation of Level III Training (i.e., procedure-specific training) will need to be provided to the IACUC office before participants can perform procedures without supervision. For more information on Level III requirements see https://researchintegrity.asu.edu/animals/training, or contact Research Support Services within DACT at dactrss@asu.edu.

Additional requirements:

☐ This protocol requires that Research Support Services group within DACT provide supervision for the first time a procedure is conducted. Contact dactrss@asu.edu to schedule.

☐ This protocol indicates that there are surgical procedures. A surgical checklist may be required to be submitted to Research Support Services within DACT (dactrss@asu.edu), prior to starting surgeries.

☐ Other requirements:

Total # of Animals:	**100**	
Species:	**Bats**	**Pain Category: C**

Protocol Approval Period: **5/26/2022 – 5/25/2025**

Sponsor:	**USFWS**
ASU Proposal/Award #:	**AWD35862**
Title:	**Investigating the winter ecology and physiology of hibernating desert southwest bats across expanded temporal and geographic scales**

Signature: Samantha Sullivan Date: 6/6/2022
IACUC Chair or ***Designee***
Cc: IACUC Office, IACUC Chair